

# Catecholaminergic neurons in the peripheral nervous system

Citation for published version (APA):

Verlinden, T. J. M. (2022). *Catecholaminergic neurons in the peripheral nervous system: a critical reappraisal of the sympathetic-parasympathetic paradigm for the classification of nerves, ganglia and neurons*. [Doctoral Thesis, Maastricht University]. Maastricht University. <https://doi.org/10.26481/dis.20221222tv>

## Document status and date:

Published: 01/01/2022

## DOI:

[10.26481/dis.20221222tv](https://doi.org/10.26481/dis.20221222tv)

## Document Version:

Publisher's PDF, also known as Version of record

## Please check the document version of this publication:

- A submitted manuscript is the version of the article upon submission and before peer-review. There can be important differences between the submitted version and the official published version of record. People interested in the research are advised to contact the author for the final version of the publication, or visit the DOI to the publisher's website.
- The final author version and the galley proof are versions of the publication after peer review.
- The final published version features the final layout of the paper including the volume, issue and page numbers.

[Link to publication](#)

## General rights

Copyright and moral rights for the publications made accessible in the public portal are retained by the authors and/or other copyright owners and it is a condition of accessing publications that users recognise and abide by the legal requirements associated with these rights.

- Users may download and print one copy of any publication from the public portal for the purpose of private study or research.
- You may not further distribute the material or use it for any profit-making activity or commercial gain
- You may freely distribute the URL identifying the publication in the public portal.

If the publication is distributed under the terms of Article 25fa of the Dutch Copyright Act, indicated by the "Taverne" license above, please follow below link for the End User Agreement:

[www.umlib.nl/taverne-license](http://www.umlib.nl/taverne-license)

## Take down policy

If you believe that this document breaches copyright please contact us at:

[repository@maastrichtuniversity.nl](mailto:repository@maastrichtuniversity.nl)

providing details and we will investigate your claim.

Catecholaminergic neurons in the peripheral nervous system: a critical reappraisal of the sympathetic-parasympathetic paradigm for the classification of nerves, ganglia and neurons

© **Thomas J.M. Verlinden**, Maastricht 2022

No parts of this book may be reproduced or transmitted in any form or by any means, without prior permission in writing by the author, or when appropriate, by the publishers of the publications.

Cover design: Greet Mommen

Layout: Tiny Wouters

Production: Ipskamp Printing

ISBN/EAN: 978-94-6421-962-3

Catecholaminergic neurons in the peripheral nervous system: a critical reappraisal of the sympathetic-parasympathetic paradigm for the classification of nerves, ganglia and neurons

**PROEFSCHRIFT**

ter verkrijging van de graad van doctor aan de Universiteit Maastricht,  
op gezag van de Rector Magnificus, Prof. dr. Pamela Habibović,  
volgens het besluit van het College van Decanen,  
in het openbaar te verdedigen op  
donderdag 22 december 2022 om 13.00 uur

door

Thomas J.M. Verlinden

**Promotor**

Prof. dr. S. E. Köhler

**Co-promotoren**

Em. prof. dr. W.H. Lamers

Dr. J.P.J.M. Hikspoors

Dr. A. Herrler

**Beoordelingscommissie**

Prof. dr. J.H.H.J. Prickaerts (voorzitter)

Dr. H. ten Donkelaar, Radboud University Medical Center, Nijmegen

Prof. dr. J.M. Rigo, Universiteit Hasselt, België

Prof. dr. Y. Temel

## Contents

Chapter 1.	General introduction	7
Chapter 2.	The human phrenic nerve serves as a morphological conduit for autonomic neurons and innervates the caval body of the diaphragm	15
Chapter 3.	Morphology of the human cervical vagus nerve: implications for vagus nerve stimulation treatment	37
Chapter 4.	Innervation of the human spleen: A complete hilum-embedding approach	59
Chapter 5.	General discussion: A systematic review on the distribution of catecholaminergic neurons in the peripheral nervous system and a critical reappraisal of the sympathetic-parasympathetic model	79
Chapter 6.	Impact	107
Addendum.	Samenvatting (Dutch summary)	111
	Dankwoord	117
	Curriculum vitae	121



# Chapter 1

General introduction





## General introduction

A long history of separate investigations to the nervous system exists. Neuroanatomists studied shape, cellular structure and neural circuitry. Neurochemists studied chemical composition, neurophysiologists bioelectric properties and neuropsychologists investigated the organization and neural substrates of behavior and cognition. In the mid-1960s, the term neuroscience was introduced to signal the beginning of an era in which each of these disciplines would work together cooperatively, sharing a common language, common concepts, and common goals.<sup>1</sup>

The anatomical nomenclature is one of the fundamental languages of neuroscience.<sup>2</sup> The unambiguous description of thousands of structures is made possible with an extensive number of highly specialized terms that are used to the exclusion of any other. However, a great amount of non-precise existing terminology exists. Although some reflect precious historical beliefs, non-precise terms obscure consensus between neuroscientists about the classification of neurons.

Anatomically, the nervous system can be divided into two divisions, the central and the peripheral nervous system.<sup>3</sup> The central nervous system consists of the brain, spinal cord, optic nerve and retina, and contains the majority of neural cell bodies (somata, perikarya). The peripheral nervous system consists of nerves and ganglia, and includes all nervous tissue outside the central nervous system.

Within the nervous system, a visceral component is distinguished that is termed the autonomic nervous system. It consists of neurons located within both the central and the peripheral nervous system. Visceral efferent pathways are characterized by having a sequence of at least two neurons between the central nervous system and the target structure. These are referred to as preganglionic and postganglionic neurons, respectively. The cell bodies of preganglionic neurons are located in the visceral efferent nuclei of the brainstem and spinal cord. Their axons, which are usually thinly myelinated, exit from the central nervous system and run to ganglia in the periphery, where they synapse with postganglionic neurons. The axons of postganglionic neurons are usually unmyelinated. Postganglionic neurons are more numerous than preganglionic ones, as one preganglionic neuron may synapse with 15-20 postganglionic neurons.<sup>1</sup> This architectural feature permits the wide distribution of many autonomic effects.

The pre- and postganglionic neurons have different embryonic origins. Preganglionic neurons find their origin in neuroblast cells, while postganglionic neurons are derived

from neural crest cells.<sup>3</sup> It is, however, common to label pairs of pre- and postganglionic neurons together as either sympathetic or parasympathetic. Another habit is to place the enteric neurons apart from the rest of the autonomic nervous system as the 'enteric nervous system'.

The term sympathetic has to be considered as non-precise existing terminology. The term underwent several semantic changes since its introduction, and is now often associated with the 'Fight and Flight' response (Table 1.1). Furthermore, there is no consensus about the classification of the sacral autonomic neurons as either sympathetic or parasympathetic.<sup>4-9</sup>

### Classic description of the sympathetic-parasympathetic model

In addition to physiological and pharmacological criteria, three anatomical arguments are used to define the sympathetic-parasympathetic model.<sup>3</sup> As the human spinal visceral preganglionic outflow concentrates around the T1-L2 and S2-S4 levels, the autonomic outflow does not appear as a continuous cell-column. The perceived gap in the nucleus between those levels has been one reason to place the sacral outflow apart from the thoracolumbar. The parallel between the parasympathetic cranial and sacral outflows is therefore often drawn.

A second argument involves the absence of white rami communicantes at the sacral level. In contrast to the sympathetic thoracolumbar outflow, preganglionic neurons at the sacral level bypass the sympathetic trunk. Pelvic splanchnic nerves arise, therefore, directly from the sacral plexus.

The third argument relates to the classic view of peripheral cell bodies being distributed bimodally. In this view, the sympathetic cell bodies are positioned mainly within the sympathetic trunk, close to the central nervous system. The parasympathetic cell bodies on the other hand, are positioned in a more distal position in the ganglia of the head, or in ganglia located close to the wall of thoracic, abdominal or pelvic organs.

As a result, nerves and ganglia are often assigned to either the sympathetic or parasympathetic limbs of the model. The paravertebral ganglia are better known as the sympathetic trunk ganglia. The ciliary, otic, submandibular and pterygopalatine ganglia of the head are considered parasympathetic. Typical sympathetic or parasympathetic nerves are the white and grey rami communicantes or the greater petrosal and pelvic splanchnic nerves respectively.

**Table 1.1** Origin and interpretation of the term sympathetic.

Author/Event	Origin and interpretation of the term sympathetic	Reference
Winslow (1669-1760)	Originally introduced the term 'sympathetic' and coined the terms small (CN VII), medium (CN X) and great sympathetic (sympathetic trunk) nerves, which played distinct roles in maintaining 'sympathy' between viscera	10
Miscellaneous	The adjectives 'small' and 'medium' sympathetic were rarely used. In many countries, 'great' was also dropped: sympathetic nerves became sympathetic nervous system	11
Andersch (1732-1777)	These authors tried unsuccessfully to replace the term sympathetic with 'sympatheticus maximus', 'nervus magnus harmonicus' and 'nervus consensualis magnus', respectively	12
Mayer (1747-1801)		
Wrisberg (1739-1808)		
<b>Semantic change</b>		
Langley (1852-1925)	Stated: "Sympathetic nerves have no special relation to sympathies", but retained the term in the 'autonomic nervous system'	11
Gaskell (1847-1914)	The so-called sympathetic system, is formed by the ganglion cells of 'visceral nerves' that migrate out from 'stationary' cerebro-spinal ganglia, into 'vagrant' ganglia.	13-15
Langley (1852-1925)	Introduced 'oro-anal system': "... the bulbar part of the cranial outflow and sacral outflow form one system for gut and appendages", and later: "... I placed them together as the 'parasympathetic system'"	11,16
	Although he recognized similarities in the action of drugs and sympathetic nerves, he deemed: "... it is necessary for descriptive purposes to keep to a nomenclature based on anatomy, ..."	11
<b>Semantic change</b>		
Barger (1878-1939) and Dale (1875-1968)	Shifted to a physiological interpretation: The term 'sympathomimetics' described the action of amines	17
Cannon (1871-1945)	Introduced the so called "fight or flight response" which became also known as the "sympathetic stress response"	18
1954 meeting of Physiological Society	Introduction of prefix 'ortho'. Prefixes to the term sympathetic must be interpreted physiologically rather than anatomically. Orthosympathetic is understood as 'real' sympathetic and parasympathetic now as 'distinct from' sympathetic	19
<b>Semantic change</b>		
Espinosa-Medina et al. in 2016	Reserved the terms sympathetic and parasympathetic to cluster neural cells based upon genetic make-up and topographic position of preganglionic neurons within the central nervous system	4

## Aim and outline of the thesis

In this thesis we present data on the peripheral distribution of catecholaminergic neurons, and use the outcome to re-evaluate the anatomical arguments on which the sympathetic-parasympathetic model is based.

In **chapter 2**, we describe our histological study of the putatively 'somatic' phrenic nerves. We analysed the entire left and right phrenic nerves in 30 human cadavers and established the presence of catecholaminergic ('sympathetic') fibres throughout their course. The sub-diaphragmic portion of the right phrenic nerve differed from its left counterpart, exhibiting all the features of an efferent nerve of the celiac plexus rather than being the continuation of the phrenic nerve. Within this nerve, catecholaminergic cell bodies were abundantly present. Furthermore, we discovered that this nerve innervates atrial natriuretic peptide-positive caval bodies in the wall of the inferior caval vein at the diaphragmatic level.

In **chapter 3**, we established that the cervical part of the vagus nerve also contains catecholaminergic fibres. These fibres appear to originate from the paravertebral ganglionic chains. We could demonstrate that the intracranial portions of the vagus nerves contained no catecholaminergic fibres, and had a smaller surface area compared to the cervical levels. In addition to catecholaminergic fibres, catecholaminergic cell bodies were encountered in the cervical portion of the vagus nerve.

We also addressed the question whether the vagus nerve innervates the human spleen (**chapter 4**), as it recently became apparent that both the vagus nerve and the spleen play a key role in the control of host defense by the autonomic nervous system. By analysing the entire hilum of the spleen, we could end the controversy whether or not direct cholinergic innervation of this organ exist.

**Chapter 5** represents a systematic literature search and general discussion of this thesis. We assembled all available data on the distribution of catecholaminergic neurons in the peripheral nervous system. 144 Queries identified 1.239 studies providing information on 389 anatomical structures. 168 Studies fulfilled all inclusion criteria. We found that our earlier observations are part of a structural architecture that we describe here for the first time. The characteristics of this novel architecture are as follows:

- Catecholaminergic neurons are embedded extensively in the peripheral nervous system, and are present in many spinal and all cranial nerves and ganglia. These include nerves and ganglia that are known for their parasympathetic function.

- Along the entire spinal autonomic outflow pathways, both proximal and distal catecholaminergic cell bodies are common in the head, thoracic and abdominal and pelvic region. This finding invalidates the “short versus long pre-ganglionic neuron” argument of the classical sympathetic-parasympathetic model.
- Contrary to the classically confined outflow levels T1-L2 and S2-S4, preganglionic neurons are present at the lower lumbar level, thus within the ‘lumbar gap’.
- Preganglionic cell bodies that are located in the intermediolateral zone of the thoracolumbar spinal cord, gradually nest more ventrally within the ventral motor nuclei at the lumbar and sacral levels and their fibers bypass the white ramus communicans and sympathetic trunk, to emerge directly from the spinal roots. Bypassing the sympathetic trunk, therefore, is not exclusive for the sacral outflow.

We conclude that the anatomy of the autonomic outflow displays a conserved architecture along the entire spinal axis, and that the classical anatomical arguments separating the spinal autonomic outflow in sympathetic and parasympathetic divisions do not hold up. Neurons, nerves and ganglia are therefore best labelled according to their topography. This allows one to conceive the peripheral nervous system as a connection matrix, as neurons are able to switch between nerves to establish unique connections. The concept of the connectome in the brain, therefore, also appears to apply to the peripheral nervous system.

## References

1. Squire L. *Fundamental neuroscience*. 4th ed. 2012: Academic Press.
2. F.I.P.A.T. *Terminologia Neuroanatomica* 2017.
3. Standing S. *Gray's Anatomy, The Anatomical Basis of Clinical Practice*. 41st Revised ed. 2016: Elsevier Health Sciences.
4. Espinosa-Medina I, et al. The sacral autonomic outflow is sympathetic. *Science*. 2016;354(6314): 893-897.
5. Janig W, et al. Renaming all spinal autonomic outflows as sympathetic is a mistake. *Auton Neurosci*. 2017;206:60-62.
6. Janig W, McLachlan EM, Neuhuber WL. The sacral autonomic outflow: against premature oversimplification. *Clin Auton Res*. 2018;28(1):5-6.
7. Janig W, Neuhuber W. Reclassification of the Sacral Autonomic Outflow to Pelvic Organs as the Caudal Outpost of the Sympathetic System Is Misleading. *J Am Osteopath Assoc*. 2017;117(7):416-417.
8. Neuhuber W, McLachlan E, Janig W. The Sacral Autonomic Outflow Is Spinal, but Not "Sympathetic". *Anat Rec (Hoboken)*. 2017;300(8):1369-1370.
9. Horn JP. The sacral autonomic outflow is parasympathetic: Langley got it right. *Clin Auton Res*. 2018; 28(2):181-185.
10. Winslow JB. *Exposition Anatomique de la Structure du Corps Humain*. 1732, Paris: Duprez et Desessartz.
11. Langley JN. *The autonomic nervous system, Part I*. 1921. Cambridge: W. HEFFER & SONS LTD.
12. Hyrtl J. *Onomatologia anatomica: Geschichte und Kritik der anatomischen Sprache der Gegenwart; mit besonderer Berücksichtigung ihrer Barbarismen, Widersinnigkeiten, Tropen, und grammatikalischen Fehler*. 1880, Wien: Braumüller.
13. Gaskell WH. On the structure, distribution and function of the nerves which innervate the visceral and vascular systems. *J Physiol*. 1886;7:1-80.
14. Gaskell WH. On the relation between the structure, function, distribution and origin of the cranial nerves. *J Physiol*. 1888;10(3):153-212.9.
15. Gaskell WH. On the relation between the structure, function, distribution and origin of the cranial nerves; together with a theory of the origin of the nervous system of vertebrata. *J Physiol*. 1889;10: 153-211.
16. Langley JN. The arrangement of the autonomic nervous system. *Lancet*. 1919;193(4996).
17. Barger G, Dale HH. Chemical structure and sympathomimetic action of amines. *J Physiol*. 1910;41(1-2): 19-59.
18. Cannon WB. *Bodily changes in pain, hunger, fear and rage: An account of recent researches into the function of emotional excitement*. 1915: D Appleton & Company.
19. Bynum WF. A short history of the Physiological Society 1926-1976. *J Physiol*. 1976;263(1):23-72.

# Chapter 2

The human phrenic nerve serves as a morphological conduit for autonomic neurons and innervates the caval body of the diaphragm

Thomas J.M. Verlinden, Paul van Dijk, Andreas Herrler, Corrie de Gier- de Vries,  
Wouter H. Lamers, S. Eleonore Köhler

*Scientific Reports. 2018;8(1):11697*



## Abstract

Communicating fibres between the phrenic nerve and sympathetic nervous system may exist, but have not been characterized histologically and immunohistochemically, even though increased sympathetic activity due to phrenic nerve stimulation for central sleep apnoea may entail morbidity and mortality. We, therefore, conducted a histological study of the phrenic nerve to establish the presence of catecholaminergic fibres throughout their course. The entire phrenic nerves of 35 formalin-fixed human cadavers were analysed morphometrically and immunohistochemically. Furthermore, the right abdominal phrenic nerve was serially sectioned and reconstructed. The phrenic nerve contained  $3 \pm 2$  fascicles in the neck that merged to form a single fascicle in the thorax and split again into  $3 \pm 3$  fascicles above the diaphragm. All phrenic nerves contained catecholaminergic fibres, which were distributed homogenously or present as distinct areas within a fascicle or as separate fascicles. The phrenicoabdominal branch of the right phrenic nerve is a branch of the celiac plexus and, therefore, better termed the “phrenic branch of the celiac plexus”. The wall of the inferior caval vein in the diaphragm contained longitudinal strands of myocardium and atrial natriuretic peptide-positive paraganglia (“caval bodies”) that were innervated by the right phrenic nerve.

## Introduction

The phrenic nerve arises from the anterior roots of the third to fifth cervical nerves and is known to innervate the diaphragm.<sup>1,2</sup> Accessory fibres from cervical segments that join the phrenic nerve are common and mainly originate from the subclavian nerve, the ansa cervicalis, and the sternohyoid nerve.<sup>3</sup> Communicating fibres between the sympathetic trunk and the phrenic nerve in the cervical region were already described by Luschka in 1853.<sup>4</sup> Some phrenic fibres may contribute to the cardiac plexus,<sup>5</sup> but the evidence is limited.<sup>6</sup> Communications between the phrenic nerve and the ansa subclavia, a structure known to contribute to the inferior cervical sympathetic cardiac nerve,<sup>7</sup> have been described more often.<sup>5,6,8</sup> Additionally, a continuation of the right phrenic nerve towards the aortic autonomic plexus in the abdomen, the so-called phrenicoabdominal branch, is often reported.<sup>7,9,10</sup> This branch contains one or several ganglia that stain positive for tyrosine hydroxylase (TH),<sup>11</sup> indicating catecholaminergic signal transmission.

Recently, the phrenic nerve has become the target of interventions that aim to regulate breathing patterns by electrical nerve stimulation.<sup>12</sup> An example is the treatment of central sleep apnoea.<sup>13,14</sup> For such an application of phrenic nerve stimulation, it is important to be aware of all components of the phrenic nerve, as they are also stimulated in such procedures. The presence of a catecholaminergic component within the phrenic nerve warrants particular attention when phrenic nerve stimulation is applied, because increased sympathetic activity is associated with increased mortality in patients with central sleep apnoea.<sup>15-17</sup>

The earlier descriptions of communicating branches between the phrenic nerve and the sympathetic nervous system were based on macroscopic dissections, which do not permit distinction between nerves and connective tissue strands. Furthermore, the dissectional approach does not reveal whether sympathetic (catecholaminergic) fibres are present in such communications. We, therefore, conducted a detailed histological study to establish the presence of catecholaminergic fibres in the phrenic nerve throughout its course from its cervical roots to its connection with the celiac plexus. Since phrenic nerve stimulation can be performed on both sides and at different levels of the nerve, we also looked at morphological differences along the course of the phrenic nerve and compared left and right phrenic nerves at different levels.

## Methods

Nerve tissue was harvested from thirty-five (16 female, 19 male) formalin-fixed cadavers between 58 and 101 ( $\bar{x} = 84 \pm 11$ ) years of age from the body donation program of the Department of Anatomy and Embryology, Maastricht University. The tissue donors gave their informed and written consent to the donation of their body for teaching and research purposes as regulated by the Dutch law for the use of human remains for scientific research and education (Wet op de Lijkbezorging, 1991). Accordingly, a handwritten and signed codicil from the donor posed when still alive and well, is kept at the Department of Anatomy and Embryology Faculty of Health, Medicine and Life Sciences, Maastricht University, Maastricht, The Netherlands. The bodies were preserved by intra-arterial infusion with 10 L fixative (composition (v/v): 96% ethanol (21%), glycerin (21%), 36% formaldehyde (2%), water (56%), and 2.4 g/L thymol), followed by 4 weeks of fixation in 96% ethanol (20%), 36% formaldehyde (2%) and water (78%). Samples were only taken from bodies without signs of previous surgical interventions on neck, thorax or abdomen.

### Phrenic nerve sampling

The cervical and thoracic portions of the phrenic nerve with surrounding connective tissue and accompanying pericardiophrenic vessels were collected and subdivided into levels A to I (- J on the left side), as depicted in Figure 2.1. To investigate whether an abdominal branch of the phrenic nerve extends to the celiac plexus (inset Figure 2.1), the abdominal phrenic nerves, including the part that traversed the diaphragm, were collected and embedded 'en bloc' for further histological processing. Furthermore, periarterial tissue accompanying left and right inferior phrenic arteries was collected to establish whether or not the phrenic nerve contributes to the nerve plexus accompanying the inferior phrenic arteries.

### Histological processing

All cervical and thoracic nerve samples were cut transversally into two parts. The upper parts were post-fixed overnight in 1% osmium tetroxide ( $\text{OsO}_4$ ) / phosphate-buffered saline (PBS) and then embedded in paraffin. The lower parts, the abdominal samples, and the 'en bloc' samples of diaphragm and abdominal phrenic nerve were subjected to standard paraffin embedding. Five micrometre-thick sections were prepared of all samples with a Leica 2245 microtome. Mounted sections were used for haematoxylin and eosin (HE) staining or immunohistochemistry. To determine the intradiaphragmatic course of the phrenic nerves, the 'en bloc' samples were sectioned every 250  $\mu\text{m}$

(4 sections per mm). For reconstruction, one abdominal phrenic nerve was sectioned completely into 5  $\mu$ m consecutive transverse sections resulting in 7,500 slides.

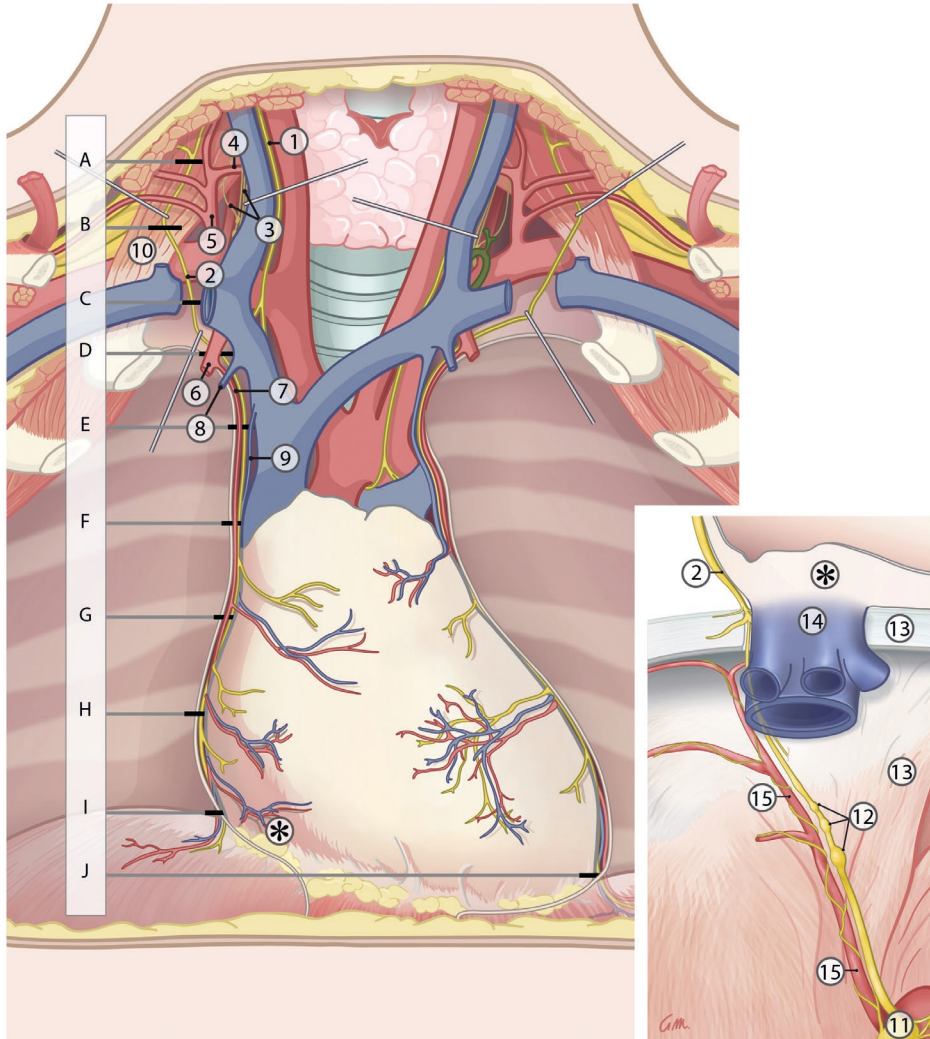


**Figure 2.1 Sampling of the phrenic nerve.** A-I indicate the sampling sites of the respective cervical and thoracic samples. J indicates the position of the extra thoracic sampling site for the left phrenic nerve. The inset shows a magnification of the peridiaphragmatic portion of the phrenic nerve (the asterisks indicate corresponding sites on the pericard). 1: Vagus nerve; 2: phrenic nerve; 3: cervical sympathetic plexus; 4: inferior thyroid artery; 5: thyrocervical trunk; 6: internal thoracic artery (cut); 7: pericardiophrenic artery; 8: internal thoracic vein; 9: pericardiophrenic vein; 10: anterior scalene muscle; 11: celiac ganglion and plexus; 12: phrenic ganglia; 13: diaphragm; 14: inferior caval vein; 15: inferior phrenic artery. Note the connection between the right phrenic nerve and the celiac autonomic nerve plexus. Illustration drawn by Greet Mommen.

To determine the surface area of catecholaminergic nerve fibres, antibodies against tyrosine hydroxylase (TH; 1:1,000, Abcam AB112, Cambridge, UK) and dopamine  $\beta$ -hydroxylase (DBH; 1:150, Abcam AB109112) were used. Antibodies against protein gene product 9.5 (PGP9.5; 1:100, Biotrend APG0714, Cologne, Germany) (a ubiquitin C-terminal hydroxylase, highly specific for neurons), S100 protein (S100; 1:1,000, Dako Z0311, Glostrup, Denmark) (used for identifying axons and dendrites), choline acetyltransferase (ChAT; 1:50, Merck, AB144P, Darmstadt, Germany) and vesicular acetylcholine transporter (VACHT) (1:2,000, MBL-Sanbio BMP 048, Japan) were used to determine the surface area of (cholinergic) nerve tissue. The antibody against natriuretic peptide A (NPPA) was purchased from Campro Scientific (RGG 9103, Veenendaal, The Netherlands; 1:200). For the detection of cardiac muscle tissue, a SERCA2a antiserum that was raised in rabbits against the BSA-coupled C terminal SERCA2a peptide NYLEPAILE (1:1,000) was used.<sup>18</sup>

Complete images of selected large slides were digitized with an Olympus BX61 scanning microscope and the DOTSLIDE program (Olympus, Zoeterwoude, The Netherlands). AMIRA software (version 6.0; base package; FEI Visualization Sciences Group Europe, Mérignac Cédex, France) was used to generate 3D reconstructions after image loading, alignment and segmentation<sup>19</sup>.

### Morphometric analysis

Slides were photographed with a Leica (type DMRD) photomicroscope.<sup>20</sup> Surface areas of myelinated axons, specifically stained axons, and the entire surface of the nerve within the perineurium, including its supporting tissue, were measured with Leica Qwin v.3.5.1 analysis software at 10x magnification. Furthermore, the number of nerve fascicles was counted. Two persons independently determined whether staining exceeded background levels. The average of these values was used as threshold.

Statistical analysis was performed with Graphpad Prism v6.0 software. Data were tested for normality with the Shapiro-Wilk normality test. Comparisons were made by Student's t-tests and one-way ANOVA followed by Bonferroni post-hoc tests. Data are presented as means  $\pm$  SD. Individually presented data are displayed after Savitzky-Golay filtering. P-values  $<0.05$  were considered as statistically significant.

## Results

### Cervical and thoracic findings

#### *Surface area measurements*

Nineteen cadavers were analysed. The mean surface area of the right and left nerves excluding epi- and perineurium was  $0.35 \pm 0.02$  and  $0.29 \pm 0.01$  mm<sup>2</sup>, yielding diameters of 1.2 and 1.1 mm, respectively. No significant differences in surface area along the proximo-distal course of the nerve were observed for either the right or left nerve ( $P \geq 0.71$ ). Furthermore, no significant differences in surface area between corresponding levels of the left and right nerves were detected (all  $P \geq 0.09$ ).

#### *Myelination*

Myelinated neurons occupied  $26 \pm 1\%$  and  $29 \pm 1\%$  of the total surface areas of the right and left nerves, respectively. No significant differences in myelination were observed along the proximo-distal course of the right and left nerve ( $P \geq 0.10$ ), or between corresponding levels of the right and left nerves (all  $P \geq 0.35$ ).

#### *Fascicles*

In the cervical area, the phrenic nerves contained  $3 \pm 2$  fascicles (as defined by having a distinct perineurium; range: 1-10 fascicles; Figures 2.2A,B and 2.3A,B) that merged to form the single fascicle usually seen in the thorax (range: 1-4; Figures 2.2C and 2.3A). Just cranial to the diaphragm the number of fascicles increased to  $3 \pm 3$  (range 1-9; Figure 2.3A,B). No significant differences were found between left and right phrenic nerves (all  $P \geq 0.08$ ).

#### *Expression of Tyrosine Hydroxylase*

Tyrosine hydroxylase (TH)-positive fibres were found in all phrenic nerves studied (Figure 2.2D), occupied  $1.6 \pm 0.5$  and  $2.0 \pm 0.6$  % of the total nerve surface area of the right and left nerves, respectively, and were present in the nonmyelinated areas (Figure 2.2C). The size of the TH-positive areas was similar along the proximo-distal course of the nerve for both the right ( $P=0.63$ ) and left nerves ( $P \geq 0.63$ ), and between corresponding levels of the left and right nerves (all  $P \geq 0.09$ ).

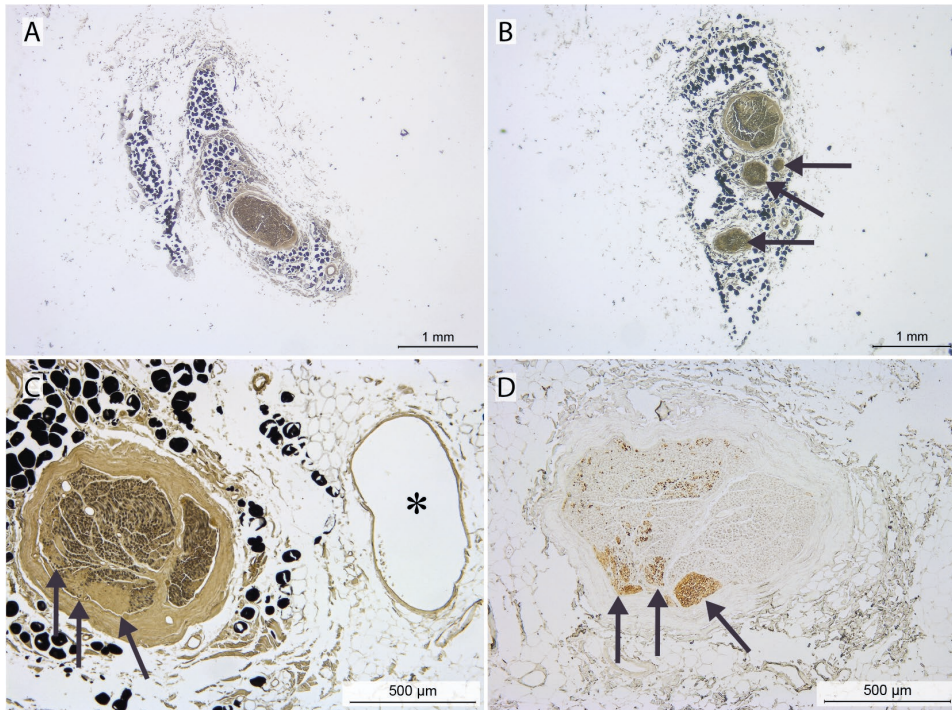


**Figure 2.2 Morphological characteristics of the phrenic nerve in neck and thorax: A-C: osmium-tetroxide staining.** Black dots represent osmium-stained adipocytes within the epineurium. D: Tyrosine Hydroxylase (TH) staining. A-C show the phrenic nerve as: a single fascicle at cervical sampling site C (A); several fascicles (arrows) in the cervicothoracic transition area at sampling site D (B); or a single fascicle at thoracic sampling site E (C). Note the close relationship of the phrenic nerve with the pericardiophrenic vein (indicated by asterisk). D: adjacent section of C, stained for the presence of TH (arrows). Note that TH-positive areas are  $\text{OsO}_4$ -negative (arrows).

#### *TH-positive fibres and fascicles*

TH-positive fibres were either distributed homogeneously or presented as distinct areas or fascicles within the phrenic perineurium or epineurium, respectively (Figure 2.3D).

The distinct areas were seen most frequently in the left and right cervical and the right thoracic region just above the diaphragm (Figure 2.3C).

## Findings near the diaphragm

### *Intradiaphragmatic course of the phrenic nerves*

The course of the right phrenic nerve along the foramen of the inferior caval vein was analysed in 4 cadavers on transverse sections of ~5 cm diameter (Figure 2.4A,B). The branching pattern of the phrenic nerve was irregular, with TH-positive branches accompanying the motor nerve. The intradiaphragmatic course of the left phrenic nerve was also analysed in 4 cadavers (Figure 2.4D-F) and was similar to that of the right phrenic nerve, except that TH-positive fibres were completely absent (Figure 2.4E,F).

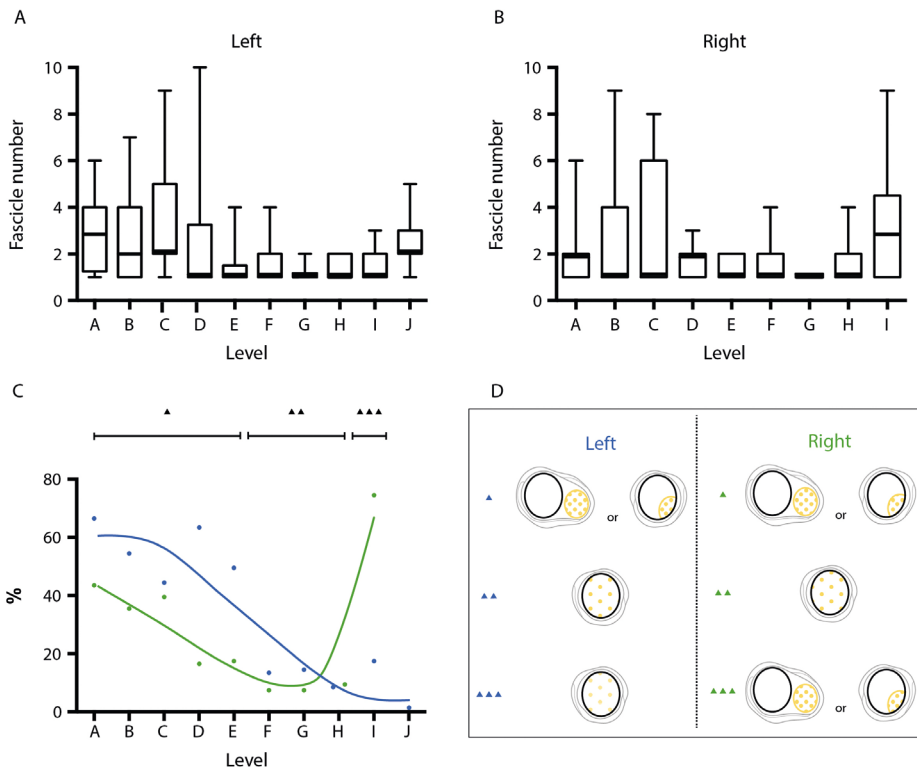


**Figure 2.3** (Tyrosine hydroxylase-positive-) Fibres and fascicles within the phrenic nerve at the different levels. A, B: Number of fascicles. Median, first and third quartile, and range are shown as boxplots, A left and B right phrenic nerve. C: Percentage of TH-positive fibres (blue: left, green: right) presenting as distinct fascicles or as distinct areas within the phrenic perineurium or epineurium, respectively (most often seen between levels A and E, and on the right side only at level I) as opposed to a homogenous distribution of TH-positive fibres (most often seen between levels F and J except for level I on the right side; for levels confer Fig. 1). Triangles in C and D are corresponding to the levels, with one triangle indicating levels A-E, two triangles levels F-H and 3 triangles levels I-J, respectively. Illustration drawn by Greet Mommen.



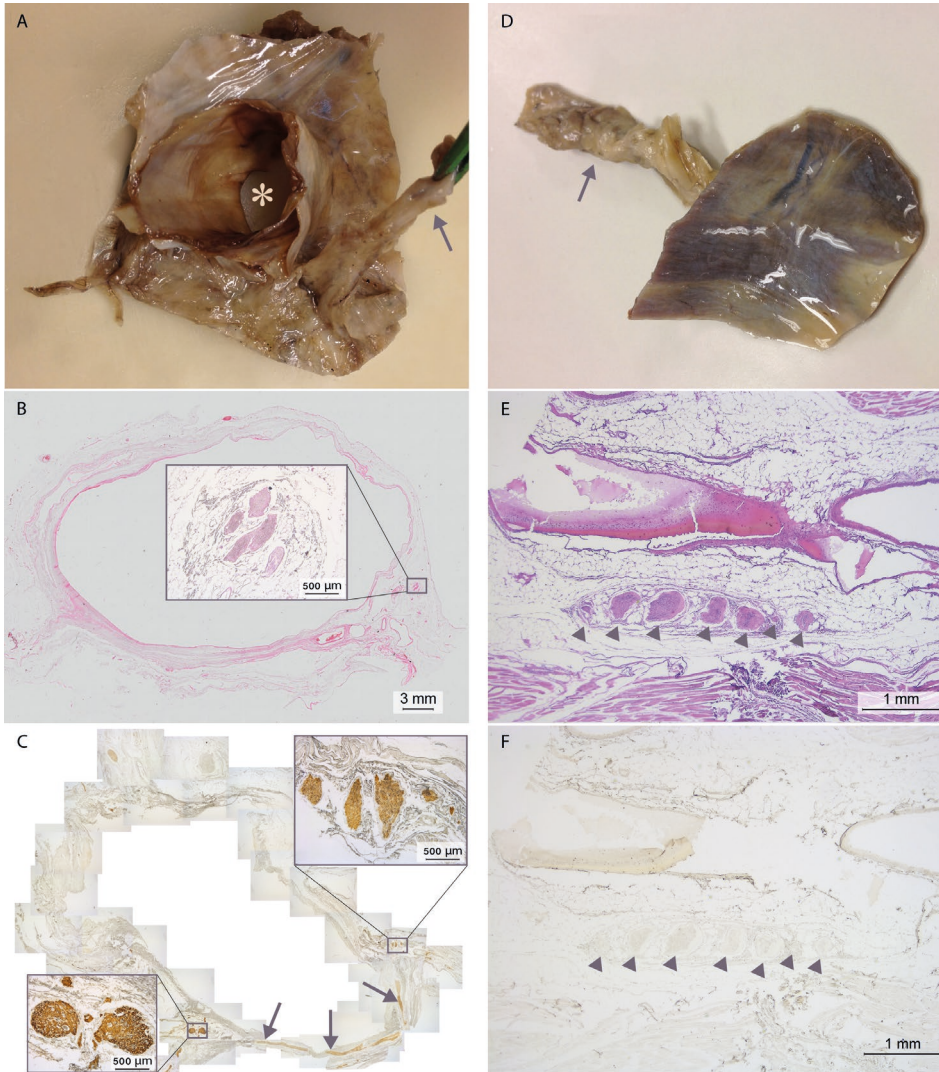


**Figure 2.4** Intradiaphragmatic course of the left and right phrenic nerves. A-C: right phrenic nerve passing through the foramen of the inferior caval vein. A: Macroscopic sample, cranial view showing the phrenic nerve (arrow), the inferior caval vein (asterisk) and a part of the surrounding diaphragm. B: HE staining of a section of the caval vein shown in A, with a magnification of the phrenic nerve consisting of several branches shown in the inset. C: S-100 staining to show the nervous connection (arrows) between the phrenic nerve (magnification shown in inset on the right) and caval body (magnification shown in inset on the left (see also Fig. 5)). D-F: left phrenic nerve passing through the left dome of the diaphragm. D: macroscopic sample with left phrenic nerve (arrow), caudal view. E: HE-stained section of the sample containing several branches of the phrenic nerve (arrows). F: TH-staining of a serial section of E. Note the absence of TH-positive fibres in this part of the phrenic nerve.

### *Caval bodies*

In the wall of the inferior caval vein of the 4 cadavers studied, we identified a total of eight tangled structures (Figures 2.4C, lower left inset and 5) that contained an extensive venous plexus surrounding large cell bodies with granular inclusions (Figure 2.5 inset) and a network of nerve fibres (Figures 2.5 and 2.6A,B) originating from the right phrenic nerve on the opposite side (Figure 2.4C). Although the large cells morphologically resembled neural cell bodies, only a fraction stained positive for PGP9.5 (Figure 2.6C) or TH (Figure 2.6D). Neither VAcHT- or ChAT-positive cells were observed (Figure 2.6F). Many of the large cells bordering the veins (Figure 2.5 inset) contained atrial natriuretic peptide (NPPA)-positive granules (Figure 2.6E). The phenotypic characteristics of these structures resemble those of paraganglia.<sup>21</sup> For this reason, we have named them “caval bodies”.

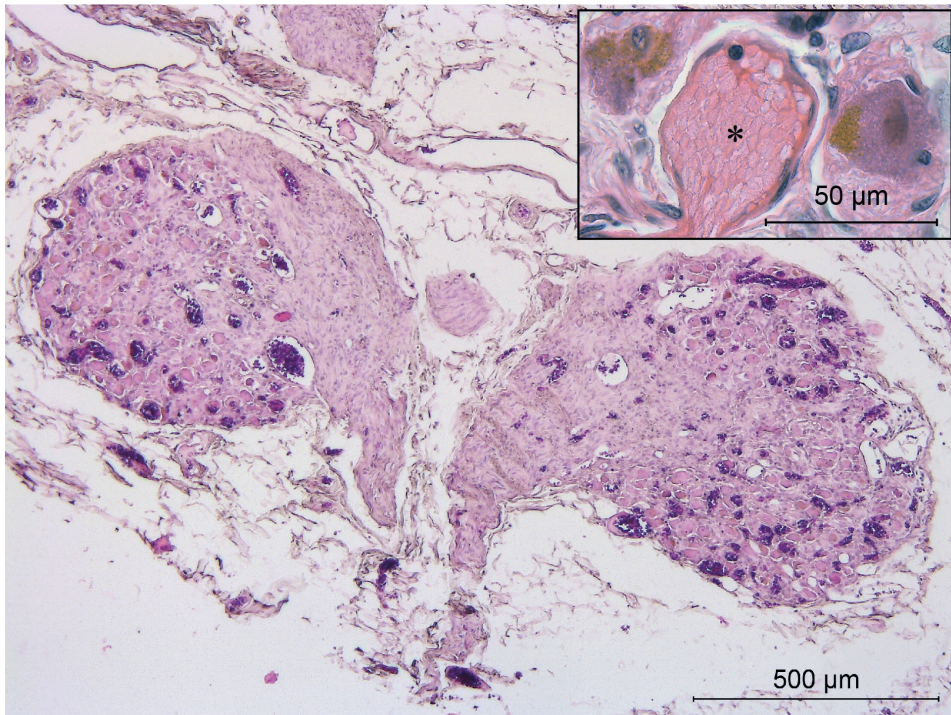


**Figure 2.5** **Caval body at the level of the diaphragm.** A: The body consists of nerve fibres (pink), an extensive venous plexus (dark purple), and large cells containing NPPA-positive granules (magnification of a caval body from another specimen is shown in inset, where NPPA-positive cells flank a venule (asterisk)).

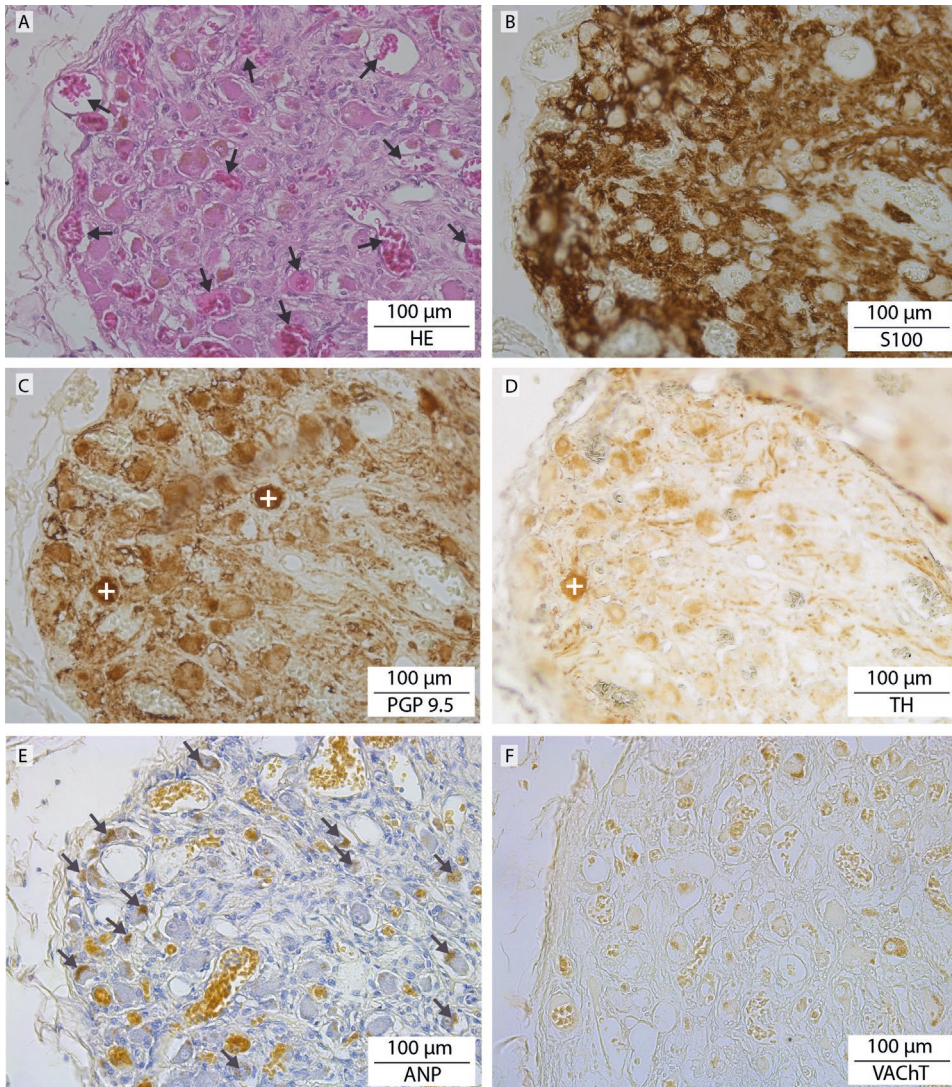


**Figure 2.6 Staining characteristics of a caval body.** Serial sections showing a magnified area of the section shown in Figure 2.5. Note the extensive venous plexus surrounding cells (A, HE; arrows), abundant nerve fibres (B, S100), scarce, strongly PGP 9.5-positive (C; +) and TH-positive cells (D; +) that only partly overlap, and abundant NPPA-positive non-neural cells (E; arrows identify intracellular granules; cf. Figure 2.5B). No VAcHT-positive staining was observed (F) (visible are some cellular pigments).

### *Myocardial muscle sleeves*

In 3 of the 4 cadavers, the wall of the inferior caval vein inside the diaphragm contained longitudinal strands of myocardium that stained positive for  $\alpha$ -smooth muscle actin and SERCA2a (Supplemental Figure S2.1).

## Findings within the abdomen

### *Abdominal course and characteristics of the right phrenic nerve*

The abdominal course of the right phrenic nerve was studied in 5 cadavers. Textbooks indicate that the nerve extends all the way to the phrenic ganglia in the periphery of the celiac plexus.<sup>7</sup> We tested this assumption by sectioning the abdominal portion of the nerve of one cadaver from the diaphragm to the caudal-most of the phrenic ganglia, (7,500 sections of 5  $\mu$ m each; Figure 2.7A-H). A 3D reconstruction of these sections (Fig. 7I) revealed that the phrenic nerve (Figure 2.7A,I (brown)) split into two main, myelinated branches that innervated the diaphragm (Figure 2.7B). A TH-positive autonomic fascicle presented as a third, separate branch distal to this level and extended all the way to the celiac ganglion (Figure 2.7C-H). We, therefore, named this branch the phrenic branch of the celiac plexus. Of note, the diameter of the branch excluding the ganglia increased towards the celiac ganglion (Figure 2.7J) and was interspersed with neuronal cell bodies (Figure 2.7E,F,H) that stained positive for PGP9.5, TH and dopamine  $\beta$ -hydroxylase DBH (see Supplemental Figure S2.2).

### *Left and right peri-arterial nerve plexuses of the inferior phrenic artery*

Nerve plexuses that accompany the left and right inferior phrenic arteries were studied in 5 cadavers and found to consist of small, purely TH-positive branches in the tunica adventitia. These plexuses, therefore, do not resemble the phrenic branch of the celiac plexus (see Supplemental Figure S2.3).

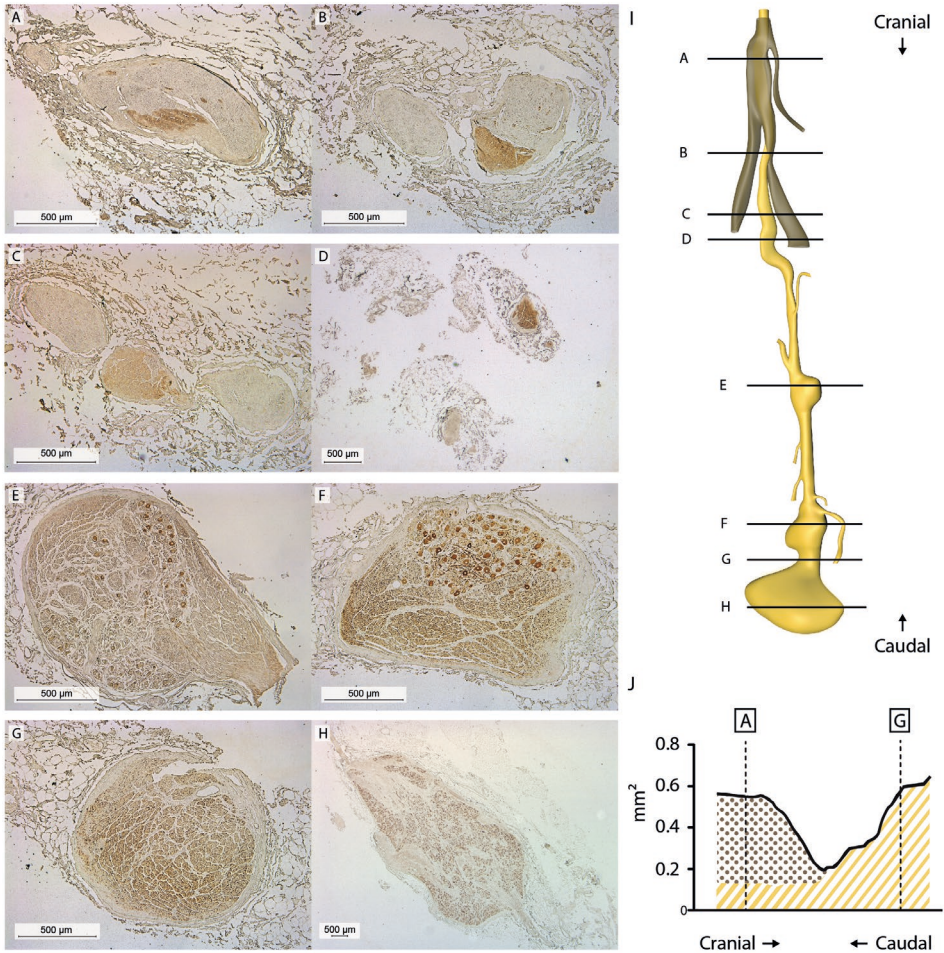


**Figure 2.7 Reconstruction of abdominal portion of the phrenic nerve.** 7,500 Sections were sampled every 5 µm. A-H: TH-stained sections corresponding to the levels depicted in the reconstruction shown in I (brown: phrenic nerve branches; yellow: phrenic branch of celiac plexus). Phrenic ganglia were found at sites E, F and H. J: Surface area measurements of the phrenic nerve (brown) and phrenic branch of the celiac plexus (yellow; without ganglia). Illustration drawn by Greet Mommen.

## Discussion

In this study, we have characterized both phrenic nerves in man with respect to fascicles, fibre composition and myelination. We demonstrate that the phrenic nerve also serves

as a conduit for catecholaminergic fibres and that the phrenicoabdominal branch of the right phrenic nerve is, instead, a branch of the celiac plexus. The “phrenic branch of the celiac plexus” is, therefore, a more appropriate name for this nerve. In addition, we report the presence of paraganglia (“caval bodies”) and myocardial sleeves in the wall of the inferior caval vein at the level of the diaphragm. The caval bodies were innervated by the right phrenic nerve.

### Morphological characterization of the left and right phrenic nerve

Our data show that the thoracic phrenic nerve generally consists of a single fascicle, which arises from the fusion of several cervical fascicles, and diverges into several fascicles again near the diaphragm. In agreement with an earlier ultrasound study at the cervical level,<sup>22</sup> we found comparable diameters for the left and right human phrenic nerves throughout their course. A small (N=2) electron-microscopic (EM) study of the phrenic nerve of the rat at the level of the entrance of the inferior caval vein into the right atrium revealed that the right phrenic nerve contained ~30% more axons than its left counterpart.<sup>23</sup>

### TH positive fibres and fascicles

Communicating nerve fibres of the phrenic nerve have been described macroscopically for the somatic subclavian and sternohyoid nerves, the ansa cervicalis, the accessory, supraclavicular, suprascapular and hypoglossal nerves<sup>3</sup> and the vagus nerve.<sup>24</sup> Communicating fibres with sympathetic nerves include the subclavian ansa, the cervical sympathetic trunk (including the middle and stellate ganglion), and the splanchnic nerves.<sup>5,6,8,24-30</sup> These fibres were also observed in other species<sup>27,29,31,32</sup> and hypothesized to be vasoregulators of the diaphragmatic vessels.<sup>27,33</sup>

This study histologically validates the presence and composition of TH positive communicating nerve fibres between the right phrenic nerve and celiac plexus (see further). In the supradiaphragmatic part of the right phrenic nerve, the TH positive fibres are present as distinct fascicles or as distinct areas within the phrenic perineurium or epineurium, respectively. Such distinct TH positive areas were only seen in the right phrenic nerve just above the diaphragm, but also in both phrenic nerves in the cervical region. Therefore, we hypothesize that TH-positive fascicles form communications with nearby nerves or organs in this area too.

## Abdominal course and characteristics of the right phrenic nerve

Previous gross-anatomy reports suggest that the phrenic nerve continues on the abdominal side of the diaphragm to the phrenic ganglia.<sup>7,9,10</sup> This branch is classically described as the 'phrenicoabdominal branch of the right phrenic nerve'.<sup>34</sup> Our 3D reconstruction of the right phrenic nerve and analysis of the composition of the left phrenic nerve revealed that the phrenic nerve motor branches do not continue beyond the diaphragm. Instead, the right phrenic nerve continues as a completely catecholaminergic nerve branch that, based on its increasing diameter, arises from the celiac ganglia and is, therefore, more appropriately termed the 'phrenic branch of celiac plexus'. TH- and DBH-positive cell bodies were encountered throughout the phrenic branch of celiac plexus, that is, also outside the two macroscopically visible ganglia that are classically described.<sup>9,11</sup> Based on these findings, we conclude that the phrenic motor nerve innervates the diaphragm, but also serves as a conduit for the peripheral autonomic nervous system. The absence of catecholaminergic fibres in the intradiaphragmatic part of the left phrenic nerve emphasizes the asymmetry of the distribution of the autonomic fibres. We hypothesize that this asymmetry corresponds with the presence of paraganglia in the wall of the (right-sided) inferior caval vein (see next paragraph).

## Paraganglia at the level of the diaphragm

An unexpected finding in this study was the identification of paraganglia in the wall of the inferior caval vein where it passed the diaphragm. Based on their morphological appearance, the extensive venous network around NPPA-positive cells and the rich innervation by fibres arising from the phrenic nerve, we hypothesize that these structures have a neuroendocrine function like paraganglia elsewhere. Fibres of the phrenic nerve encircling the inferior caval vein have also been described in the foetus.<sup>35</sup> The presence of NPPA-positive granules further suggests that these cells have a role in regulating plasma volume in a similar manner as NPPA-containing cardiomyocytes. By analogy to the vagal B-type atrial receptors,<sup>36</sup> which monitor central venous pressure as stretch of the atrial wall, the phrenic or autonomic nerve endings could act as low-pressure receptors for the central venous pressure. As elsewhere,<sup>37</sup> the NPPA-positive cells could be under efferent catecholaminergic neural control. It would be interesting to investigate whether right phrenic nerve stimulation affects plasma levels of NPPA (fragments) and influences volume homeostasis. Blood pressure management is a key element in the treatment of patients suffering from HF and many other conditions.

Further characterization of these neuroendocrine structures is desirable, since neuroendocrine, chemosensory and neuroimmunomodulatory functions exist in other paraganglia like the carotid body.<sup>21</sup>

### Myocardial muscle strands

Another unexpected finding was the presence of longitudinal cardiac muscle strands in the wall of the inferior caval vein. A caval sphincter supplied by the right phrenic nerve is a well-known feature of diving mammals.<sup>38</sup> However, this sphincter is usually described as consisting of striated skeletal muscle that is continuous with the diaphragm.<sup>38</sup> The expression of  $\alpha$ -smooth muscle actin indicates that the myocardium in these strands is poorly differentiated.<sup>39</sup> Myocardial 'sleeves' with such properties have also been described in pulmonary veins and at the base of the pulmonary trunk, where their presence can establish extranodal pacemaker activity.<sup>40</sup>

### Clinical implications

We observed myelinated and non-myelinated nerve fibres in both phrenic nerves without differences between left and right or along the proximo-distal course of the nerves. Such information is important for nerve stimulation, because myelinated nerve fibres have a much lower amplitude-duration threshold upon nerve stimulation than non-myelinated fibres.<sup>41,42</sup> Typical stimulation protocols for (transvenous) phrenic nerve stimulation can vary up to a hundred-fold in intensity (0.1-10 mA), 5-fold in duration (60-300  $\mu$ s) and 2-fold in frequency (20-40 Hz).<sup>13</sup> If applied for central sleep apnoea, the stimulation should target the myelinated fibres and should, therefore, be accomplished with the lowest possible amplitude-duration thresholds that result in the intended rhythmic activation of the diaphragm. This is necessary to prevent any undesired stimulation of the nonmyelinated catecholaminergic fibres that are also present within the phrenic nerve. This concern is relevant, because (direct) electric stimulation of the right subclavian ansa did elevate noradrenaline and cAMP concentrations in plasma harvested in the coronary sinus of dogs.<sup>43</sup> Such a catecholaminergic stimulation of the heart may, therefore, further increase the chronic upregulation of sympathetic activity that is already present in patients with central sleep apnoea<sup>44,45</sup> and that is associated with increased mortality these patients.<sup>15-17</sup>



## References

- 1 Galen C. On the Usefulness of the Parts of the Body (De Usu Partium). Translated from the Greek with an introduction and commentary by Margaret Tallmadge May. Vol. Book XIII, Chap. 5 (Ithaca, N.Y., Cornell University Press, 1968).
- 2 Mendelsohn AH, et al. Cervical variations of the phrenic nerve. *Laryngoscope* 2011;121:1920-1923.
- 3 Loukas M, Kinsella CR, Jr, Louis RG, Jr, Gandhi S, Curry B. Surgical anatomy of the accessory phrenic nerve. *Ann Thorac Surg* 2006;82:1870-1875.
- 4 Luschka H. Der nervus phrenicus des menschen; eine monographie. (Laupp, 1853).
- 5 Mitchell GA. The innervation of the heart. *Br Heart J* 1953;15:159-171.
- 6 Than M, Dharap AS. Variations in the formation of the cardiac plexus--a study in human fetuses. *Z Morphol Anthropol* 1996;81:179-188.
- 7 Standing S. *Gray's Anatomy*. (Elsevier Health Sciences, 2008).
- 8 Paturet. *Traité d'anatomie humaine, Tome IV: Système nerveux*. (Masson, Paris, 1964).
- 9 Rusu MC. Considerations on the phrenic ganglia. *Ann Anat* 2006;188:85-92.
- 10 Robinson B. in *The abdominal and pelvic brain* Ch. XII, 121 (Frank S. Betz company, 1907).
- 11 Tubbs RS, et al. Immunohistochemical study of the phrenic ganglion. *Anat Sci Int* 2008;83:159-161.
- 12 Judson JP, Glenn WW. Radio-frequency electrophrenic respiration. Long-term application to a patient with primary hypoventilation. *JAMA* 1968;203:1033-1037.
- 13 Abraham WT, et al. Phrenic nerve stimulation for the treatment of central sleep apnea. *JACC Heart Fail* 2015;3:360-369.
- 14 Zhang X, et al. Safety and feasibility of chronic transvenous phrenic nerve stimulation for treatment of central sleep apnea in heart failure patients. *Clin Respir J* 2017;11(2):176-184.
- 15 Brunner-La Rocca HP, Esler MD, Jennings GL, Kaye DM. Effect of cardiac sympathetic nervous activity on mode of death in congestive heart failure. *Eur Heart J* 2001;22:1136-1143.
- 16 Kaye DM, et al. Adverse consequences of high sympathetic nervous activity in the failing human heart. *J Am Coll Cardiol* 1995;26:1257-1263.
- 17 Cohn JN, et al. Plasma norepinephrine as a guide to prognosis in patients with chronic congestive heart failure. *N Engl J Med* 1984;311:819-823.
- 18 Moorman AF, et al. Presence of functional sarcoplasmic reticulum in the developing heart and its confinement to chamber myocardium. *Dev Biol* 2000;223:279-290.
- 19 Hikspoors JP, et al. Development of the human infrahepatic inferior caval and azygos venous systems. *J Anat* 2015;226:113-125.
- 20 Verlinden TJ, Rijkers K, Hoogland G, Herrler A. Morphology of the human cervical vagus nerve: implications for vagus nerve stimulation treatment. *Acta Neurol Scand*. 2016;133(3): 173-182.
- 21 Kumar P, Prabhakar NR. Peripheral chemoreceptors: function and plasticity of the carotid body. *Compr Physiol* 2012;2:141-219.
- 22 Canella C, et al. Anatomical study of phrenic nerve using ultrasound. *Eur Radiol* 2010;20:659-665.
- 23 Song A, Tracey DJ, Ashwell KW. Development of the rat phrenic nerve and the terminal distribution of phrenic afferents in the cervical cord. *Anat Embryol (Berl)* 1999;200:625-643.
- 24 Muller Botha GS. The anatomy of phrenic nerve termination and the motor innervation of the diaphragm. *Thorax* 1957;12:50-56.
- 25 Caliot P, Bousquet V, Cabanie P, Midy D. The nerve loops crossing below the subclavian artery and their anatomical variations. *Anat Clin* 1984;6:209-213.
- 26 Aoyagi T. Zur histologie des n. phrenicus des Zwerchfells und der motorischen nervenendigungen in demselben. *Mitt. med. Fak. Tokyo* 1913;10:233.
- 27 Balkowiec A, Szulczyk P. Properties of postganglionic sympathetic neurons with axons in phrenic nerve. *Respir Physiol* 1992;88:323-331.
- 28 Felix W. Anatomische, experimentelle und klinische Untersuchungen über den Phrenicus und über die Zwerchfellinnervation. *Deut Zeit f Chir* 1922;171.
- 29 Baluk P, Gabella G. Innervation of the guinea pig trachea: a quantitative morphological study of intrinsic neurons and extrinsic nerves. *J Comp Neurol* 1989;285:117-132.

- 30 Merkel FS. Die anatomie des menschen. (Bergmann, 1918).
- 31 Mills E. Activity of aortic chemoreceptors during electrical stimulation of the stellate ganglion in the cat. *J Physiol* 1968;199:103-114.
- 32 Langford LA, Schmidt RF. An electron microscopic analysis of the left phrenic nerve in the rat. *Anat Rec* 1983;205:207-213.
- 33 Kuré KaSM. Trophischer Einfluß des Sympathikus auf das Zwerchfell. *Z. ges. exp. Med.* 1922;26:190.
- 34 F.C.o.A.T. Terminologia anatomica: International anatomical terminology. (Thieme Publishing Group, 2011).
- 35 Pearson AA, Sauter RW. Observations on the phrenic nerves and the ductus venosus in human embryos and fetuses. *Am J Obstet Gynecol* 1971;110:560-565.
- 36 Paintal AS. A study of right and left atrial receptors. *J Physiol* 1953;120:596-610.
- 37 Luchner A, Schunkert H. Interactions between the sympathetic nervous system and the cardiac natriuretic peptide system. *Cardiovasc Res* 2004;63:443-449.
- 38 Harrison RJ, Tomlinson JDW. Observations on the venous system in certain Pinnipedia and Cetacea. *Proceedings of the Zoological Society of London* 1956;126:205-233.
- 39 Ya J, et al. Expression of the smooth-muscle proteins alpha-smooth-muscle actin and calponin, and of the intermediate filament protein desmin are parameters of cardiomyocyte maturation in the prenatal rat heart. *Anat Rec* 1997;249:495-505.
- 40 Roux N, Havet E, Mertl P. The myocardial sleeves of the pulmonary veins: potential implications for atrial fibrillation. *Surg Radiol Anat* 2004;26:285-289.
- 41 Groves DA, Brown VJ. Vagal nerve stimulation: a review of its applications and potential mechanisms that mediate its clinical effects. *Neurosci Biobehav Rev* 2005;29:493-500.
- 42 Mollet L, et al. Intensity-dependent modulatory effects of vagus nerve stimulation on cortical excitability. *Acta Neurol Scand* 2013;128:391-396.
- 43 Loukas M, Zhan XL, Tubbs RS, Mirchandani D, Shoja MM. The ansa subclavia: a review of the literature. *Folia Morphol (Warsz)* 2008;67:166-170.
- 44 Pepper GS, Lee RW. Sympathetic activation in heart failure and its treatment with beta-blockade. *Arch Intern Med* 1999;159:225-234.
- 45 Naughton MT, et al. Effects of nasal CPAP on sympathetic activity in patients with heart failure and central sleep apnea. *Am J Respir Crit Care Med* 1995;152:473-479.

Supplemental materials

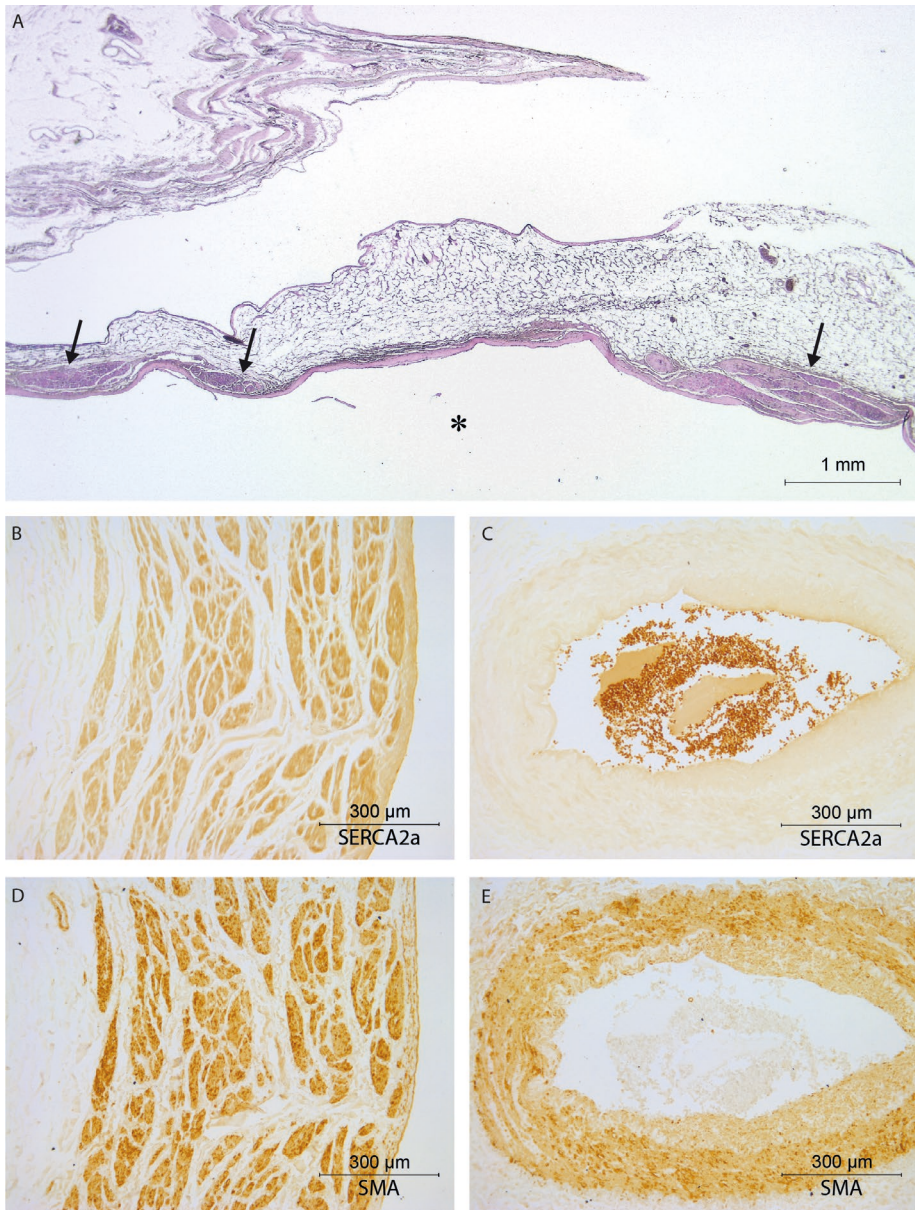


**Figure S2.1 Myocardial strands.** A: HE: Clustered, longitudinally arranged cardiac muscle fibres residing in the wall of the inferior caval vein (arrows) (lumen of inferior caval vein indicated by asterisk). B: SERCA2-positive staining of myocardial strands. C: SERCA2a-negative staining of adjacent arterial smooth muscle wall. D: SMA-positive staining of myocardial strands. E: SMA-positive staining of adjacent arterial smooth muscle wall.

The human phrenic nerve serves as a morphological conduit for autonomic nerves

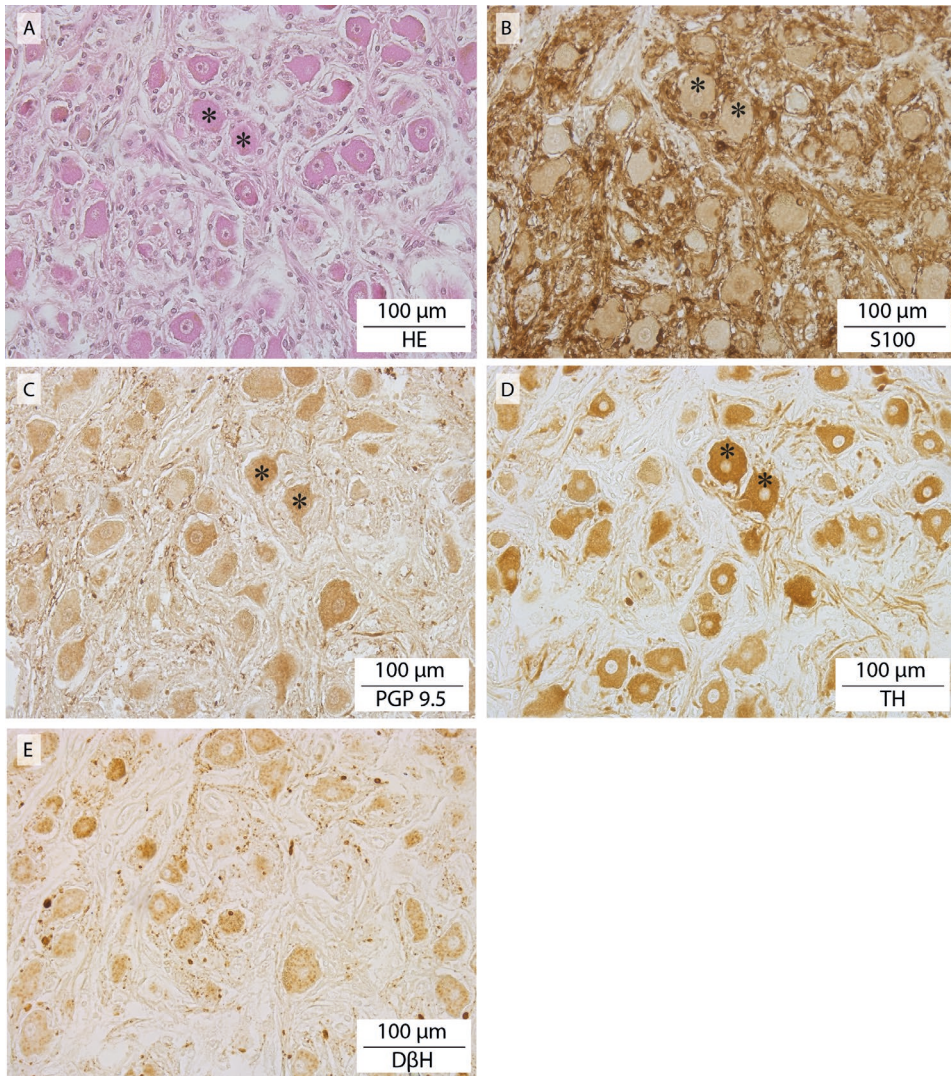


**Figure S2.2** Ganglion in the phrenic branch of the celiac plexus. Serial sections stained with A: HE; B: S-100; C: PGP.9.5; D: TH; and E: DβH. Identical cells are indicated with an asterisk.

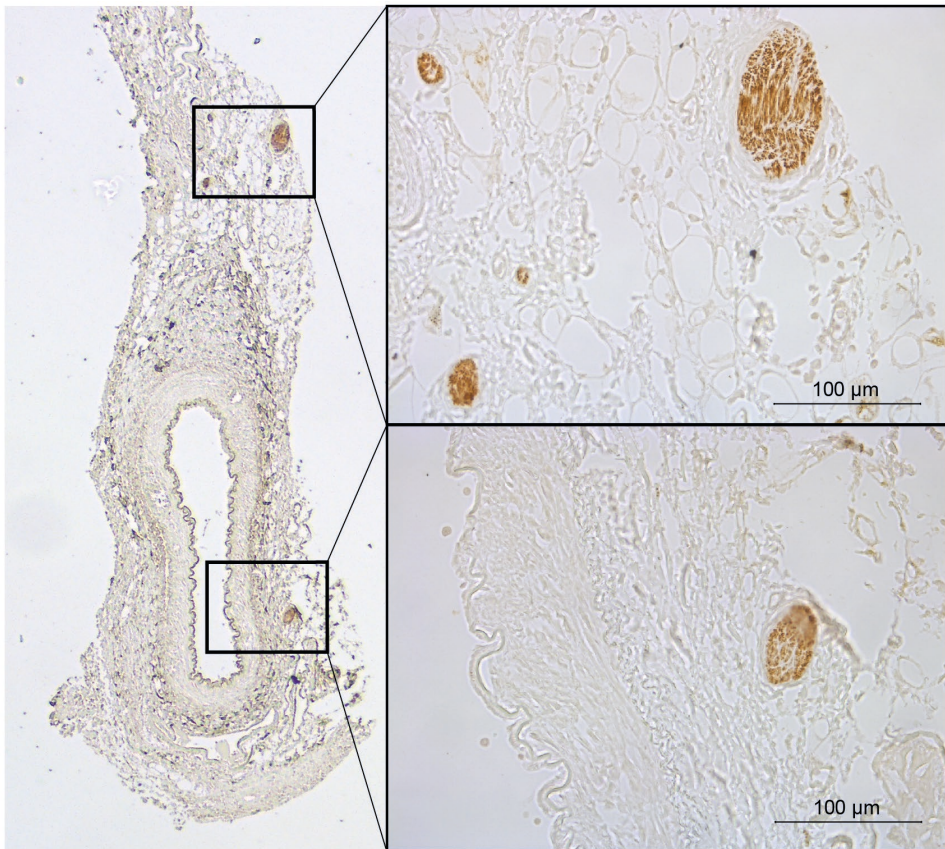


**Figure S2.3** Peri-arterial nerve plexus of the inferior phrenic artery. Left inferior phrenic artery stained for the presence of TH.

# Chapter 3

Morphology of the human cervical vagus nerve:  
Implications for vagus nerve stimulation treatment

Thomas J.M. Verlinden, Kim Rijkers, Govert Hoogland, Andreas Herrler

*Acta Neurologica Scandinavica. 2016. 133(3): 173-182*

## Abstract

### Objectives

The vagus nerve has gained a role in the treatment of certain diseases by use of vagus nerve stimulation (VNS). This study provides detailed morphological information regarding the human cervical vagus nerve at the level of electrode implant.

### Results

Eleven pairs of cervical vagus nerves and four pairs of intracranial vagus nerves were analyzed by use of computer software. It was found that the right cervical vagus nerve has an 1.5 times larger effective surface area on average than the left nerve ( $1,089,492 \pm 98,337 \mu\text{m}^2$  vs.  $753,915 \pm 102,490 \mu\text{m}^2$  respectively ( $P < 0.05$ )) and that there is broad spreading within the individual nerves. At the right side, the mean effective surface area at the cervical level ( $1,089,492 \pm 98,337 \mu\text{m}^2$ ) is larger than at the level inside the skull base ( $630,921 \pm 105,422$ ) ( $P < 0.05$ ). This could imply that the vagus nerve receives anastomosing and 'hitchhiking' branches from areas other than the brainstem. Furthermore, abundant tyrosine hydroxylase (TH) and dopamine  $\beta$  hydroxylase (DBH) positive staining nerve fibres could be identified, indicating catecholaminergic neurotransmission. In 2 out of 22 cervical nerves, ganglion cells were found that also stained positive for TH and DBH. Stimulating the vagus nerve may therefore induce the release of dopamine and noradrenaline. A sympathetic activation could therefore be part of mechanism of action of VNS. Furthermore, it was shown that the right cervical vagus nerve contains on average 2 times more TH positive nerve fibres than the left nerve ( $P < 0.05$ ), a fact that could be of interest upon choosing stimulation side. We also suggest that the amount of epineurial tissue could be an important variable for determining individual effectiveness of VNS, because the absolute amount of epineurial tissue is widely spread between the individual nerves (ranging from  $2,090,000 \mu\text{m}^2$  to  $11,683,000 \mu\text{m}^2$ ).

### Conclusions

We conclude by stating that one has to look at the vagus nerve as a morphological entity of the peripheral autonomic nervous system, a composite of different fibres and (anastomosing and hitchhiking) branches of different origin with different neurotransmitters, which can act both parasympathetic and sympathetic. Electrically stimulating the vagus nerve therefore is not the same as elevating the 'physiological parasympathetic tone', but may also implement catecholaminergic (sympathetic) effects.

## Introduction

The (ortho)sympathetic and parasympathetic function of the autonomic nervous system (ANS) is essential to nearly all physiological processes. The vagus nerve is mainly known for its parasympathetic function. Apart from its physiological function, the vagus nerve has gained a role in the treatment of certain diseases as well. The most important example of this role is the use of electrical stimulation of the vagus nerve (vagus nerve stimulation, VNS) for the treatment of epilepsy.<sup>1,2</sup> VNS is among others explored as treatment option for depression,<sup>3</sup> cardiac disease states,<sup>4,5</sup> and inflammatory diseases like rheumatoid arthritis.<sup>6,7</sup>

The exact mechanisms of VNS however, remain elusive. Central effects are thought to be responsible for the anti-epileptic and antidepressant effects of VNS, while (mainly) peripheral and systemic effects are thought to be responsible for the immunomodulatory and cardiac effects.<sup>7</sup> It has not been clarified yet whether the treatment effects can be explained by afferent/efferent, direct/indirect or ortho-/antidromic signalling. Furthermore, physiologic signalling towards intracranial structures can be afferent or efferent in origin depending on which division of the ANS is considered (i.e. parasympathetic or sympathetic). Dual peripheral and central effects are thereby likely too, through vago-vagal and vago-central (i.e. parasympathetic-sympathetic) reflexes.<sup>7</sup> Stimulation intensity (output current), frequency, pulse width, signal on-time, signal off time, surgical procedures and the choice of site are parameters that possibly influence the success rate of VNS therapy for the different pathologies. Classically, VNS is performed on the left side because of early observations that right-sided VNS caused a greater reduction in heart rate than left-sided VNS.<sup>7</sup> Left-sided VNS became standard. The side effect profile of VNS investigated prospectively by Ben-Menachem et al.<sup>1</sup> and Handforth et al.<sup>8</sup> however, is positive and offers patients with refractory epilepsy prospects of good efficacy with only minor and often resolvable side effects.<sup>9</sup>

Data on vagus nerve morphology are scarce.<sup>10-16</sup> They include animal studies and qualitative studies on human vagus nerves. Quantitative data on human vagus nerve morphology at the level of electrode implant however, are lacking. By giving a detailed morphological description of the human cervical vagus nerve using a computerized analyzing system we aimed to answer the following questions: What is the composition of human cervical vagus nerve? How many fascicles run through the nerve? What is its degree of myelination? Is the myelin equally distributed within the fascicles? What is the amount of epineurial (connective) tissue? How large is its effective surface area? Which



percentage of this surface area is used by catecholaminergic neurotransmission? Do these variables differ between the right and left nerve? Do these variables differ between different nerves / individuals?

## Methods

Eleven pairs of cervical vagus nerves (right and left) were harvested by two anatomists from not previously dissected, fresh formalin-fixed (femoral infusion of ~10l fixative, followed by 4 weeks of fixation in a formalin bath) specimens, ranging in age between 67 and 91 years. No previous surgical interventions of head and neck had been performed.

### Vagus nerve sampling

The nerves were exposed using techniques that are similar to surgery for vagus nerve electrode placement.<sup>17,18</sup> A five centimeters linear incision through the skin and platysma muscle was made one centimeter above the clavicle extending cranially and parallel to the anterior border of the sternocleidomastoid muscle. This muscle was retracted laterally to expose the carotid sheath. The omohyoid muscle was then dissected from the carotid sheath and retracted cranially. The carotid sheath was opened and the vagus nerve was exposed between the common carotid artery and jugular vein. At this level the vagus nerve was transected caudally and cranially, at a course of 3 cm, whereafter the nerve was sampled (Figure 3.1).

From four additional specimens, vagus nerves (right and left) were collected inside the skull base (by means of opening the skull via a radial incision) between the brainstem and jugular foramen, proximal to the fusion of the vagus nerve with the accessory nerve.

### Histological preparation

All cervical nerves were divided into 3 pieces, to provide the 'mean morphology' over the whole trajectory used for electrode placement. Every piece then was divided into 2 halves. The first halves, were post-fixated overnight with 1% osmium tetroxide ( $\text{OsO}_4$ ) in phosphate buffered saline (PBS) before they followed paraffin embedding procedures. These paraffin blocks were cut into 4 $\mu\text{m}$  transverse sections and mounted on slides. These slides were used for morphometric analysis. The other halves followed standard paraffin blocking and cutting (4  $\mu\text{m}$  transverse sections) procedures, and were used for immunohistochemistry staining with anti-tyrosine hydroxylase (TH) (1:1000, Abcam AB112, Cambridge, UK) or anti-dopamine B hydroxylase (DBH) (1:150, Abcam, AB109112, Cambridge, UK) for surface area measurement of catecholamine containing

fibres. Shrinkage of about 30% in tissue diameter, before and during fixation and processing is thereby a recognized phenomenon.<sup>19</sup>

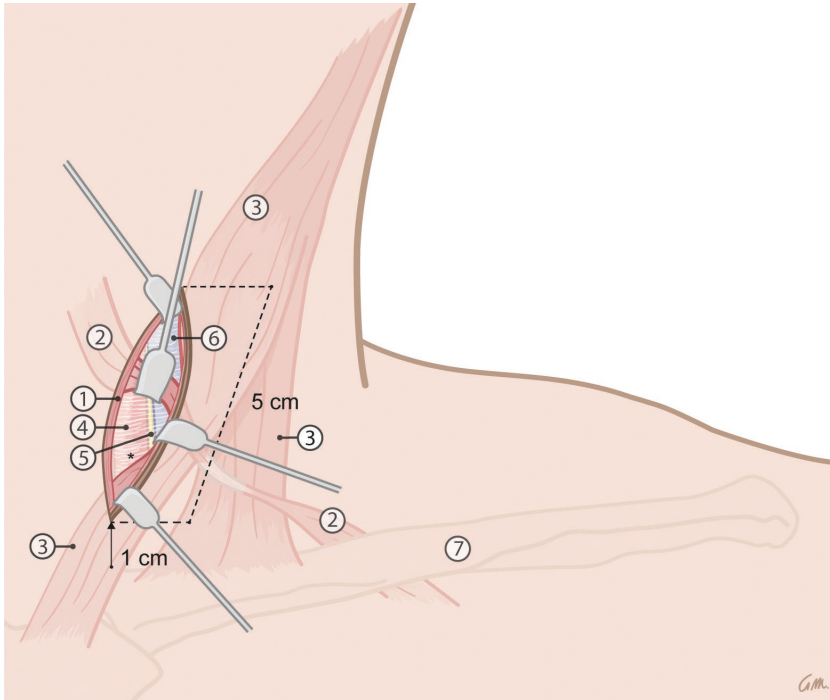


**Figure 3.1** Harvesting of the vagus nerves using exposure techniques similar to the surgical approach applied during implantation of the electrodes of the VNS device. Legend: 1. platysma muscle, 2. omohyoid muscle, 3. sternocleidomastoid muscle, 4. common carotid artery, 5. vagus nerve, 6. internal jugular vein and 7. clavicle \* carotid sheath.

### Morphometric analysis (detailed description to be found in supplement)

The slides were photographed with a Leica (type DMRD) photomicroscope in black and white using standardized settings. Surface areas of the specific stainings were measured with Leica Qwin v.3.5.1 analysis software at 10x magnification, including the following parameters: total surface area, effective surface area (nerve tissue exclusively within perineurium), connective tissue area, fascicle count and relative amount of myelination. Furthermore, the distribution of myelin within the fascicles was measured by dividing the effective surface area into 3 thirds (inner, middle and outer). Two persons

independently determined the gray value corresponding to positive staining. The average of their values was used as threshold.

Statistical analysis was performed with Graphpad Prism v5.0 software. Data were tested for normality with the use of Shapiro-Wilk normality test. Comparisons were made with the use of Student's t-tests. Data are presented as mean  $\pm$  SEM. P values less than 0.05 were considered statistically significant.

## Results

Eleven pairs of cervical vagus nerves were successfully harvested and studied. Transverse sections typically show several fascicles, connective tissue, fat and vessels. Figure 3.2 shows an example of a typical right and left human cervical vagus nerve of one specimen at the level of electrode implant. In 8 out of 11 specimens, the right nerve contained more fascicles than the left. On average, the right nerve contains 8.2 ( $\pm$ 1.7) fascicles, compared to 5.3 ( $\pm$ 0.9) within the left nerve ( $P=0.15$ ).

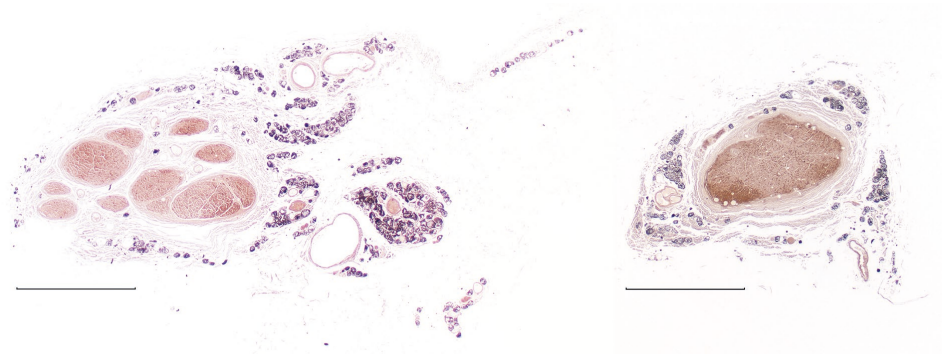


**Figure 3.2** Example of a human cervical right (left picture) and left (right picture) vagus nerve within one individual (OsO<sub>4</sub> fixation, bar indicates 500  $\mu$ m).

### Surface area measurements

The mean effective surface area on the right side is significant larger than on the left (1,089,492  $\pm$  98,337  $\mu$ m<sup>2</sup> vs. 753,915  $\pm$  102,490  $\mu$ m<sup>2</sup> respectively  $P<0.05$ ). In 10 out of 11 specimens, the right nerve possesses a larger effective surface area.

Figure 3.3 shows a boxplot of the effective surface area of the individual nerves in relation to the mean and confidence interval of 95%. For both sides, 4 out of 11 nerves

are not displayed within this 95% confidence interval, while Shapiro-Wilk normality test shows a normal distribution for both the right ( $P=0.99$ ) and left ( $P=0.31$ ) nerve. To illustrate, Figure 3.4 displays the largest and smallest left vagus nerve.

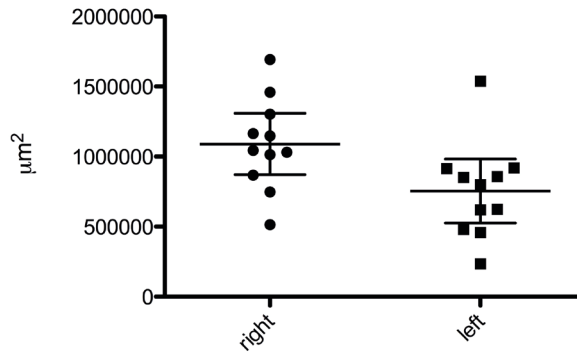


Figure 3.3 Mean effective surface area  $\pm$ 95% CI.

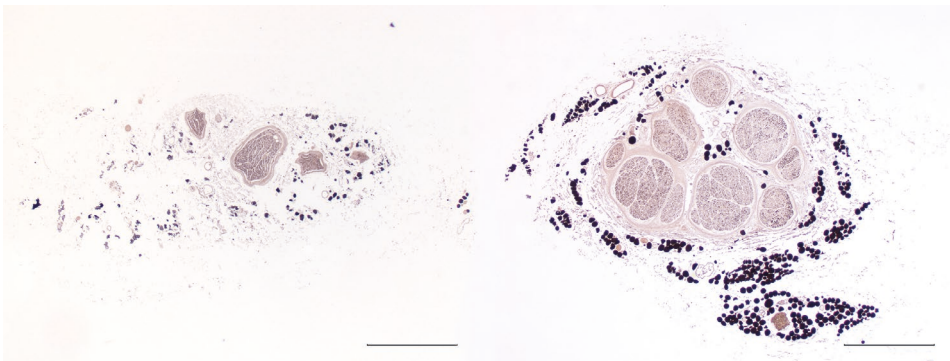
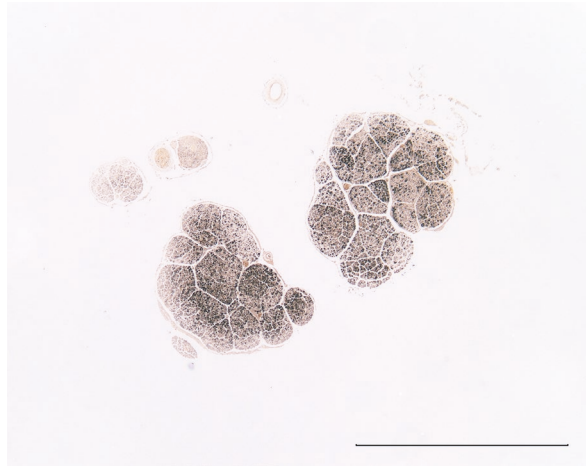


Figure 3.4 Example of two single left vagus nerves to illustrate the largest difference in surface area in-between nerves (OsO<sub>4</sub> fixation. Bar indicates 500 µm).

At the intracranial level ( $n=4$ ), no differences between the right ( $630,921 \pm 105,422 \mu\text{m}^2$ ) and left ( $855,808 \pm 655,902 \mu\text{m}^2$ ) nerve in terms of effective surface area were observed ( $P=0.54$ ).

On the right side, the mean effective intracranial surface area ( $630,921 \pm 105,422 \mu\text{m}^2$ ) is significantly less than the mean effective surface area at the cervical level of electrode implant ( $1,089,492 \pm 98,337 \mu\text{m}^2$ ) ( $P<0.05$ ), whereas on the left side, the mean effective

surface areas do not differ between the intracranial and cervical level ( $P=0.69$ ). The typical intracranial vagus nerve hardly possessed connective tissue and fat in the epineurium, and possessed multiple fascicles (Figure 3.5).



**Figure 3.5** Example of a (left) human vagus nerve inside the skull base (OsO<sub>4</sub> fixation, bar indicates 500 μm).

### Connective tissue

The mean total surface area of the cervical vagus nerve including epineurium (i.e. containing connective tissue, fat and vasa nervorum) did not differ between the right ( $8,448,000 \pm 739,000 \mu\text{m}^2$ ) and the left ( $6,992,000 \pm 905,500 \mu\text{m}^2$ ) cervical vagus nerve ( $P=0.23$ ).

The individual nerve's amount of epineurial tissue ranges from  $2,090,000 \mu\text{m}^2$  to  $11,683,000 \mu\text{m}^2$ . The boxplot (Figure 3.6) of the individual nerve's amount of epineurial tissue in relation to its mean and confidence interval of 95% however, shows that 5, respectively 7 of the 11 nerves are not displayed within this 95% CI, while the Shapiro-Wilk normality test shows a normal distribution for both the right ( $P=0.98$ ) and left ( $P=0.94$ ) nerve.

### Myelination

No difference in the amount of myelination relative to the effective surface area between the right ( $26.8\% \pm 1.5$ ) and left ( $28.0\% \pm 1.7$ ) nerve could be observed ( $P=0.62$ ). The myelin appeared to be distributed equally within the three thirds of the fascicles. The surface areas of the outer thirds of the right and left nerve fascicles show  $40.0\% \pm 1.5$  and  $37.9\% \pm 2.7$  positive OSO<sub>4</sub> staining, respectively. The surface areas of the outer

two thirds of the right and left nerve fascicles show  $66.5\% \pm 2.6$  and  $63.6\% \pm 2.6$  positive  $\text{OSO}_4$  staining, respectively.

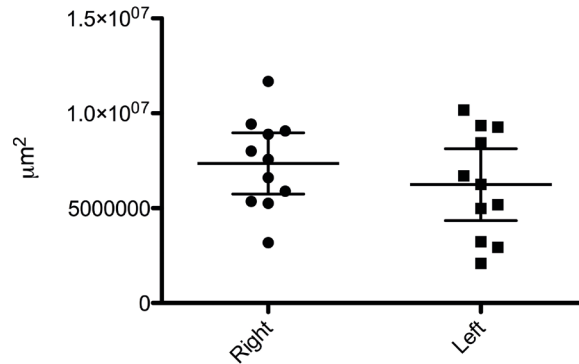


**Figure 3.6** Mean amount of epineurial tissue  $\pm 95\%$  CI.

### Catecholamines

At the cervical level, all nerves stained positive for tyrosine hydroxylase, varying from 0.6% to 8.5% of the total effective surface area. The mean area of tyrosine hydroxylase (TH) positive staining is significantly larger on the right side ( $43,393 \mu\text{m}^2 \pm 7,771$  i.e. 3.3%) compared to the left ( $20,748 \mu\text{m}^2 \pm 4,532$  i.e. 1.9%) ( $P < 0.05$ ).

In 2 cases, ganglion cells in the right cranial cervical vagus nerve were detected that stained positive for TH (Figure 3.7A). These nuclei stained positive for dopamine  $\beta$  hydroxylase DBH as well (Figure 3.7B). Furthermore, axons that stained positive for TH (Figure 3.7C) also stained positive for DBH (Figure 3.7D). In some cases, there was no positive DBH (Figure 3.7F) staining at sites of TH positive stained axons (Figure 3.7E).

No positive staining for TH or DBH could be observed at the intracranial level.

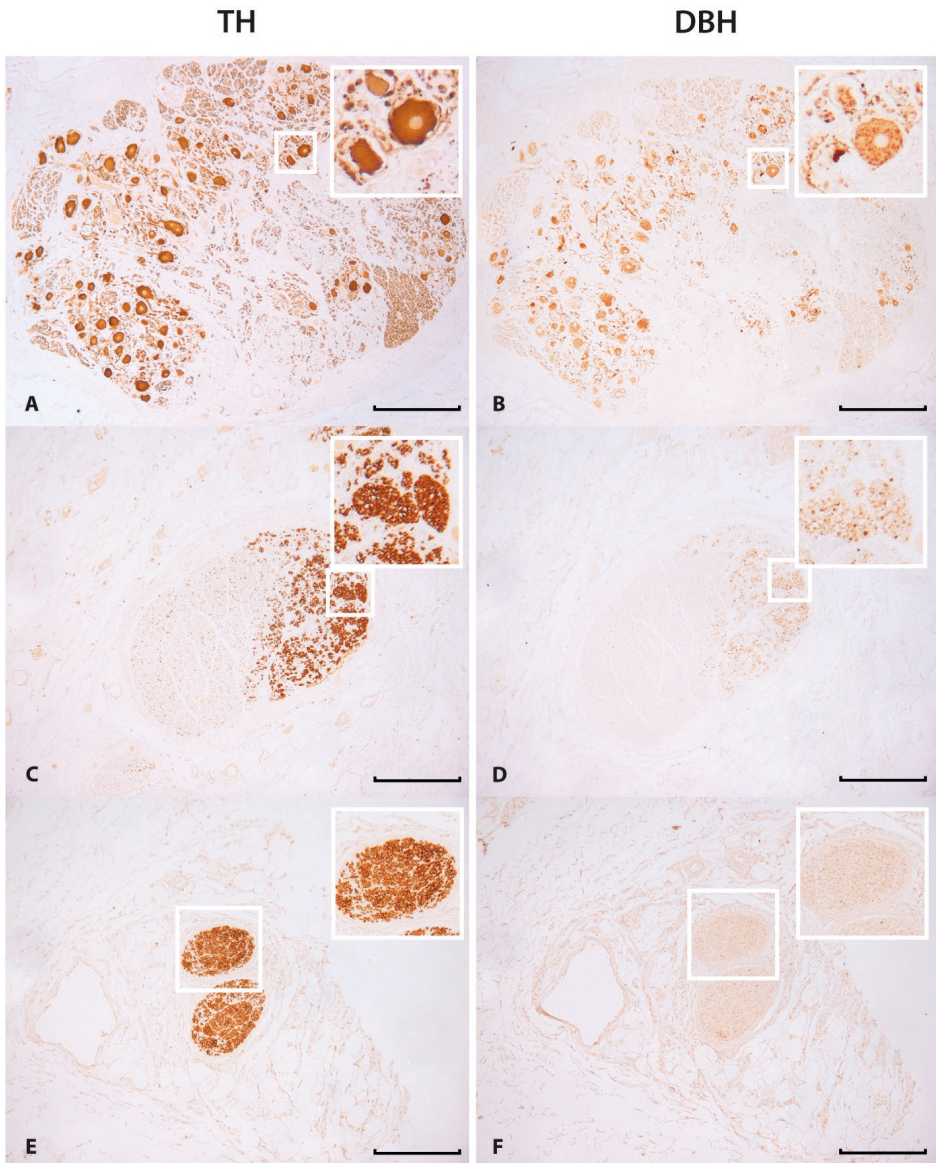


**Figure 3.7** (A–F) Tyrosine hydroxylase (TH) and dopamine beta-hydroxylase (DBH) staining (bar indicates 250  $\mu\text{m}$ ). (A) TH-positive ganglion cells in right cervical vagus nerve. (B) Ganglion cells that also stained positive for DBH. (C) TH-positive axons. (D) Axons that also stained positive for DBH. (E) TH-positive axons. (F) Axons that did not stain positive for DBH. Insets in the right upper corner show magnifications of the area surrounded with a white square.

## Discussion

This is the first study that provides quantitative data about human cervical vagus nerve morphology at the level of electrode implant for vagus nerve stimulation (VNS). The following conclusions can be drawn from our results:

### Surface area measurements

Although the total surface areas of the right and left cervical vagus nerves do not differ significantly, the effective surface area (nerve tissue exclusively within the perineurium) does. The effective surface area of the right cervical vagus nerve is 1.5x larger than the left nerve. This could have implications for the choice of side of stimulation when considering the possible amount of axons that will be stimulated. The (majority of the) right nerve fibres extend in the abdomen as the posterior trunk, running (among others) through the celiac and superior mesenteric ganglia, thereby supplying more viscera (possibly including the spleen) than the anterior trunk. This could explain (a.o. see further) the right-left difference in surface area at the cervical level. The effective surface area of 4 out of 11 nerves do not find themselves inside the  $\pm 95\%$  CI. This large variation in surface area may affect VNS success rates. The variation in surface area may also be explained by the inferior cardiac branch, which branches off the vagus nerve at variable levels. It has even been reported to branch off the recurrent laryngeal nerve<sup>11</sup> (see Figure 3.8). The possible co-stimulation of the cardiac branch upon VNS could therefore vary between individuals.

Our finding that the mean effective surface area at the right cervical level is significantly larger than at the level inside the right skull base, could implicate that the vagus nerve receives anastomosing and 'hitchhiking' branches from areas other than the brainstem. Other factors may contribute to this difference, such as the fusion of the accessory nerve with the vagus nerve and the difference in the amount of myelination. However, on the left side these factors did not contribute to a significant difference and also the relative amount of myelination between right and left nerve appeared equal.



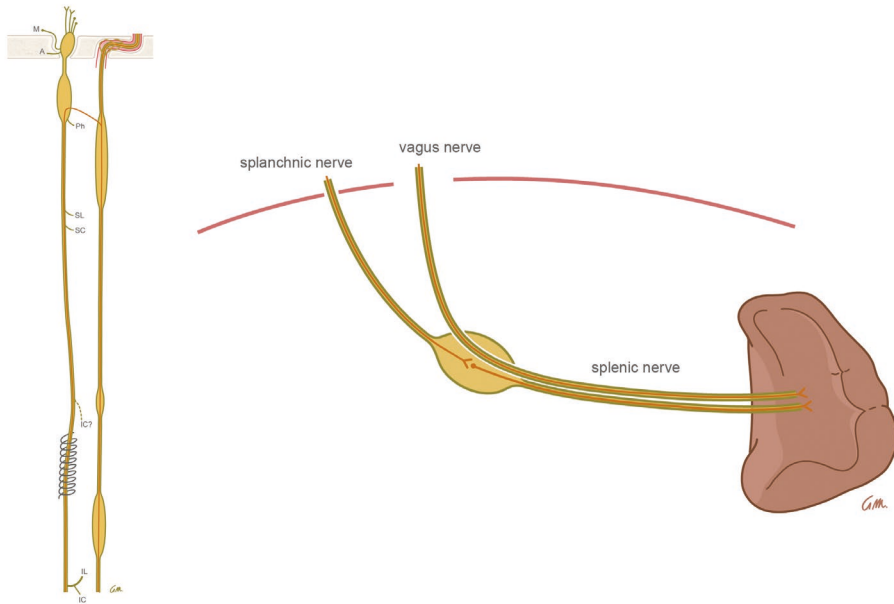


**Figure 3.8** Left: Anastomosing and ‘hitchhiking’ branches within the vagus nerve (left) from sympathetic chain (right). Right: hypothesis that the splenic nerve’s catecholaminergic release originates directly from the vagus nerve upon VNS. M: meningeal branch, A: auricular branch, Ph: pharyngeal branch, SL: superior laryngeal branch, SC: superior cardiac branch, IC: inferior cardiac branch and IL: inferior laryngeal branch.

## Myelination

High-degree myelinated fibres have the lowest amplitude-duration thresholds and are preferentially activated by low level VNS to result in therapeutic effects.<sup>20,21</sup> It is thereby suggested that the myelinated axons are responsible for the anticonvulsive effect since destruction of C-fibres does not alter the effect of VNS upon induced seizures in rats.<sup>22</sup> Fibres located closer to the perineurium of a fascicle are exposed to a stronger electric field since they are closer to the electrode.<sup>23</sup> We found that in humans the cervical vagus nerve contains relatively equal amounts of myelination on both the right and left side and that the amount of myelination within the individual nerves lie within the 95% CI. Furthermore, this myelination is equally distributed within the nerve fascicles. Upon VNS, the electrode does not fully encircle the vagus nerve, but wraps approximately 270 degrees around it. This partial positioning of the electrode contributes to potential ‘quiet spots’ where higher stimulation may be required for the activation of the nerve fibres present.<sup>23</sup> However, the large variation in epineurial connective tissue might influence the effectiveness of VNS to a greater extent (see further).

## Connective tissue

The nerves were exposed using techniques that are similar to surgery for vagus nerve electrode placement.<sup>17,18</sup> Attention was paid to isolate the nerve from its surroundings, while not harming the nerve proper. As already depicted in figure 6, the absolute amount of epineurial tissue, (i.e. connective tissue (including perineurium), fat and vasa nervosum) varied widely between the individual nerves, ranging from 2,090,000  $\mu\text{m}^2$  to 11,683,000  $\mu\text{m}^2$ . The amount of 'epineurial tissue' could isolate the nerve tissue proper from the electrical impulses generated by the electrical stimulation upon VNS-treatment. Helmers et al.<sup>23</sup> calculated in their mathematical working model of VNS (with 1.5 mA current and 500- $\mu\text{s}$  pulse width) that the presence of 1,300,000  $\mu\text{m}^2$  fibrous tissue around the nerve led to a decrease of 46.5% in A and B fibre activation. The conductivity of the extraneural medium is of prime importance to fibre recruitment. An insulating 'extraneural' medium generally requires more current to reach the stimulus threshold.<sup>24</sup> We suggest that the amount of epineurial tissue could be an important variable for determining individual effectiveness of VNS. These findings support the general belief that careful surgical exposure of the nerve prior to electrode application is extremely important.

## Catecholaminergic neurotransmission

Tyrosine hydroxylase positive nerve fibres were detected within the cervical vagus nerve. This confirms the early finding of H. Gray and H.V. Carter in 1858<sup>25</sup> who found communicating branches between the vagus nerve and sympathetic trunk. To date, no quantitative data about TH positive nerve fibres in human nerves exist, especially concerning the level of electrode implant upon VNS. The right cervical vagus nerve contains on average 2 times more TH positive nerve fibres than the left cervical nerve. The presence of DBH positive staining in the matching axons confirms the presence of not only dopamine but also noradrenaline (NA). No TH or DBH positive nerve fibres could be identified inside the skull base, confirming the early findings<sup>25</sup> that the origin/destination of these positive fibres must be the sympathetic chain. Above-mentioned findings have important implications for the contribution of the VNS treatment principle hypotheses.

## Central mechanism-of-action hypothesis

Stimulating the vagus nerves may implicate the release of dopamine and noradrenaline centrally as well as peripherally. Dopamine and noradrenaline might be released centrally via the sympathetic chain, thereby reaching all central areas that are innervated

by the sympathetic nervous system. This implies that VNS may have a catecholaminergic (sympathetic) effect that could contribute to the mechanism of action. This hypothesis is supported by the finding that VNS-induced antiepileptic effects are associated with increased hippocampal NA levels.<sup>26</sup> Furthermore, the locus coeruleus, the principal brain noradrenergic nucleus, mediates at least some of the seizure-attenuating effects of VNS.<sup>27</sup> The sympathetic component might also receive interest because of its role in regulating cerebral perfusion, since VNS has shown to induce cerebral (thalamic) blood flow changes in experimental settings.<sup>3</sup> Altogether, an increased release of noradrenaline in widespread cerebral regions upon VNS is thought to be one mechanism of action.<sup>2</sup> Furthermore, VNS is thought to have anti-inflammatory effects that are suspected to result from increased corticosteroid release by VNS-induced HPA-axis activation.<sup>28</sup> Lesions of the noradrenergic projections to the hypothalamus in rats impair the increase in plasma corticosterone induced by intraperitoneally injected IL-1.<sup>29</sup> Further imaging studies are necessary to characterize the activity of 'sympathetic and dopaminergic brain regions' upon VNS treatment. Since in many experimental studies however, the electronic device upon 'VNS' is (necessarily) implanted around the vagus nerve and common carotid artery (including sympathetic fibres therefore) together, the positive results from these studies might additionally be explained by the sympathetic component that was stimulated by chance.

### Peripheral mechanism-of-action hypothesis

(Peripheral) anti-inflammatory effects of VNS appear to rely on an intact catecholamine containing splenic nerve.<sup>30,31</sup> Our findings support this hypothesis by stating that the splenic nerve's catecholaminergic release possibly originates directly from the vagus nerve itself, and not from a synapse in the celiac ganglion, as has been proposed by Rosas-Ballina et al.<sup>30</sup> Catecholamine containing nerve fibres in the anterior nerve of Latarjet for instance have been described previously.<sup>32</sup> A possible direct catecholaminergic, sympathetic effect upon vagus nerve stimulation treatment could be the mechanism of action (see Figure 3.8) since  $\beta$  and  $\alpha$  receptors are present in different types of immunocompetent cells, and because of the direct contact between TH positive nerve terminals and lymphocytes in the spleen.<sup>33</sup> Despite several studies on spleen innervation,<sup>34-38</sup> the question whether the human spleen receives (catecholaminergic) innervation from the vagus nerve has not been answered yet. The origin of catecholamines within the subdiaphragmatic vagus nerves remains controversial. Ahlman et al.<sup>39</sup> and Liedberg et al.<sup>40</sup> demonstrated that the abdominal vagus nerve receives catecholamines from the superior cervical ganglion, which may be supported by our findings, as well as from the stellate ganglion and possibly also from the

intrathoracic sympathetic ganglia. Muryobayashi et al.<sup>41</sup> found that the origin of catecholamines in the abdominal vagus is restricted to the superior cervical ganglion. However, these studies were conducted on cats and dogs. Since we found that the cervical vagus nerve on the right side contains more TH positive nerve fibres, and the right (posterior) vagus nerve extends in the abdomen through the celiac trunk and possibly the splenic plexus, experimental studies studying the anti-inflammatory effect of VNS could investigate the difference in effects upon right vs. left nerve stimulation. In theory, stimulation of the direct sympathetic supply to the spleen should induce even stronger anti-inflammatory effects.

In two of our cases, ganglion cells were found in the human cervical vagus nerve at the level of electrode implant. These nuclei stained positive for TH as well as DBH, implicating a catecholaminergic origin. The presence of these nuclei here implies that the destination of at least part of the catecholaminergic fibers are 2<sup>nd</sup> order neurons that travel peripherally down the vagus nerve.

Experimental studies have demonstrated beneficial effects of VNS for the treatment of various cardiac disease states such as arrhythmias.<sup>4</sup> These cardiac effects appear to rely on both parasympathetic and sympathetic activation. For instance, the anti-arrhythmic effect of VNS in undiseased hearts, is abolished by treatment with propranolol.<sup>42</sup> On the other hand, several investigators have shown a reduction in the anti-arrhythmic effect of VNS following treatment with atropine, supporting the role of muscarinic receptor activation in these studies.<sup>42,43</sup> Furthermore, Hopkins et al.<sup>44</sup> stated that the intrinsic cardiac nervous system can become directly involved in cardiac pathology. At the level of the intrinsic cardiac nervous system, complex functional interconnectivity exists. These act as a stabilizing feature to prevent various cardiac disease states. Components within this neuroaxis may interact abnormally to alter myocyte function.<sup>45</sup> These findings have lead to the concept of VNS-induced restoration of the loss of autonomic balance, in order to provide treatment effects such as electrical stability.<sup>5,6</sup> Furthermore, Levy demonstrated that in the presence of a substantial background of sympathetic activity, the same level of vagal activity exerted a more prominent effect upon different cardiac effector tissues than in the absence of substantial sympathetic background activity.<sup>46</sup> Concurrent stimulation of both sympathetic and parasympathetic cardiac nerves increases myocardial contractility without increasing heart rate.<sup>5</sup> The presence of catecholaminergic fibres within the vagus nerve at the level of electrode implant could therefore be of special interest when stimulating the nerve in patients with cardiac disease. This fact could be of particular interest upon choosing the side of stimulation. Since the right vagus nerve at the level of electrode implant contains more

catecholaminergic fibres it would therefore be interesting to study whether the effects of human VNS on the right nerve possibly exerts a greater beneficial effect.

## Conclusion

Our finding that the human cervical vagus nerve differs at the level of electrode implant between both sides in various ways has interesting implications for the choice of stimulation side for VNS. Future studies should test this in various conditions instead of merely try to standardize the procedure. In support of the general belief, careful surgical exposure of the vagus nerve prior to electrode application seems extremely important due to various amounts of epineurial tissue. Furthermore we conclude by stating that one has to look at the vagus nerve as a morphological entity of the peripheral autonomic nervous system. “The parasympathetic vagus nerve” does not exist. Rather we have to speak of the morphological vagus nerve, a composite of different fibres and branches with different neurotransmitters, which can act parasympathetic, sympathetic, somato-efferent or viscerio-afferent in function. This ‘morphological’ view at nerves is further illustrated by the difference in effective surface area and amount of fascicles at different levels within in the nerve, indicating various anastomising and “hitchhiking” branches within morphological nerve entities of different origin. Electrically stimulating the vagus nerve therefore is not the same as a pure elevation of the ‘physiologic vagal parasympathetic tone’, but also implements catecholaminergic (sympathetic) effects. We recommend surgeons and scientists taking this in consideration when investigating the autonomic nervous system and related areas.

## References

1. Ben-Menachem E, et al. Vagus nerve stimulation for treatment of partial seizures: 1. A controlled study of effect on seizures. First International Vagus Nerve Stimulation Study Group. *Epilepsia*. 1994;35(3): 616-626.
2. Beekwilder JP, Beems T. Overview of the clinical applications of vagus nerve stimulation. *J Clin Neurophysiol*. 2010;27(2):130-138.
3. Nemeroff CB, et al. VNS therapy in treatment-resistant depression: clinical evidence and putative neurobiological mechanisms. *Neuropsychopharmacology*. 2006;31(7):1345-1355.
4. Brack KE, Winter J, Ng GA. Mechanisms underlying the autonomic modulation of ventricular fibrillation initiation--tentative prophylactic properties of vagus nerve stimulation on malignant arrhythmias in heart failure. *Heart Fail Rev*. 2013;18(4):389-408.
5. Kobayashi M, et al. Cardiac autonomic nerve stimulation in the treatment of heart failure. *Ann Thorac Surg*. 2013;96(1):339-345.
6. Koopman FA, et al. Restoring the balance of the autonomic nervous system as an innovative approach to the treatment of rheumatoid arthritis. *Mol Med*. 2011;17(9-10):937-948.
7. Bonaz B, et al. Vagus nerve stimulation: from epilepsy to the cholinergic anti-inflammatory pathway. *Neurogastroenterol Motil*. 2013;25(3):208-221.
8. Handforth A, et al. Vagus nerve stimulation therapy for partial-onset seizures: a randomized active-control trial. *Neurology*. 1998;51(1):48-55.
9. Ben-Menachem E. Vagus nerve stimulation, side effects, and long-term safety. *J Clin Neurophysiol*. 2001; 18(5):415-418.
10. Pereyra PM, et al. Development of myelinated and unmyelinated fibers of human vagus nerve during the first year of life. *J Neurol Sci*. 1992;110(1-2):107-113.
11. Standring S. *Gray's Anatomy*. 2008: Elsevier Health Sciences.
12. Hoffman HH, Schnitzlein HN. The numbers of nerve fibers in the vagus nerve of man. *Anat Rec*. 1961; 139:429-435.
13. Kawagishi K, et al. Tyrosine hydroxylase-immunoreactive fibers in the human vagus nerve. *J Clin Neurosci*. 2008;15(9):1023-1026.
14. Onkka P, et al. Sympathetic nerve fibers and ganglia in canine cervical vagus nerves: localization and quantitation. *Heart Rhythm*. 2013;10(4):585-591.
15. Asala SA, Bower AJ. An electron microscope study of vagus nerve composition in the ferret. *Anat Embryol (Berl)*. 1986;175(2):247-253.
16. Ruffoli R, et al. The chemical neuroanatomy of vagus nerve stimulation. *J Chem Neuroanat*. 2011;42(4): 288-296.
17. Reid SA. Surgical technique for implantation of the neurocybernetic prosthesis. *Epilepsia*. 1990;31 Suppl 2:S38-539.
18. Patil A, Chand A, Andrews R., Single incision for implanting a vagal nerve stimulator system (VNSS): technical note. *Surg Neurol*. 2001;55(2):103-105.
19. Stickland NC. A detailed analysis of the effects of various fixatives on animal tissue with particular reference to muscle tissue. *Stain Technol*. 1975;50(4):255-264.
20. Groves DA, Brown VJ. Vagal nerve stimulation: a review of its applications and potential mechanisms that mediate its clinical effects. *Neurosci Biobehav Rev*. 2005;29(3):493-500.
21. Mollet L, et al. Intensity-dependent modulatory effects of vagus nerve stimulation on cortical excitability. *Acta Neurol Scand*. 2013;128(6):391-396.
22. Krahl SE, Senanayake SS, Handforth A. Destruction of peripheral C-fibers does not alter subsequent vagus nerve stimulation-induced seizure suppression in rats. *Epilepsia*. 2001;42(5):586-589.
23. Helmers SL, et al. Application of a computational model of vagus nerve stimulation. *Acta Neurol Scand*. 2012;126(5):336-343.
24. Frieswijk TA, et al. Force-current relationships in intraneural stimulation: role of extraneural medium and motor fibre clustering. *Med Biol Eng Comput*. 1998;36(4):422-430.

25. Gray H, Carter, Henry Vandyke, *Anatomy Descriptive and Surgical*: 1858:498. London: John W. Parker and Son, West strand.
26. Raedt R, et al. Increased hippocampal noradrenaline is a biomarker for efficacy of vagus nerve stimulation in a limbic seizure model. *J Neurochem*. 2011;117(3):461-469.
27. Krahl SE, et al. Locus coeruleus lesions suppress the seizure-attenuating effects of vagus nerve stimulation. *Epilepsia*. 1998;39(7):709-714.
28. Dantzer R, et al. Neural and humoral pathways of communication from the immune system to the brain: parallel or convergent? *Auton Neurosci*. 2000;85(1-3):60-65.
29. Chuluyan HE, et al. Noradrenergic innervation of the hypothalamus participates in adrenocortical responses to interleukin-1. *Neuroendocrinology*. 1992;56(1):106-111.
30. Rosas-Ballina M, et al. Splenic nerve is required for cholinergic antiinflammatory pathway control of TNF in endotoxemia. *Proc Natl Acad Sci U S A*. 2008;105(31):11008-11013.
31. Tracey KJ. Understanding immunity requires more than immunology. *Nat Immunol*. 2010;11(7):561-564.
32. Lundberg J, et al. Catecholamine-containing nerve fibres in the human abdominal vagus. *Gastroenterology*. 1976;70(3):472-474.
33. Hori T, et al. The autonomic nervous system as a communication channel between the brain and the immune system. *Neuroimmunomodulation*. 1995;2(4):203-215.
34. Reilly FD. Innervation and vascular pharmacodynamics of the mammalian spleen. *Experientia*. 1985; 41(2):187-192.
35. Bellinger DL, et al. Acetylcholinesterase staining and choline acetyltransferase activity in the young adult rat spleen: lack of evidence for cholinergic innervation. *Brain Behav Immun*. 1993;7(3):191-204.
36. Heusermann U, Stutte HJ., Electron microscopic studies of the innervation of the human spleen. *Cell Tissue Res*. 1977;184(2):225-236.
37. Kudoh G, Hoshi K, Murakami T. Fluorescence microscopic and enzyme histochemical studies of the innervation of the human spleen. *Arch Histol Jpn* 1979;42(2):169-180.
38. Nance DM, Burns J. Innervation of the spleen in the rat: evidence for absence of afferent innervation. *Brain Behav Immun*. 1989;3(4):281-290.
39. Ahlman BH, et al. Evidence for innervation of the small intestine from the cervical sympathetic ganglia. *J Surg Res*. 1978;24(3):142-149.
40. Liedberg G, et al. Adrenergic contribution to the abdominal vagus nerves in the cat. *Scand J Gastroenterol*. 1973;8(2):177-180.
41. Muryobayashi T, et al. Fluorescence histochemical demonstration of adrenergic nerve fibers in the vagus nerve of cats and dogs. *Jpn J Pharmacol* 1968;18(3):285-293.
42. Li M, et al. Vagal nerve stimulation markedly improves long-term survival after chronic heart failure in rats. *Circulation*. 2004;109(1):120-124.
43. Wang X, Gerdes AM. Chronic pressure overload cardiac hypertrophy and failure in guinea pigs: III. Intercalated disc remodeling. *J Mol Cell Cardiol*. 1999;31(2):333-343.
44. Hopkins DA, et al. Pathology of intrinsic cardiac neurons from ischemic human hearts. *Anat Rec*. 2000; 259(4):424-436.
45. Armour JA. Potential clinical relevance of the 'little brain' on the mammalian heart. *Exp Physiol* 2008; 93(2):165-176.
46. Levy MN. Cardiac sympathetic-parasympathetic interactions. *Fed Proc* 1984;43(11):2598-2602.

## Supplemental materials

### Morphometric analysis

The slides were photographed with a Leica (type DMRD) photomicroscope in black and white using standardized settings. These comprised an equal white balance and shutter speed, in order to acquaint an equivalent black and white photograph. By using black and white photography a linear grey scale was achieved. By this it was possible to determine the amount of positive staining, expressed as a number on one linear numeric scale (instead of the inaccurate and surrounding complexity of determining positive staining using RGB photographs within three combined axes (consisting of red, green and blue)). Surface areas of the specific stainings were measured with Leica Qwin v.3.5.1 analysis software at 10x magnification, including the following parameters: total surface area, effective surface area (nerve tissue exclusively within perineurium), connective tissue area, fascicle count and relative amount of myelination. Furthermore, the distribution of myelin within the fascicles was measured by dividing the effective surface area into 3 thirds (inner, middle and outer, see Figure S3.1). The Leica Qwin analysis software is capable of determining the amount of pixels as from a chosen gray value on the linear scale and to convert this into a surface area expressed in square micrometer. Figure S3.2 illustrates this with a graph. This enabled us to determine, for instance, the amount of pixels darker than for instance grayscale 130 or grayscale 250. Two persons independently determined the gray value corresponding to positive staining. The average of their values was used as threshold. Figure S3.3 illustrates how the effective surface area (area covered by pixels that are darker than 250) can be determined, even on a morphologically poor quality slide. Figure S3.4 depicts an example of  $\text{OsO}_4$  quantification using the same technique as a measure of myelination.

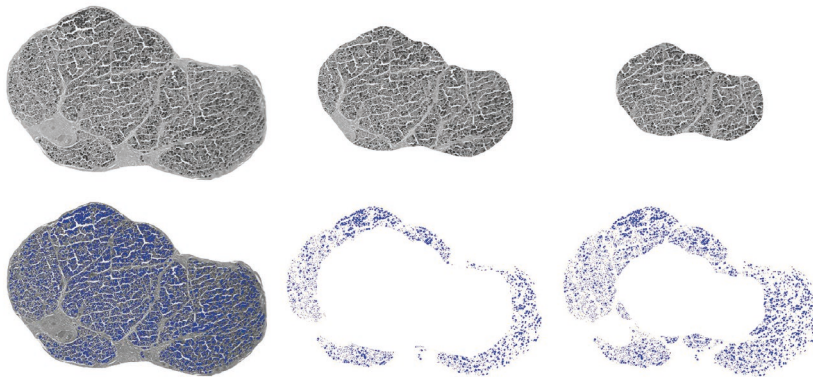


**Figure S3.1** Determining the distribution of  $\text{OsO}_4$  positive staining within the three thirds of a single fascicle (example).



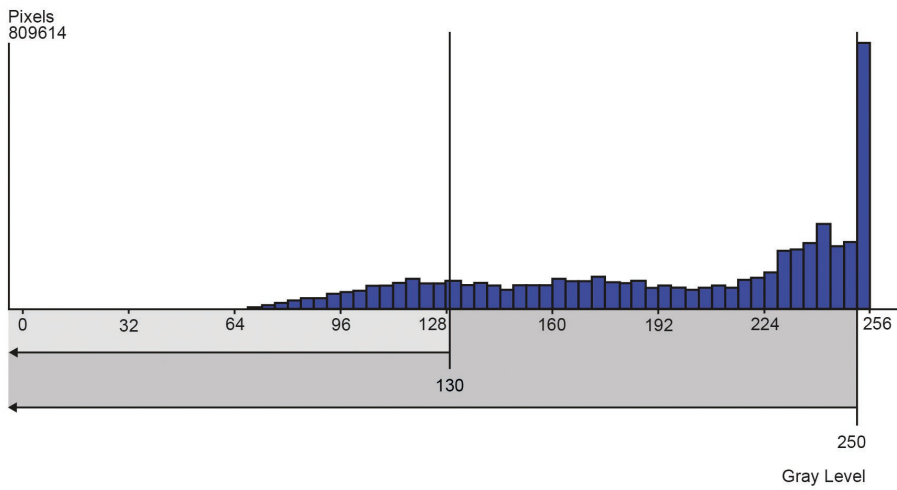


**Figure S3.2** Determining the amount of pixels as from a chosen gray value (for example 130 and 250) on the linear (grey) scale.

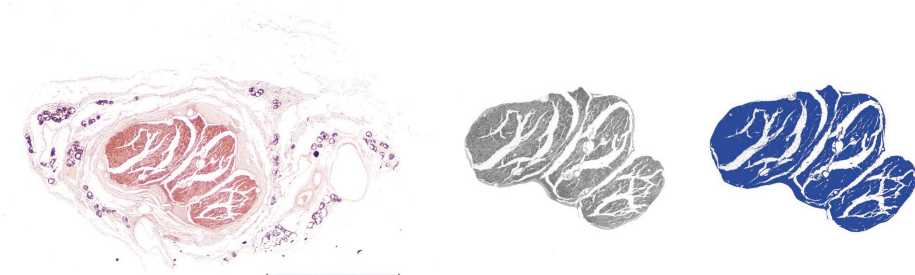


**Figure S3.3** Example of measuring effective surface area. (OsO<sub>4</sub> Fixation, bar indicates 500  $\mu$ m).

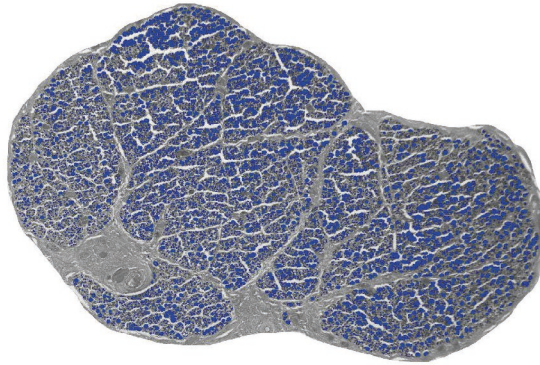


Figure S3.4 Positive  $\text{OsO}_4$  staining measured using analysis software within 1 fascicle (example).



# Chapter 4

Innervation of the human spleen:  
a complete hilum-embedding approach

Thomas J.M. Verlinden, Paul van Dijk, Jill P.J.M. Hikspoors, Andreas Herrler,  
Wouter H. Lamers, S. Eleonore Köhler

*Brain Behavior and Immunity* 2019. 77: 92-100

## Abstract

### Introduction

The spleen is hypothesized to play a role in the autonomic nervous system (ANS)-mediated control of host defence, but the neuroanatomical evidence for this assumption rests on a sparse number of studies, which mutually disagree with respect to the existence of cholinergic or vagal innervation.

### Methods

We conducted an immuno- and enzyme-histochemical study of the innervation of the human spleen using a complete hilum-embedding approach to ensure that only nerves that entered or left the spleen were studied, and that all splenic nerves were included in the sampled area. Furthermore, a complete embedded spleen was serially sectioned to prepare a 3D reconstruction of the hilar nerve plexus.

### Results

All detected nerves entering the spleen arise from the nerve plexus that surrounds branches of the splenic artery and are catecholaminergic. Inside the spleen these nerves continue within the adventitia of the white pulpal central arteries and red pulpal arterioles. Staining for either choline acetyltransferase or acetylcholinesterase did not reveal any evidence for cholinergic innervation of the human spleen, irrespective of the type of fixation (regularly fixed, fresh-frozen post-fixed or fresh-frozen cryoslides). Furthermore, no positive VIP staining was observed (VIP is often co-expressed in postganglionic parasympathetic nerves).

### Conclusion

Our comprehensive approach did not produce any evidence for a direct cholinergic (or VIP-ergic) innervation of the spleen. This finding does not rule out (indirect) vagal innervation via postganglionic non-cholinergic periarterial fibres.

## Introduction

The autonomic nervous system (ANS) has an acknowledged role in host defence.<sup>1</sup> Nerves are located in the perivascular adventitia of immune organs and, in addition, are found in juxtaposition to the cellular mediators of both innate and adaptive immunity.<sup>2</sup> The spleen is hypothesized to play a role in the ANS-mediated control of host defence,<sup>3</sup> but the neuroanatomical evidence for this assumption rests upon a sparse number of studies with mutually divergent claims. Some argue that the spleen lacks vagal or cholinergic innervation,<sup>4-11</sup> whereas others state that the spleen does receive such innervation.<sup>12-14</sup> Most of these studies were based on nerve tracing techniques. Since vascular branches to stomach, pancreas and greater omentum also originate from the distal end of the splenic artery (see Figure 4.1), this technique may not always identify the injection site accurately and may include perivascular adventitial branches of the vagus nerve.<sup>15</sup> The few studies that were performed in humans also produced contradictory data. Electron-microscopic analysis of splenic biopsies and fetal immunohistochemical studies only demonstrated catecholaminergic nerve fibres that accompanied the peripheral branches of the splenic artery.<sup>16,17</sup> Another study confirmed the presence of catecholaminergic nerves within the spleen, but also found cholinergic nerve fibres around the trabecular arteries upon staining for the presence of acetylcholinesterase.<sup>18</sup>

Difficulties in establishing the innervation of the human spleen arise from the variable branching pattern of splenic arteries within the large splenic hilum.<sup>19-22</sup> We, therefore, conducted a histological study of the innervation of the human spleen using a complete hilum-embedding approach to ensure that only nerves that entered or left the spleen were studied and that all splenic nerves were included in the sampled area. We used PGP-9.5 and S-100 to identify nerves and partially characterized the neurochemical nature of these nerves by staining for the presence of the cholinergic markers choline acetyltransferase (ChAT) and acetylcholinesterase (AChE), the catecholaminergic markers tyrosine hydroxylase (TH) and dopamine  $\beta$ -hydroxylase (DBH), and vasoactive intestinal peptide (VIP). The main finding of our study was that all splenic nerves arise from the plexus surrounding the splenic artery, are catecholaminergic, and continue inside the spleen within the adventitia of the intrasplenic arteries and arterioles.

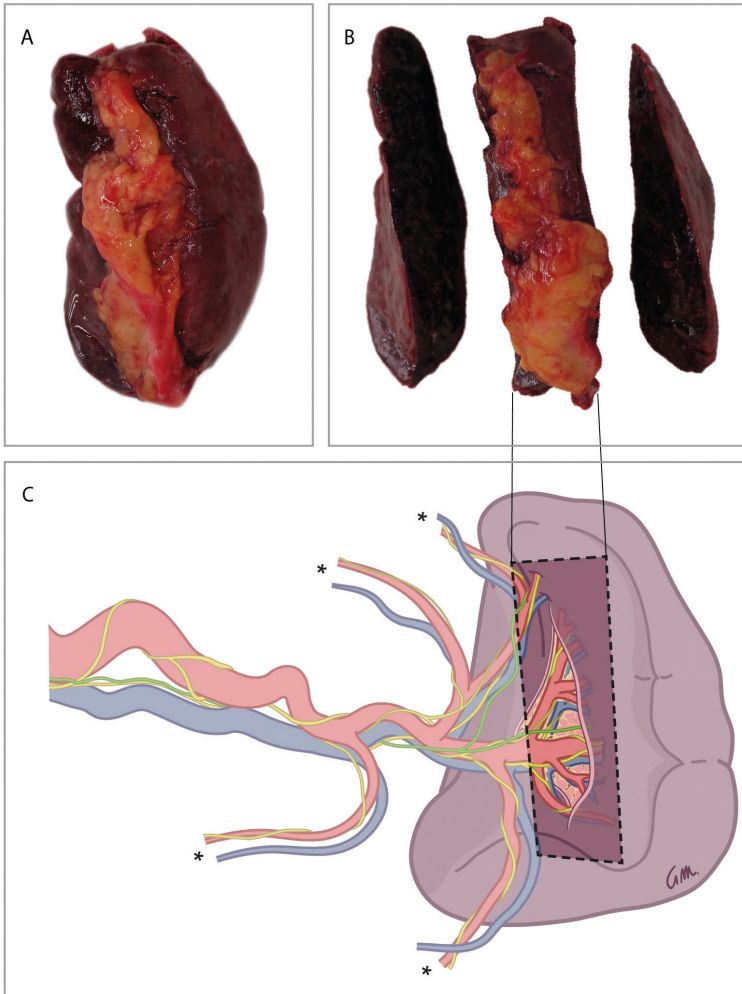


**Figure 4.1 Isolation of the spleen hilum for histological analysis.** The main goal of the procedures was to leave the topography of the hilum intact. A: Complete spleen as sampled from a human cadaver; B: removal of splenic parts not directly connected to the hilum; C: schematic drawing of the spleen, including the splenic artery (red) and vein (blue), lymph vessels (green) and nerves (yellow). Note the peripheral branches of the splenic vessels and nerves that approach the spleen, but do not enter (asterisks). Instead, such vessels and nerves head for nearby mesenteries and organs. The hilar area corresponding to the embedded samples is indicated by the stippled rectangle.

## Methods

### Harvesting of splenic tissue

Spleens were harvested from forty-six formalin-fixed (42), fresh-frozen (3) or non-fixed, non-frozen (4h post-mortem (1)) cadavers between 58 and 101 ( $\bar{x}$  = 84 ± 11) years of age from the body donation program of the Department of Anatomy and Embryology, Faculty of Health, Medicine and Life Sciences, Maastricht University, Maastricht, The Netherlands. The tissue donors gave their informed and written consent for the donation of their body for teaching or research purposes as regulated by the Dutch law for the use of human remains for scientific research and education (Wet op de Lijkbezorging, 1991). Accordingly, a handwritten and signed codicil from the donor posed when still alive and well, is kept at the Department of Anatomy and Embryology of Maastricht University. Formalin-fixed bodies were preserved by intra-arterial infusion with 10 L fixative (composition (v/v): 96% ethanol (21%), 100% glycerol (21%), 36% formaldehyde (2%), water (56%), and 2.4 g/L thymol), followed by 4 weeks of fixation in 96% ethanol (20%), 36% formaldehyde (2%) and water (78%). Samples were only taken from bodies without signs of previous abdominal surgical interventions. After opening the abdomen, the spleen was removed together with its mesenteries (i.e. presplenic, gastrosplenic, phrenicosplenic, splenocolic, pancreaticosplenic (or tip of pancreas tail itself) and splenorenal folds). Both the mass of the spleen and its mesenteries were then trimmed away to such an extent that the hilum was retained in its original intact state (Figure 4.1). These blocks were embedded in paraffin or frozen to prepare cryosections.

### Histological processing

Sections were mounted onto large glass slides (76 x 52 mm). The complete hila sections were fitted on a single glass slide for 20 spleens. The remaining hila were divided and mounted on consecutive glass slides. Serial transverse sections, 5 µm thick for paraffin or 14 µm thick for cryosections, were prepared throughout the hilum with a Leica 2245 microtome. For general examination, tissues were stained with haematoxylin & eosin (HE). Weigert van Gieson (WVG) staining was used for the detection of connective tissue. Antibodies against S100 protein (S100) and protein gene product 9.5 (PGP 9.5) were used as general neural markers. S100 protein identifies nerve-supporting tissue,<sup>23</sup> while PGP 9.5 is a ubiquitin C-terminal hydroxylase, that specifically stains nerve axoplasm.<sup>24</sup> For the specific identification of catecholaminergic neurons, antibodies against tyrosine hydroxylase (TH) and dopamine β-hydroxylase (DBH) (the rate-determining enzymes for dopamine and noradrenaline synthesis, respectively) were used. For the detection of cholinergic innervation, both enzyme-histochemical staining (based on Karnovsky's and



Roots' acetylcholinesterase (AChE) method<sup>25</sup> with iso-octamethylpyrophosphoramidate for inhibition of butyrylcholinesterase) was performed, and immunohistochemical staining using antibodies against choline acetyltransferase (ChAT). Furthermore, immunohistochemical staining for vasoactive polypeptide (VIP), a neurotransmitter that is frequently co-expressed with acetylcholine,<sup>26</sup> was carried out. Specific attention was given to the combined staining of S100 and PGP 9.5 with other neural markers. CD31, CD45 and CD68 were used for the detection of endothelium, leukocytes and macrophages, respectively. Sections for control incubations (sweat glands, skin and ileum) were obtained from the same cadavers and were processed histologically as described for the splenic tissue, ensuring that negative results cannot to be attributed to methodological issues. Table 4.1 provides details about dilutions, sources, and characteristics of the antisera and enzymes used. Two persons independently determined whether staining exceeded background levels using a Leica DM4 microscope.

**Table 4.1 Dilutions, sources, and characteristics of antisera and enzymes used.**

A	B	C	D	E	F	G	H	I
WvG	C							I,vG
S100	P	X		DAKO-Z0311 1:1000 TengT/10%NGS for 60 min.	1		6	
PGP 9.5	P	X	X	Biotrend APS0714 PGP9.5 1:100 4%FCS/PBS O/N	2	4	6	
TH	P	X	X	Abcam AB112 1:1000 TengT/10%NGS O/N	1	4	6	M
DBH	P	X	X	Abcam AB109112 1:150 TengT/10%NGS O/N	1	4	6	
ChAT	P	X	X	Merck-Millipore AB144P 1µl/ml 1:50 PBST/10%NHS O/N	3	4	7	
VIP	P	X	X	Peninsula Lab. Int. T4246 1:2000 TengT/10%NGS O/N	1	4	6	
CD31	P	X	X	DAKO-Z0823 1:100 2%FCS/10%NGS O/N	3	5	6	M
CD45	P		X	DAKO-701 1:200 PBST/0.5%BSA O/N	2	4	6	
CD68	P	X	X	Abcam AB125047 1:100 TengT/10%NGS O/N	1	4	8	
AChE	C*			Acetylcholine iodide 5 mg (Sigma) + Iso-octamethyl pyrophosphoramidate 4mM 0.2ml (Sigma) + Ferricyanide for 120 min.			7	

A: Type of staining: WvG: histochemistry, S100-CD68: immunohistochemistry, AChE: enzyme histochemistry; B: Type of section: C: Cryosection (14µ), P: Paraffin section (5µ); C: Peroxidase block with 3% H<sub>2</sub>O<sub>2</sub> / methanol for 10 min.; D: Antigen retrieval with sodium citrate at pH6.0 for 30 min.; E: Primary antibody or enzyme staining; F: Secondary antibody: 1: Vector BA1000 GAR-bio 1:500 PBST for 30 min., 2: Vector BA9200 GAM-bio 1:500 PBST for 30 min., 3: DAKO K0690 Link-biotin for 30 min.; G: Amplify: 4: Vector P6200-HRP for 30 min., 5: DAKO K0690 Link-streptavidin HRP for 30 min.; H: Chromogen: 6: DAB Sigma D5905, 7: AEC-it NOVEX-RED 002007, 8: Vector SG SK-4700; I: Counter staining: M: Mayer haematoxylin nuclear staining, I: Iron haematoxylin nuclear staining, vG: von Gieson connective tissue staining; \* Fixation: 30 sec. 4%Formaldehyde / 0.1M Calcium Acetate at pH 6.0.

### 3-D Reconstruction of splenic nerves

Two spleens were embedded completely including their splenorenal and splenogastric folds and mounted on single glass slides. One of these spleens was used for preparing a 3D reconstruction of the hilar nerve plexus. Serial transverse sections (5 µm) were made

every 200  $\mu\text{m}$  through this intact spleen. For the 3D reconstruction, complete images of selected large slides were digitized with an Olympus BX61 microscope and the DOTSLIDE program (Olympus, Leiderdorp, The Netherlands), which allows fully automated, high-resolution scanning of entire slides. AMIRA software (version 5.5; base package; FEI Visualization Sciences Group Europe, Mérignac Cédex, France) was used to generate 3D reconstructions after image loading, alignment and segmentation.<sup>27</sup>

## Results

Nerves entered the spleen within the vascular adventitia via the hilum. No vessels or nerves were seen to enter the spleen outside its mesentery (i.e. through the capsule). Inside the spleen, nerves surrounded the trabecular arteries and their branches, the central arteries (Figure 4.2), and could be followed up to the arteriolar level. Nerves that were not associated with periadventitial tissue were not encountered within the white or red pulpa (Figure 4.3).

Abundant TH- and DBH-positive staining was observed within all nerves, that is, structures that stained for the presence of both PGP 9.5 and S100 (Figure 4.2). Importantly, although non-neural positive ChAT staining of spleen macrophages was observed (Figure 4.4 and Supplemental Figure S4.1), ChAT- or AChE-positive neurons were never seen, irrespective of whether formalin-fixed, fresh-frozen post-fixed, or fresh-frozen cryo-slides were used (Figure 4.2). Nerves in human axillary sweat glands and skin, on the other hand, did stain positive for ChAT- or AChE (Figures 4.5, 4.6). Furthermore, although classic parasympathetic nerves usually synapse on their postganglionic nerves close to or within organs,<sup>28</sup> no (postganglionic) nerve cell bodies were encountered within or close to the spleen. VIP is often observed in postganglionic parasympathetic nerves,<sup>26</sup> but VIP-positive staining was never observed (Figure 4.2; positive control shown in Supplemental Figure S4.2). Care was taken to differentiate S100 staining of macrophages from that of neurons by comparing its staining pattern with that of the second pan-neural marker PGP 9.5. A more limited distribution of PGP 9.5 staining of nerves compared to the S100 distribution, however, existed, because of its characteristic restriction to the thin axoplasm (Figure 4.7).

From one completely embedded spleen, a reconstruction of the S-100-positive (hilar) nerves was made (Figure 4.8 and Supplemental Figure S4.3). This reconstruction demonstrates that all nerves entered via the splenic hilum, including those innervating the hilar poles. Furthermore, we found isolated perivascular nerves in the connective

tissue of the mesentery that appeared to approach the spleen, but turned away towards the adjacent mesenteries and organs (Figure 4.1C) instead of entering the spleen.

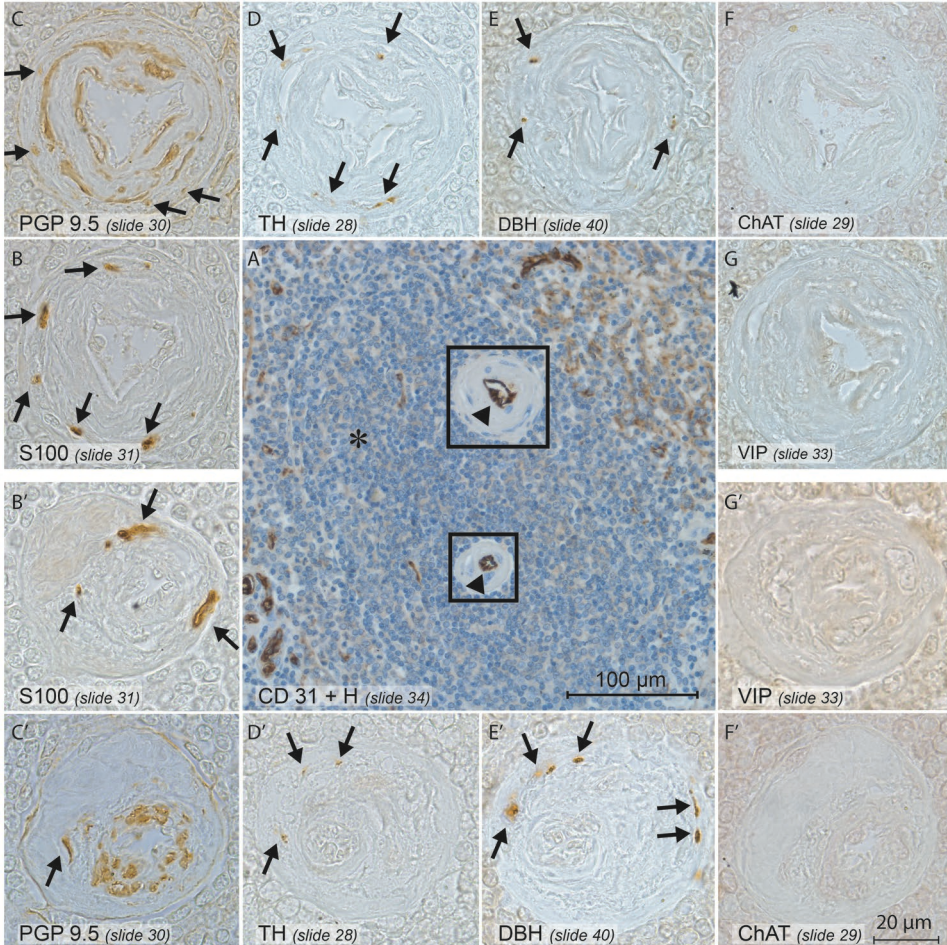


**Figure 4.2** Serial sections showing nerves in the adventitia of central arteries. Arrows show stained nerves. Magnifications of the corresponding central arteries, indicated by the rectangles, are shown. A: CD 31 + haematoxylin double-staining demonstrates endothelium of central arteries (arrowheads). B: S-100 staining and C: PGP 9.5 staining (general nervous tissue markers). D: Tyrosine hydroxylase (TH) and E: Dopamine  $\beta$ -hydroxylase (DBH) staining of catecholaminergic nerves. F: Absence of choline acetyltransferase (ChAT) staining (cholinergic phenotyping; for a positive control see Figures 4.5 and 4.6). G: Absence of vasoactive polypeptide staining (VIP) (for a positive control see Supplemental Figure S4.2). \*: follicle (white pulpa)

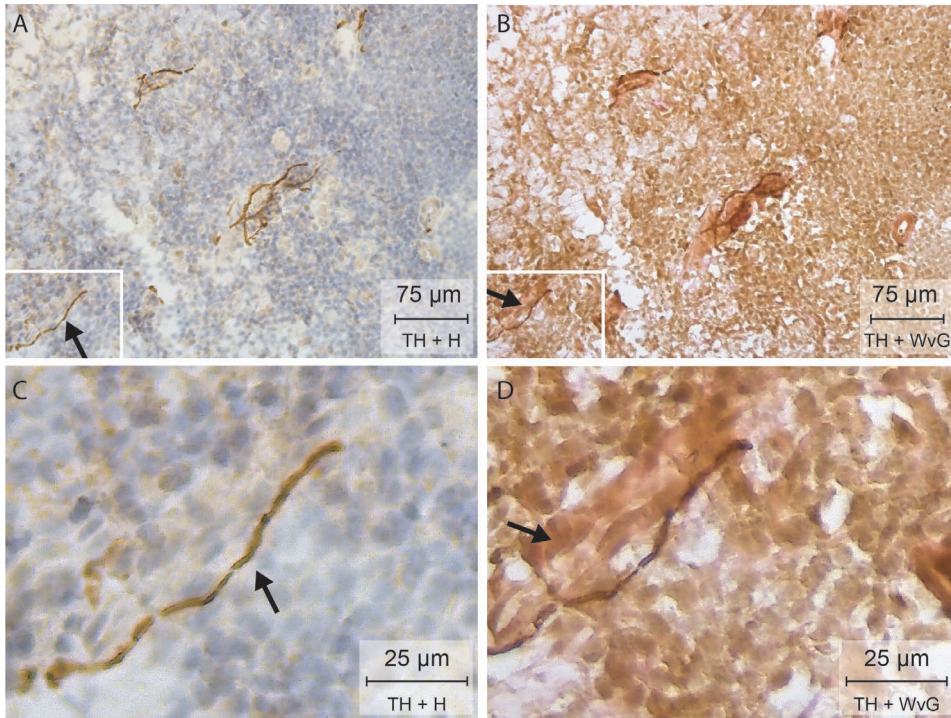


**Figure 4.3 Nerves in the adventitia of arteries.** A: Tyrosine hydroxylase (TH) + haematoxylin (H) staining (15 µm thick slide) demonstrating catecholaminergic nerve fibres (brown). C and D are magnifications of the insets in A and B, respectively. Although nerves do not seem to be associated with other structures in the pulpa (arrows A + C), double staining with Weigert van Gieson (WvG) and TH (B + D) reveals that all nerves are associated with the adventitia of red pulpal arterioles (reddish-brown).

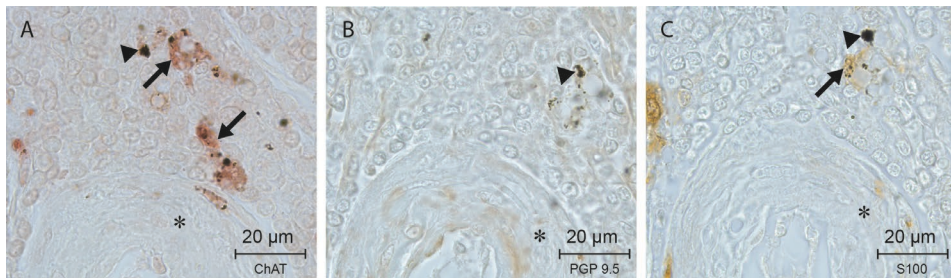


**Figure 4.4 Non-neural expression of ChAT close to a central artery (indicated by asterisks).** A: choline acetyltransferase (ChAT) staining (arrows) of macrophages. B: Absence of PGP 9.5 neural staining in an adjacent section of the same area. C: False-positive S-100 staining (arrow). A-C: Black dots represent phagocytosed material (indicated by arrowheads).

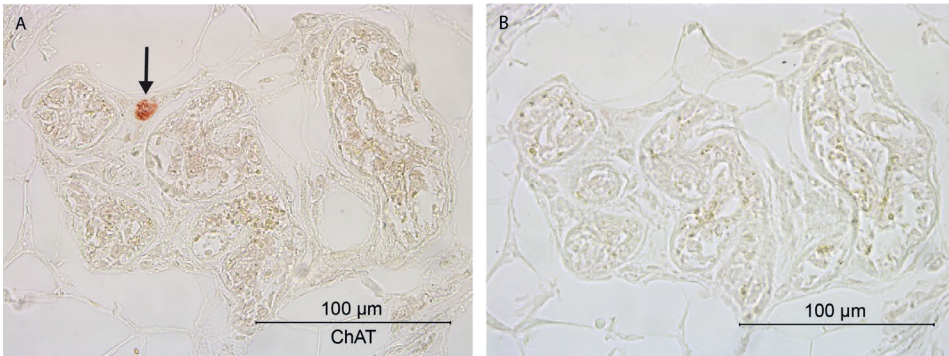


**Figure 4.5** Positive and negative controls for choline acetyltransferase staining. A: cholinergic nerve (arrow) innervating human axillary sweat gland. B: corresponding adjacent section of A showing negative control.

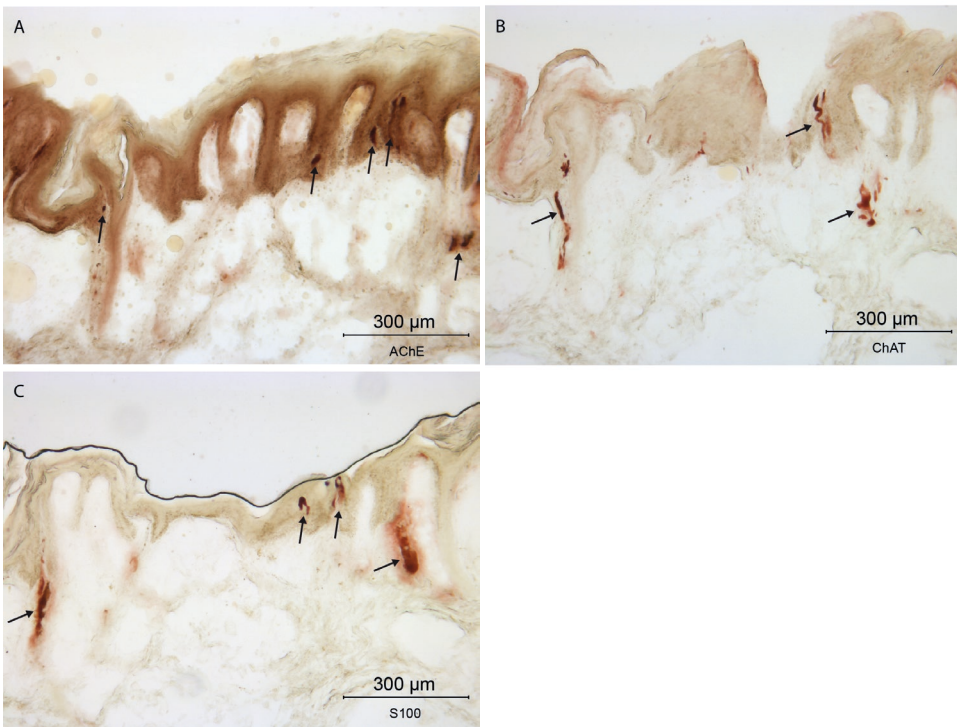


**Figure 4.6** Positive controls for acetylcholinesterase and choline acetyltransferase staining. Human skin samples were stained for AChT and ChAT (non-fixed, fresh frozen cryoslides). Positive nerves innervating the skin are indicated by arrows. A: acetylcholinesterase-positive nerves (cholinergic phenotyping). B: choline acetyltransferase-positive nerves (cholinergic phenotyping). C: S100 (general nervous tissue marker). Black line represents light diffraction at stratum corneum.

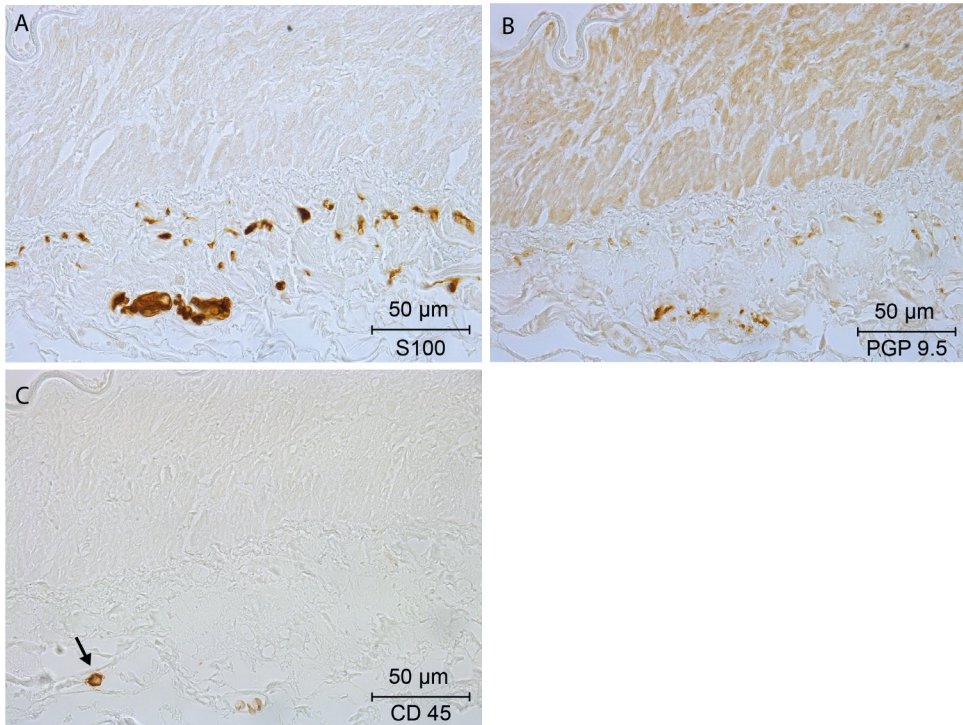


**Figure 4.7 PGP 9.5 vs S100 staining.** Comparison of panels A and B shows more limited distribution of PGP 9.5 staining of nerves (B) compared to the S100 distribution (A) because of its characteristic restriction to the thin axoplasm. No false-positive staining of leukocytes (identified by CD45) by S100 (compare panels A and C) was observed. (The intravascular leukocyte in panel C is indicated by an arrow).

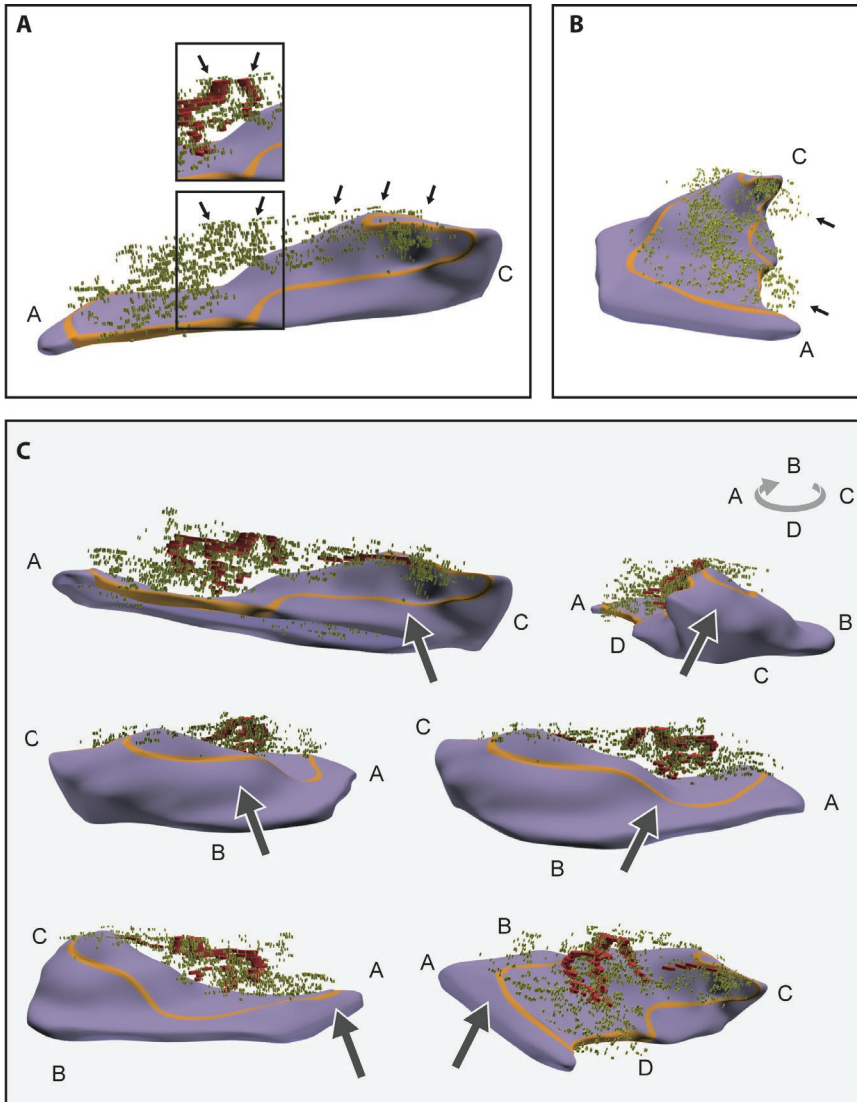


**Figure 4.8 Screenshots of the 3D reconstruction.** A: nerves (greenish-yellow) in the hilum of the spleen (purple). The boundary of the hilum is outlined in orange. A: Lateral view showing that nerves to the tips of the spleen (indicated with A and C) arise from the hilar splenic plexus (arrows). Detail of hilar splenic plexus around the splenic artery (red) is shown in the inset. B: View showing that not all nerves approaching the splenic hilum enter the spleen (arrows). C: Screenshots from different angles (letters A-D indicate the four sides of the spleen), demonstrate that nerves do not enter the spleen outside the hilar area. The arrows indicate regions of the spleen outside the hilar area that are all free of nerves. The nerves are shown as separate dots rather than continuous structures, since slides were sampled every 200  $\mu\text{m}$ . No smoothing filter has been applied, nor have (interpretative) connections between the nerve dots been drawn. For a better 3D impression, it is advised to inspect the interactive 3D-PDF (Supplemental Figure S4.3).

## Discussion

In this study, we demonstrated that all nerves innervating the spleen are present in the plexus surrounding the branches of the splenic artery. We observed catecholaminergic nerves entering the splenic parenchyma in the adventitia of the trabecular arteries, white pulpal central arteries and red pulpal arterioles, but found no enzymatic or immunohistochemical evidence for the presence of cholinergic innervation.

### Methodological considerations

We characterized splenic innervation histologically, using a complete hilum-embedding approach and 3D reconstruction. We used this comprehensive approach, because the spleen possesses a complex anatomical architecture without consistent segmental arterial (and nerve) supply,<sup>19-22</sup> and vascular branches to stomach, pancreas and greater omentum also stem from the distal end of the splenic artery.

Because of the relatively long time interval between death and fixation, the use of cadavers is suboptimal to underscore a negative finding based on the detection of intact and still functional proteins. For this reason, we included, in addition to the standard formalin fixation of the bodies (fixed <24h post mortem), non-fixed frozen (<24h post mortem) and 4h-post-mortem non-fixed, non-frozen specimens in our analysis. Irrespective of the type of preservation (formalin-fixed, fresh-frozen, or non-fixed, non-frozen), fixation (fixed before embedding or after sectioning (cryoslides) or staining techniques used (enzyme-histochemical and immunohistochemical), the outcome of the analyses did not change, in agreement with earlier studies.<sup>16,17</sup>

The age of the cadavers in this study ranged from 58 to 101 years, with two-thirds between 73 and 95 years of age. It has been reported in rats that ageing is associated with a reduction in the density of intrasplenic noradrenergic nerves.<sup>30,31</sup> However, this decline in noradrenergic nerve density is strain-dependent<sup>31</sup> and already present at midlife without further decline later in life in at least some rat strains.<sup>32</sup> Furthermore, the same group was unable to demonstrate cholinergic innervation in young adult rat spleens.<sup>8</sup> Since we did observe catecholaminergic innervation in all our samples, a direct effect of age on our conclusions seems unlikely. The effects of ageing on lymphoid-organ innervation do show, nevertheless, that validation in young adult subjects is important.

Our strategy to search and characterize splenic innervation was based on identifying catecholaminergic and cholinergic nerves that enter the spleen by their co-expression of



the neural markers S-100 and PGP 9.5, since non-axonal cholinergic, catecholaminergic and VIP-ergic staining has been observed in the gastrointestinal tract, spleen and testis by us and others.<sup>14,33-35</sup> We required the co-expression of two pan-neural markers, since the periarterial lymphatic sheath,<sup>36</sup> interdigitating reticulum cells<sup>37</sup> and macrophages<sup>17</sup> in the spleen show immunoreactivity with S-100, as we also observed in the present study. Although some reports claim that PGP 9.5 does not stain all nerves,<sup>38</sup> its main limitation in our hands was that it only stained the thin axoplasm of nerves. Although we did find macrophages expressing choline-acetyltransferase (which does fit in the theory of the inflammatory reflex<sup>39</sup>), our findings underscore the few reports on human splenic innervation<sup>16-18</sup> that failed to find evidence for cholinergic innervation, despite using validated histological techniques. Since VIP is a frequently co-expressed peptide in cholinergic nerves and often used to identify cholinergic nerves<sup>26</sup> and since VIP-positive nerves were found in rat spleens,<sup>40</sup> we also looked for its expression. The co-expression of VIP and TH /DBH in neurons of the thoracic sympathetic chain ganglia of the pig shows, however, that VIP is not a very reliable marker for cholinergic nerves.<sup>41-43</sup>

### Potential roles of periarteriolar catecholaminergic innervation

Synaptic contacts between tyrosine hydroxylase-positive nerve terminals and lymphocytes have been identified in the spleens of mice, rats, cats and dogs<sup>5,6,44-48</sup> and these lymphocytes are hypothesized to be the targets of these nerves.<sup>39</sup> Recently, a similar assumption was made based on the observation that nerves run freely within the human pulpa in close apposition to leukocytes.<sup>11</sup> In line with previous EM studies,<sup>16</sup> we, however, did not encounter such nerves within the splenic pulpa. Although the immunostain suggested that such free nerve endings existed, double staining with Weigert van Gieson revealed the presence of a vascular adventitia surrounding the nerve ending.

Instead of directly innervating leukocytes, these peripheral extensions may exert a chemotactic function, since stromal cells express the B2 adrenergic receptor and produce the chemokine CXCL13 which together recruit lymphocytes.<sup>49</sup> In support of such a scenario, we found that the perivascular nerve branches were present up to the level of white pulpal central arteries and red pulpal arterioles.

The absence of direct synaptic contacts between nerves and lymphocytes does, however, not rule out noradrenaline signalling to lymphocytes, since some lymphocytes express adrenoceptors.<sup>39</sup> The spleen has a unique open circulation, in which a reticular connective tissue forms non-endothelial vascular spaces in which lymphocytes move freely, enabling the immunological process of 'homing'. It has been proposed that these

minute connective tissue spaces serve as noradrenaline channels that allow paracrine signalling to the adrenoreceptors on immune cells.<sup>50,51</sup>

### A cholinergic phenotype does not necessarily identify vagal nerves in the peripheral autonomic nervous system

The lack of cholinergic nerves in the rodent spleen led previously to the hypothesis that the spleen is innervated indirectly by the vagus nerve via a synapse in the celiac ganglion.<sup>3</sup> Some authors have claimed retrograde labelling of the dorsal motor nucleus of the vagus nerve in rodents via a supra- and infra-hilar route (i.e. via the tips of the spleen),<sup>13,52</sup> but other studies have failed to label vagus nuclei after applying label in splenic tissue at different sides along the hilar axis.<sup>9</sup> We did not encounter nerve cell bodies close to or within the spleen, as is typical for vagus nerve targets. To further address the issue of vagal innervation via the tips of the spleen, we reconstructed the vessels and all nerves in the splenic mesentery and hilum of one cadaver. This reconstruction showed that nerves that entered via the tips of the spleen all arose from the periarteriolar hilar plexus. Another argument for vagal innervation of the spleen via its tips was the lack of staining of these nerves for TH.<sup>13,52</sup> However, lack of TH staining does not necessarily imply a vagal identity.

Vagal nerve fibres and cholinergic phenotype do not necessarily correspond. Cholinergic neurons are not only characteristic for sympathetic preganglionic nerves, but are also often present in the sympathetic postganglionic nerves. The best-known example is the cholinergic innervation of the sweat glands and arrector pili muscles. Furthermore, it was recently proposed that the pelvic splanchnic nerves are best described as having a sympathetic origin.<sup>53</sup> while most of its postganglionic fibres are cholinergic. Similarly, it has been suggested that cholinergic fibres in mouse spleen originate from sympathetic neurons located in the para- and/or prevertebral ganglia.<sup>14</sup> Although these proposals spark much debate, the boundaries between ortho- and parasympathic innervation seem to be blurring. We demonstrated recently, for instance, that a substantial fraction of the nerve fibres within the vagus nerve is catecholaminergic.<sup>54</sup> These catecholaminergic fibres are not found in the intra-cranial part of the vagus nerve, implying that they arise from communicating fibres that originate from the superior cervical, stellate and thoracic ganglia.<sup>54-58</sup> The possibility that catecholaminergic (or other non-cholinergic, non-vipergic) fibres that travel in the vagus nerve (and will be activated during vagal stimulation) contribute to the innervation of the human spleen is, therefore, an interesting hypothesis.

## Literature

1. Elenkov IJ, et al. The sympathetic nerve--an integrative interface between two supersystems: the brain and the immune system. *Pharmacol Rev.* 2000;52(4):595-638.
2. Nance DM, Sanders VM. Autonomic innervation and regulation of the immune system (1987-2007). *Brain Behav Immun.* 2007;21(6):736-745.
3. Rosas-Ballina M, et al. Splenic nerve is required for cholinergic antiinflammatory pathway control of TNF in endotoxemia. *Proc Natl Acad Sci U S A.* 2008;105(31):11008-11013.
4. Tranzer JP, Thoenen H. Elektronenmikroskopische Untersuchungen am peripheren sympathischen Nervensystem der Katze; physiologische und pharmakologische Aspekte. *Naunyn-Schmiedebergs Arch. Pharmak. Exp. Path.* 1967;257:73-75.
5. Fillenz M. The innervation of the cat spleen. *Proc R Soc Lond B Biol Sci.* 1970;174(1037):459-468.
6. Reilly FD, McCuskey RS, Meineke HA. Studies of the hemopoietic microenvironment. VIII. Andrenergic and cholinergic innervation of the murine spleen. *Anat Rec.* 1976;185(1):109-117.
7. Nance DM, Burns J. Innervation of the spleen in the rat: evidence for absence of afferent innervation. *Brain Behav Immun.* 1989;3(4):281-290.
8. Bellinger DL, et al. Acetylcholinesterase staining and choline acetyltransferase activity in the young adult rat spleen: lack of evidence for cholinergic innervation. *Brain Behav Immun.* 1993;7(3):191-204.
9. Cano G, et al. Characterization of the central nervous system innervation of the rat spleen using viral transneuronal tracing. *J Comp Neurol.* 2001;439(1):1-18.
10. Bratton BO, et al. Neural regulation of inflammation: no neural connection from the vagus to splenic sympathetic neurons. *Exp Physiol.* 2012;97(11):1180-1185.
11. Hoover DB, et al. Loss of Sympathetic Nerves in Spleens from Patients with End Stage Sepsis. *Front Immunol.* 2017;8:1712.
12. Stöhr PH, Jr. *Mikroskopische Anatomie des vegetativen Nervensystems., in Handbuch der Mikroskopischen Anatomie des Menschen.* Springer: Berlin-Göttingen-Heidelberg. 1957.
13. Buijjs RM, et al. Spleen vagal denervation inhibits the production of antibodies to circulating antigens. *PLoS One.* 2008;3(9):e3152.
14. Gautron L, et al. Neuronal and nonneuronal cholinergic structures in the mouse gastrointestinal tract and spleen. *J Comp Neurol.* 2013;521(16):3741-3767.
15. Anderson C, et al. Letter to the editor: Parasympathetic innervation of the rodent spleen? *Am J Physiol Heart Circ Physiol.* 2015;309(12):H2158.
16. Heusermann U, Stutte HJ. Electron microscopic studies of the innervation of the human spleen. *Cell Tissue Res.* 1977;184(2):225-236.
17. Anagnostou VK, et al. Ontogeny of intrinsic innervation in the human thymus and spleen. *J Histochem Cytochem.* 2007;55(8):813-820.
18. Kudoh G, Hoshi K, Murakami T. Fluorescence microscopic and enzyme histochemical studies of the innervation of the human spleen. *Arch Histol Jpn.* 1979;42(2):169-180.
19. Skandalakis PN, et al. The surgical anatomy of the spleen. *Surg Clin North Am.* 1993;73(4):747-768.
20. Michels NA. Variations in the blood-supply of the liver, gall bladder, stomach, duodenum, pancreas and spleen; 200 dissections. *Am J Med Sci.* 1948;216(1):115.
21. Garcia-Porrero JA, Lemes A. Arterial segmentation and subsegmentation in the human spleen. *Acta Anat (Basel).* 1988;131(4):276-283.
22. Vandamme JP, Bonte J. Systematisation of the arteries in the splenic hilus. *Acta Anat (Basel).* 1986; 125(4):217-224.
23. Gonzalez-Martinez T, et al. S-100 proteins in the human peripheral nervous system. *Microsc Res Tech.* 2003;60(6):633-638.
24. Krammer HJ, et al. Immunohistochemical visualization of the enteric nervous system using antibodies against protein gene product (PGP) 9.5. *Ann Anat.* 1993;175(4):321-325.
25. Kobayashi H, et al. A rapid technique of acetylcholinesterase staining. *Arch Pathol Lab Med.* 1994; 118(11):1127-1129.

26. Lindh B, Hokfelt T. Structural and functional aspects of acetylcholine peptide coexistence in the autonomic nervous system. *Prog Brain Res.* 1990;84:175-191.
27. Hiksloops JP, et al. Development of the human infrahepatic inferior caval and azygos venous systems. *J Anat.* 2015;226(2):113-125.
28. Standing S. *Gray's Anatomy, The Anatomical Basis of Clinical Practice.* 41st Revised ed. 2016: Elsevier Health Sciences.
29. Brendolan A, et al. Development and function of the mammalian spleen. *Bioessays.* 2007;29(2):166-177.
30. Bellinger DL, et al. A longitudinal study of age-related loss of noradrenergic nerves and lymphoid cells in the rat spleen. *Exp Neurol.* 1992;116(3):295-311.
31. Bellinger D, et al. Age-related changes in noradrenergic sympathetic innervation of the rat spleen is strain dependent. *Brain Behav Immun.* 2002;16(3):247-261.
32. Perez SD, et al. Sympathetic innervation of the spleen in male Brown Norway rats: a longitudinal aging study. *Brain Res.* 2009;1302:106-117.
33. Schirmer SU, et al. The cholinergic system in rat testis is of non-neuronal origin. *Reproduction.* 2011;142(1):157-166.
34. Qiu YH, et al. Expression of tyrosine hydroxylase in lymphocytes and effect of endogenous catecholamines on lymphocyte function. *Neuroimmunomodulation.* 2004;11(2):75-83.
35. Zhang QL, et al. Vasoactive intestinal peptide: mediator of laminin synthesis in cultured Schwann cells. *J Neurosci Res.* 1996;43(4):496-502.
36. Uccini S, et al. Immunoreactivity for S-100 protein in dendritic and in lymphocyte-like cells in human lymphoid tissues. *Virchows Arch B Cell Pathol Incl Mol Pathol.* 1986;52(2):129-141.
37. Nakajima T, et al. S-100 protein in Langerhans cells, interdigitating reticulum cells and histiocytosis X cells. *Gan.* 1982;73(3):429-432.
38. Eaker EY, Sallustio JE. The distribution of novel intermediate filament proteins defines subpopulations of myenteric neurons in rat intestine. *Gastroenterology.* 1994;107(3):666-674.
39. Rosas-Ballina M, et al. Acetylcholine-synthesizing T cells relay neural signals in a vagus nerve circuit. *Science.* 2011;334(6052):98-101.
40. Bellinger DL, et al. Vasoactive intestinal polypeptide (VIP) innervation of rat spleen, thymus, and lymph nodes. *Peptides.* 1997;18(8):1139-1149.
41. Hill EL, Elde R. Vasoactive intestinal peptide distribution and colocalization with dopamine-beta-hydroxylase in sympathetic chain ganglia of pig. *J Auton Nerv Syst.* 1989;27(3):229-239.
42. Majewski M. Synaptogenesis and structure of the autonomic ganglia. *Folia Morphol (Warsz).* 1999;58(3 Suppl 2):65-99.
43. Gazza F, et al. Double labelling immunohistochemistry on the peripheral autonomic neurons projecting to the bulbospongiosus muscle in male impuberal pigs. *Vet Res Commun.* 2003;27 Suppl 1:603-605.
44. Felten DL, et al. Noradrenergic sympathetic innervation of the spleen: I. Nerve fibers associate with lymphocytes and macrophages in specific compartments of the splenic white pulp. *J Neurosci Res.* 1987;18(1):28-36, 118-121.
45. Felten SY, Olschowka J. Noradrenergic sympathetic innervation of the spleen: II. Tyrosine hydroxylase (TH)-positive nerve terminals form synaptolike contacts on lymphocytes in the splenic white pulp. *J Neurosci Res.* 1987;18(1):37-48.
46. Kirpekar SM, Wakade AR, Prat JC. Histochemical demonstration for the release of norepinephrine from the sympathetic nerves in the cat spleen. *Experientia.* 1972;28(1):36-37.
47. Dahlstroem AB, Zetterstroem BE. Noradrenaline Stores in Nerve Terminals of the Spleen: Changes during Hemorrhagic Shock. *Science.* 1965;147(3665):1583-1585.
48. Zetterstrom BE, et al. Possibilities of a direct adrenergic influence on blood elements in the dog spleen. *Acta Chir Scand.* 1973;139(2):117-122.
49. Murray K, et al. Neuroanatomy of the spleen: Mapping the relationship between sympathetic neurons and lymphocytes. *PLoS One.* 2017;12(7):e0182416.
50. Saito H. The relationship between the sympathetic nerves and immunocytes in the spleen. *Kaibogaku Zasshi.* 1991;66(1):8-19.
51. Vizi ES, et al. Neurochemical, electrophysiological and immunocytochemical evidence for a noradrenergic link between the sympathetic nervous system and thymocytes. *Neuroscience.* 1995;68(4):1263-1276.

52. Kooijman S, de Jonge WJ, Rensen PC. Reply to "Letter to the editor: Parasympathetic innervation of the rodent spleen?". *Am J Physiol Heart Circ Physiol*. 2015;309(12):H2159.
53. Espinosa-Medina I, et al. The sacral autonomic outflow is sympathetic. *Science*. 2016;354(6314):893-897.
54. Verlinden TJ, et al. Morphology of the human cervical vagus nerve: implications for vagus nerve stimulation treatment. *Acta Neurol Scand*. 2016;133(3):173-182.
55. Lundberg JM, et al. Efferent innervation of the small intestine by adrenergic neurons from the cervical sympathetic and stellate ganglia, studied by retrograde transport of peroxidase. *Acta Physiol Scand*. 1978;104(1):33-42.
56. Ahlman BH, et al. Evidence for innervation of the small intestine from the cervical sympathetic ganglia. *J Surg Res*. 1978;24(3):142-149.
57. Liedberg G, et al. Adrenergic contribution to the abdominal vagus nerves in the cat. *Scand J Gastroenterol*. 1973;8(2):177-180.
58. Muryobayashi T, et al. Fluorescence histochemical demonstration of adrenergic nerve fibers in the vagus nerve of cats and dogs. *Jpn J Pharmacol*. 1968;18(3):285-293.

## Supplemental materials

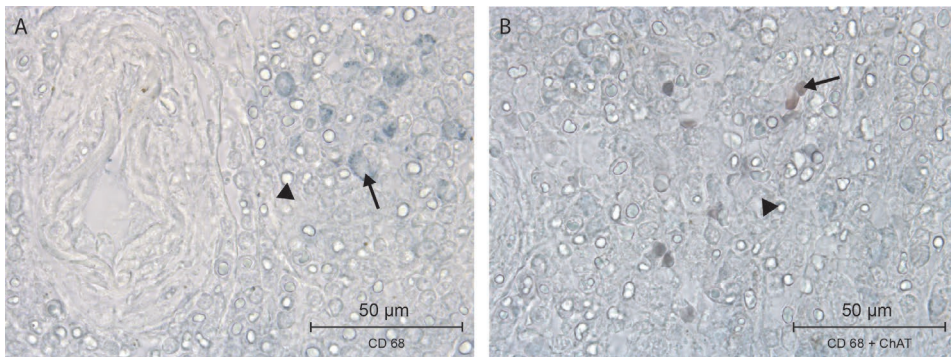


**Figure S4.1** Double staining of CD68 and ChAT of human splenic pulpa. A: CD68-positive staining of macrophages (blue, arrow). B: Double staining of CD68 positive-macrophages (blue) with ChAT (brown). The arrow indicates an example of overlap. The use of water-soluble mounting solution led to the formation of light diffraction artefacts (arrowheads).

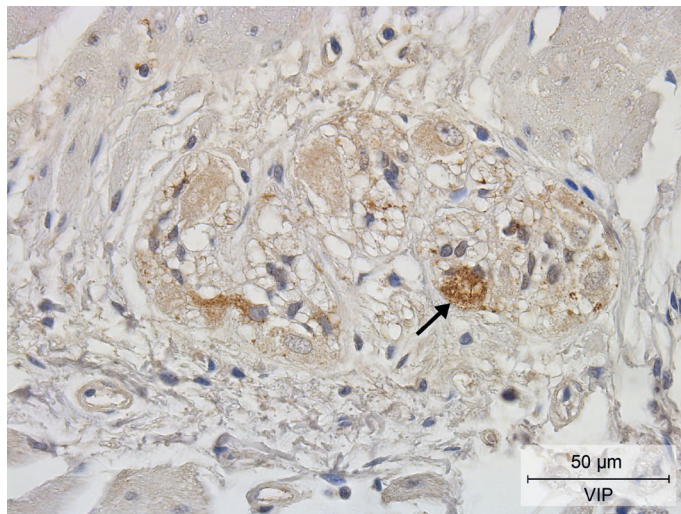


**Figure S4.2** Positive control for VIP staining in human ileum. Positive neural cell body and fibre staining can be observed (brown, arrow) in Auerbach's plexus. Haematoxylin counterstaining stains cell nuclei blue.

**Figure S4.3** 3D Reconstruction of innervation of spleen (Can be found online at <https://doi.org/10.1016/j.jbbi.2018.12.009>). 3D reconstruction showing nerves (greenish-yellow) entering the spleen (purple). The boundary of the hilum is indicated with an orange line. Note that not all arteries (red) were reconstructed. The nerves are shown as separate dots rather than continuous structures, since slides were sampled every 200 µm. No smoothing filter has been applied, nor have (interpretative) connections between the nerve dots been drawn. Instructions for working with the interactive 3D model are shown upon opening this supplemental file. Note that the file (3D PDF) must be opened with Adobe Acrobat Reader ([www.adobe.com](http://www.adobe.com)).



# Chapter 5

General discussion

A systematic review on the distribution of catecholaminergic neurons in the peripheral nervous system and a critical reappraisal of the sympathetic-parasympathetic model

Thomas J.M. Verlinden, Wouter H. Lamers, Andreas Herrler, S. Eleonore Köhler

*Submitted as: "The perceived differences in the anatomy of the thoracolumbar and sacral autonomic outflow are quantitative only"*



## Abstract

### Introduction

We assembled all available data on the peripheral distribution of catecholaminergic neurons, and used the outcome to re-evaluate the anatomical arguments on which the present binary sympathetic-parasympathetic model is based.

### Methodology

Pubmed was searched for original studies in mammals that demonstrated the presence of catecholaminergic neurons immunohistochemically or confirmed communications between nerves and sympathetic structures with validated techniques.

### Results & discussion

144 Queries identified 1,239 studies providing information on 389 anatomical structures. 168 Studies fulfilled all inclusion criteria.

Catecholaminergic nerve fibers are present in many spinal and all cranial nerves and ganglia, including nerves and ganglia that are known for their parasympathetic function. Along the entire spinal autonomic outflow pathways, both proximal and distal catecholaminergic cell bodies are common in the head, thoracic and abdominal and pelvic region, which invalidates the “short versus long pre-ganglionic neuron” argument. These findings further demonstrate that neurons are not dedicated to specific nerves, and shows that the concept of the connectome in the brain also applies to the peripheral nervous system.

Contrary to the classically confined outflow levels T1-L2 and S2-S4, preganglionic neurons have been found at the lower lumbar level. Preganglionic cell bodies that are located in the intermediolateral zone of the thoracolumbar spinal cord, gradually nest more ventrally within the ventral motor nuclei at the lumbar and sacral levels and their fibers bypass the white ramus communicans and sympathetic trunk, to emerge directly from the spinal roots. Bypassing the sympathetic trunk, therefore, is not exclusive for the sacral outflow. We conclude that the anatomy of the autonomic outflow displays a conserved architecture along the entire spinal axis.

## Introduction

The universally accepted model of the sympathetic and parasympathetic efferent limbs of the autonomic nervous system was formulated at the turn of the 19<sup>th</sup> to the 20<sup>th</sup> century.<sup>1</sup> In addition to physiological and pharmacological criteria, anatomical arguments have been invoked to define the sympathetic-parasympathetic model.<sup>2-4</sup> These anatomic arguments have three main components. The first argument relates to the bimodal distribution of peripheral cell bodies, with the sympathetic cell bodies located in ganglia close to the central nervous system, and the parasympathetic cell bodies in a distal position, within or close to the wall of target organs. A second argument involves the absence of white rami communicantes at the sacral level. In contrast to the sympathetic thoracolumbar outflow, preganglionic neurons at the sacral level bypass the sympathetic trunk. Pelvic splanchnic nerves arise, therefore, directly from the sacral plexus. The third argument concerns the gap in the central autonomic outflow at the lumbar level. As the autonomic outflow concentrates around the T1-L2 and S2-S4 levels, the preganglionic neurons do not appear as a continuous cell-column. The parallel between the parasympathetic cranial and sacral outflows is therefore often drawn.

Recently, the sympathetic-parasympathetic model was challenged by demonstrating that the autonomic outflows at the thoracolumbar and sacral levels possess a highly similar molecular signature.<sup>5</sup> This paradigm shift met with considerable resistance,<sup>6-10</sup> largely because it contradicted a longstanding concept. In this review, we re-evaluate the anatomical arguments that are used to support the sympathetic-parasympathetic model. First, we describe the distribution of catecholaminergic neurons in the peripheral nervous system. We show that such neurons are found in parasympathetic, spinal and cranial nerves and ganglia throughout the body. Catecholaminergic cell bodies also have a widespread peripheral distribution, including distal locations not only in the abdominal and pelvic, but also in the thoracic region and the head, including nerves and ganglia that are known for their parasympathetic function. The observed mixed composition of ganglia and nerves throughout the body contradicts the argument of the bimodal distribution of cell bodies. These findings further demonstrate that neurons are not dedicated to specific nerves, and suggest that the peripheral nervous system functions as a connection matrix.

The two other anatomical arguments mentioned above also do not hold up to scrutiny. Contrary to the classical model, we will show that preganglionic neurons are present within in the lumbar gap. Whereas the intermediolateral nucleus is well defined in the

thoracolumbar spinal cord, the preganglionic cell bodies at the sacral level are found not only in the intermediolateral zone, but also in the ventral horn. This ventral extension is a gradual process that already starts at the lower thoracic level. A second, probably correlated change is that these ventral lumbar preganglionic neurons, like the sacral, tend to bypass the sympathetic trunk. Bypassing the sympathetic trunk, therefore, is not exclusive for the sacral outflow. We conclude that the anatomy of the autonomic outflow displays a conserved architecture along the entire spinal axis, albeit that a gradient in characteristics is observed.

## Methods

### Data source and study selection

Abstracts, titles and MESH entry terms in Pubmed were searched to identify original studies that either established the existence of catecholaminergic neurons histologically by demonstrating the presence of the enzymes tyrosine hydroxylase or dopamine  $\beta$ -hydroxylase, or confirmed communications between nerves and sympathetic structures with validated techniques, such as neural tract tracing, experimental neural degeneration, crushing or denervation, and neural recordings. Studies relying on macroscopic dissections alone were not included. Languages were restricted to English and German. Only mammalian species were included. Search terms included every nervous structure listed in the Anatomical Terminology<sup>11</sup> under the headings 'cranial nerves', 'spinal nerves' and 'parasympathetic part of autonomic part of peripheral nervous system'. The last search was performed on November 28<sup>th</sup>, 2021. The reference lists of retrieved articles were also reviewed for additional studies that fulfilled the search criteria.

### Search strategy for the systematic literature search

The search of each structure consisted of two separate approaches. The first approach looked for the histologically confirmed presence of catecholaminergic neurons, and was executed by combining the entry terms of tyrosine hydroxylase or dopamine  $\beta$ -hydroxylase with (query term: *AND*) the nervous structure of interest. The second approach searched for communications between nerves and sympathetic structures, using the entry terms of sympathetic structures listed in the Anatomical Terminology<sup>11</sup> *AND* the nervous structures from search 1, *AND* neuroanatomical tract-tracing techniques (Mesh) *OR* horseradish peroxidase (Mesh) *OR* communication *OR*

communicating OR communications OR anastomosis OR anastomosing OR connecting OR connection.

## Findings and discussion

### The distribution of catecholaminergic neurons

A total of 43 queries for the cranial and 101 for the spinal nerves were performed, which provided information on 389 anatomical structures in 996 and 243 identified studies, respectively. All abstracts were screened for the inclusion criteria with respect to applied techniques, language and species, resulting in 168 eligible studies (Table 5.1 and online interactive Table 2 (extended Microsoft Excel-based Table)). Sixty references from the 19<sup>th</sup> and 20<sup>th</sup> centuries were found that studied the anatomical arguments upon which the sympathetic-parasympathetic model was built (online interactive Table 5.3).

#### *Nerve fibers*

Throughout the body, catecholaminergic nerve fibers have been demonstrated in many spinal and all cranial nerves and ganglia (Table 5.1). Catecholaminergic nerve fibers are also present in established parasympathetic nerves,<sup>4,11</sup> such as the greater petrosal nerve in mice, rats, cats, and monkeys<sup>12-15</sup> and the pelvic splanchnic nerves in humans.<sup>16-18</sup> We found no species-specific differences. Although we focused on mammals, we also encountered similar observations in birds<sup>19,20</sup> and amphibia,<sup>21,22</sup> suggesting evolutionary conservation of the observed features.

**Table 5.1** List of nerves containing catecholaminergic neurons or demonstrated communications with sympathetic structures.

Nerve	First author, year and reference	Species		Nerve	First author and reference	Species
Oculomotor	Oikawa, 2004 <sup>204</sup>	Human		Trochlear	Hosaka, 2014 <sup>75</sup>	Human
	Maklad, 2001 <sup>15</sup>	Mouse			Oikawa, 2004 <sup>204</sup>	Human
Trigeminal, ciliary, submandibular, pterygopalatine, otic, trigeminal ganglion	Ruskell, 1983 <sup>205</sup>	Monkey		Abducens	Maklad, 2001 <sup>15</sup>	Mouse
	Teshima, 2019 <sup>77</sup>	Mouse	X, *(Hand2+)		Oikawa, 2004 <sup>204</sup>	Human
	Hosaka, 2016 <sup>206</sup>	Human		Facial, geniculate ganglion	Maklad, 2001 <sup>15</sup>	Mouse
	Matsubayashi, 2016 <sup>207</sup>	Human			Lyon, 1992 <sup>208</sup>	Cynomolgus
	Yamauchi, 2016 <sup>76</sup>	Human	X	Johnston, 1974 <sup>209</sup>	Human	
	Hosaka, 2014 <sup>75</sup>	Human	X	Ohman-Gault, 2017 <sup>210</sup>	Mouse	
	Szczurkowski, 2013 <sup>71</sup>	Chinchilla	X	Matsubayash, 2016 <sup>207</sup>	Human	
	Kiyokawa, 2012 <sup>58</sup>	Human fetus	X	Yamauchi, 2016 <sup>76</sup>	Human	
	Rusu, 2010 <sup>211</sup>	Human		Hosaka, 2014 <sup>75</sup>	Human	
	Thakker, 2008 <sup>67</sup>	Human	X	Reuss, 2009 <sup>212</sup>	Rat	

Table 5.1 (continued)

Nerve	First author, year and reference	Species		Nerve	First author and reference	Species	
Trigeminal, ciliary, submandibular, pterygopalatine, otic, trigeminal ganglion (cont'd)	Kaleczyc, 2005 <sup>66</sup>	Pig	X, *(DBH+)	Facial, geniculate ganglion (cont'd)	Maklad, 2001 <sup>15</sup>	Mouse	
	Reynolds, 2005 <sup>24</sup>	Rat	X, *(DBH+)		Johansson, 1998 <sup>213</sup>	Rat	
	Maklad, 2001 <sup>15</sup>	Mouse			Shibamori, 1994 <sup>14</sup>	Rat	
	Grimes, 1998 <sup>65</sup>	Rhesus Monkey	X, *(DBH+)		Takeuchi, 1993 <sup>214</sup>	Cynomolgus	
	Kirch, 1995 <sup>63</sup>	Human	X		Fukui, 1992 <sup>215</sup>	Cat	
	Ng, 1995 <sup>74</sup>	Rat, Monkey	X		Anniko, 1987 <sup>170</sup>	Mouse	*(NA+)
	Tan, 1995 <sup>64</sup>	Cat, Monkey	X		Matthews, 1986 <sup>13</sup>	Cat	
	Simons, 1994 <sup>70</sup>	Rat	X, *(DBH+)		Wilson, 1985 <sup>12</sup>	Cynomolgus, Rhesus	
	Marfurt, 1993 <sup>23</sup>	Rat, Guinea pig	X		Thomander, 1984 <sup>216</sup>	Cat	
	Tyrrell, 1992 <sup>62</sup>	Rat	X		Schimozaawa, 1978 <sup>217</sup>	Mouse	
	Shida, 1991 <sup>73</sup>	Rat	X		Yamauchi, 2016 <sup>76</sup>	Human	
	Soinila, 1991 <sup>72</sup>	Rat	X		Shibamori, 1994 <sup>14</sup>	Rat	
	Yau, 1991 <sup>218</sup>	Cat			Hozawa, 1993 <sup>158</sup>	Guinea Pig	*(DBH+)
	ten Tusscher, 1989 <sup>219</sup>	Rat			Yamashita, 1992 <sup>220</sup>	Guinea Pig	
	Kuwayama, 1988 <sup>69</sup>	Rat	X		Hozawa, 1990 <sup>157</sup>	Cynomolgus	*(DBH+)
	Landis, 1987 <sup>60</sup>	Rat	X, *(DBH+)		Anniko, 1987 <sup>170</sup>	Mouse	*(NA+)
	Uemura, 1987 <sup>61</sup>	Japanese Monkey, Cat, Dog	X		Paradies-garten, 1976 <sup>221</sup>	Cat	
	Jonakait, 1984 <sup>48</sup>	Rat (embryo)	X		Densert, 1975 <sup>171</sup>	Rabbit and Cat	*(NA+)
	Lackovic, 1981 <sup>169</sup>	Human	*(NA+)				
	Glossopharyngeal, petrosal ganglion	Oda, 2013 <sup>78</sup>	Human		X	Vagus, superior (nodose) ganglion	Bookout, 2021 <sup>46</sup>
Ichikawa, 2007 <sup>36</sup>		Rat	X	Verlinden, 2016 <sup>79</sup>	Human		X, *(DBH+)
Matsumoto, 2003 <sup>222</sup>		Rat		Hosaka, 2014 <sup>75</sup>	Human		
Wang, 2002 <sup>35</sup>		Rat	X	Seki, 2014 <sup>223</sup>	Human		
Satoda, 1996 <sup>225</sup>		Cynomolgus		Onkka, 2013 <sup>224</sup>	Dog		
Ichikawa, 1995 <sup>33</sup>		Rat	X	Ibanez, 2010 <sup>61</sup>	Human		X
Ichikawa, 1993 <sup>32</sup>		Rat	X	Kawagishi, 2008 <sup>37</sup>	Human		X
Helke, 1991 <sup>31</sup>		Rat	X	Ichikawa, 2007 <sup>36</sup>	Rat		X
Helke, 1990 <sup>28</sup>		Rat	X	Matsumoto, 2003 <sup>222</sup>	Rat		
Katz, 1990 <sup>29</sup>		Rat	X	Nozdrachev, 2003 <sup>226</sup>	Cat		
Kummer, 1990 <sup>30</sup>		Guinea pig	X	Forgie, 2000 <sup>227</sup>	Mouse		
Katz, 1987 <sup>27</sup>		Rat	X	Yang, 1999 <sup>154</sup>	Rat		X, *(DBH+)
Katz, 1986 <sup>26</sup>		Rat	X	Gorbunova, 1998 <sup>44</sup>	Rabbit		
Jonakait, 1984 <sup>48</sup>		Rat (embryo)	X, *(DBH+)	Ichikawa, 1998 <sup>34</sup>	Rat		X
Katz, 1983 <sup>25</sup>		Rat	X	Sang, 1998 <sup>45</sup>	Mouse		X
			Ichikawa, 1996 <sup>42</sup>	Rat	X		
Accessory Hypoglossal	Hosaka, 2014 <sup>75</sup>	Human		Uno, 1996 <sup>43</sup>	Dog	X	
	Hosaka, 2014 <sup>75</sup>	Human		Fateev, 1995 <sup>228</sup>	Cat		
	Tubbs, 2009 <sup>82</sup>	Human	X	Ichikawa, 1995 <sup>33</sup>	Rat	X	
	Tseng, 2005 <sup>229</sup>	Hamster		Zhuo, 1995 <sup>41</sup>	Rat	X	
	Tseng, 2001 <sup>230</sup>	Hamster		Zhuo, 1994 <sup>40</sup>	Rat	X	
	Hino, 1993 <sup>231</sup>	Dog		Kummer, 1993 <sup>38</sup>	Rat	X	
	Fukui, 1992 <sup>215</sup>	Cat		Yoshida, 1993 <sup>39</sup>	Cat	X	
	O'Reilly, 1990 <sup>232</sup>	Rat		Ruggiero, 1993 <sup>233</sup>	Rat		
				Dahlqvist, 1992 <sup>80</sup>	Rat	X, *(DBH+)	
	Greater auricular	Matsubayashi, 2016 <sup>207</sup>	Human				

Table 5.1 (continued)

Nerve	First author, year and reference	Species		Nerve	First author and reference	Species	
Phrenic	Verlinden, 2018 <sup>119</sup>	Human	*(DBH+)	Vagus, superior and inferior (nodose) ganglion (cont'd)	Helke, 1991 <sup>31</sup>	Rat	X
	Lackovic, 1981 <sup>169</sup>	Human	*(NA+)		Helke, 1990 <sup>28</sup>	Rat	X
Suprascapular	Hosaka, 2014 <sup>75</sup>	Human		Kummer, 1990 <sup>30</sup>	Guinea pig	X	
Mammary	Eriksson, 1996 <sup>234</sup>	Human, Rat		Ling, 1990 <sup>235</sup>	Hamster		
Lateral antebrachial cutaneous nerve of forearm (musculocutaneous)	Marx, 2011 <sup>236</sup>	Human		Baluk, 1989 <sup>237</sup>	Guinea pig		
	Marx, 2010 <sup>238</sup>	Human		Katz, 1987 <sup>27</sup>	Rat	X	
Radial	Marx, 2010 <sup>239</sup>	Human		Dahlqvist, 1986 <sup>174</sup>	Rat	*(NA+)	
Superficial branch of radial	Marx, 2010 <sup>239</sup>	Human		Lucier, 1986 <sup>240</sup>	Cat		
	Marx, 2011 <sup>236</sup>	Human		Matthews, 1986 <sup>13</sup>	Cat		
	Balogh, 1999 <sup>241</sup>	Human		Smith, 1986 <sup>242</sup>	Guinea Pig		
Palmar branch of ulnar	Marx, 2011 <sup>236</sup>	Human		Blessing, 1985 <sup>243</sup>	Rat		
Medial antebrachial cutaneous nerve of forearm	Marx, 2010 <sup>244</sup>	Human		Smith, 1985 <sup>245</sup>	Guinea pig		
Intercostal	Lackovic, 1981 <sup>169</sup>	Human	*(NA+)	Jonakait, 1984 <sup>48</sup>	Rat (embryo) X, *(DBH+)		
Genitofemoral	Lackovic, 1981 <sup>169</sup>	Human	*(NA+)	Katz, 1983 <sup>25</sup>	Rat	X	
Ilioinguinal	Lackovic, 1981 <sup>169</sup>	Human	*(NA+)	Hisa, 1982 <sup>246</sup>	Dog		
Sciatic	Creze, 2017 <sup>153</sup>	Human fetus		Lackovic, 1981 <sup>169</sup>	Human	*(NA+)	
	Hosaka, 2014 <sup>75</sup>	Human		Lundberg, 1978 <sup>247</sup>	Cat and Guinea Pig		
	Loesch, 2010 <sup>151</sup>	Rat		Ungváry, 1976 <sup>248</sup>	Cat		
	Castro, 2008 <sup>150</sup>	Rat		Nielsen, 1969 <sup>172</sup>	Cat	*(NA+)	
	Wang, 2002 <sup>249</sup>	Mouse		Tompkins, 1985 <sup>152</sup>	Human		
	Li, 1999 <sup>250</sup>	Rat		Jänig, 1984 <sup>251</sup>	Cat		
	Li, 1996 <sup>252</sup>	Rat		Ben-Jonathan, 1978 <sup>178</sup>	Cat	*(NA+)	
	Li, 1995 <sup>253</sup>	Rat					
	Li, 1994 <sup>255</sup>	Rat		Tibial	Koistinaho, 1991 <sup>254</sup>	Human fetus	
	Koistinaho, 1991 <sup>254</sup>	Human fetus		Sural	Fang, 2017 <sup>256</sup>	Rabbit	
				Pudendal	Nyangoh Timoh, 2017 <sup>257</sup>	Human fetus	
	D'Hooge, 1990 <sup>177</sup>	Dog	*(NA+)	Bertrand, 2016 <sup>258</sup>	Human fetus		
	Studelska, 1989 <sup>259</sup>	Rat		Hinata, 2015 <sup>260</sup>	Human		
	Dahlström, 1987 <sup>176</sup>	Rat	*(NA+)	Hieda, 2013 <sup>261</sup>	Human		
	Dahlström, 1986 <sup>175</sup>	Rat	*(NA+)	Alsaid, 2011 <sup>262</sup>	Human fetus		
	Larsson, 1986 <sup>168</sup>	Rat	*(DBH+, NA+)	Alsaid, 2009 <sup>263</sup>	Human fetus		
	Schmidt, 1984 <sup>167</sup>	Rat	*(DBH+)	Roppolo, 1985 <sup>264</sup>	Monkey		
	Larsson, 1984 <sup>166</sup>	Rat	*(DBH+, NA+)	Perineal	Moszkowicz, 2011 <sup>265</sup>	Human fetus	
	Evers- Von Bültzingslöwen, 1983 <sup>165</sup>	Rabbit	*(DBH+)		Colombel, 1999 <sup>266</sup>	Human	
	Dahlström, 1982 <sup>173</sup>	Rat	*(NA+)	Nerve to levator ani	Hinata, 2014 <sup>267</sup>	Human	
	Jakobsen, 1981 <sup>164</sup>	Rat	*(DBH+)		Hinata, 2014 <sup>268</sup>	Human	
	Häggendal, 1980 <sup>163</sup>	Rat	*(DBH+)	Pelvic splanchnic	Jang, 2015 <sup>18</sup>	Human	
	Reid, 1975 <sup>162</sup>	Rat	*(DBH+)		Imai, 2006 <sup>17</sup>	Human	
	Keen, 1974 <sup>160</sup>	Rat	*(DBH+, NA+)		Takenaka, 2005 <sup>16</sup>	Human	
	Nagatsu, 1974 <sup>161</sup>	Rat	*(DBH+)	Spinal root, dorsal root ganglia (cont'd)	Deng, 2000 <sup>269</sup>	Rat	
	Dairman, 1973 <sup>159</sup>	Rat	*(DBH+)		Jones, 1999 <sup>270</sup>	Rat	
	Thoenen, 1970 <sup>271</sup>	Rat			Ma, 1999 <sup>272</sup>	Rat	

**Table 5.1** (continued)

Nerve	First author, year and reference	Species		Nerve	First author and reference	Species	
Spinal root, dorsal root ganglia	Massrey, 2020 <sup>98</sup>	Human	X		Shinder, 1999 <sup>273</sup>	Rat	
	Morellini, 2019 <sup>274</sup>	Rat	*DBH+, NAT+		Thompson, 1998 <sup>275</sup>	Rat	
	Oroszova, 2017 <sup>58</sup>	Rat	X		Karlsson, 1994 <sup>276</sup>	Rat	
	McCarthy, 2016 <sup>57</sup>	Mouse	X		Vega, 1991 <sup>50</sup>	Rat	X
	Brumovsky, 2012 <sup>56</sup>	Mouse	X		Kummer, 1990 <sup>30</sup>	Guinea pig	X
	Lj, 2011 <sup>55</sup>	Mouse	X		Katz, 1987 <sup>27</sup>	Rat	X
	Dina, 2008 <sup>54</sup>	Rat	X,*(DBH+, NAT+)		Price, 1985 <sup>49</sup>	Rat	X
	Brumovsky, 2006 <sup>53</sup>	Mouse	X		Jonakait, 1984 <sup>48</sup>	Rat (embryo)	X, *(DBH+)
	Ichikawa, 2005 <sup>52</sup>	Mouse	X		Price, 1983 <sup>47</sup>	Rat	X
	Holmberg, 2001 <sup>51</sup>	Mouse	X		Lackovic, 1981 <sup>169</sup>	Human	*(NA+)

For each nerve, studies confirming catecholaminergic nerve fibers or experimentally proven communications are listed with first author, year of publication and species investigated. Studies that demonstrate catecholaminergic (CA) cell bodies are indicated by X. Studies that demonstrate additional 'sympathetic' phenotypic properties are indicated by \*. A more extensive interactive Microsoft Excel-based Table, provided with filter tools for study characteristics and findings is provided in interactive Table 2. DBH: dopamine- $\beta$ -hydroxylase, NA: noradrenaline, NAT: noradrenaline transporter.

### Cell bodies

Catecholaminergic cell bodies have a more widespread distribution than generally acknowledged,<sup>2,4,11</sup> and are found in ganglia including the trigeminal,<sup>23,24</sup> inferior glossopharyngeal,<sup>25-36</sup> superior<sup>30,37</sup> and inferior<sup>25,27,28,30,31,33,34,36-46</sup> vagal ganglia, and in dorsal root ganglia at all spinal levels.<sup>27,30,47-58</sup> Moreover, the generally accepted parasympathetic ganglia of the head,<sup>2</sup> which include the ciliary,<sup>59-68</sup> the otic,<sup>68</sup> the pterygopalatine<sup>68-71</sup> and the submandibular ganglia,<sup>68,72-77</sup> all contain catecholaminergic cell bodies. Catecholaminergic cell bodies are not only found in ganglia, but also in the cranial nerves themselves, such as the (lingual branch of the) glossopharyngeal nerve,<sup>26,78</sup> the cervical<sup>79</sup> and laryngeal branches of the vagus nerve,<sup>80,81</sup> and the hypoglossal nerve.<sup>82</sup> In addition, catecholaminergic cell bodies are found in both the ventral and dorsal spinal nerve roots,<sup>83-98</sup> and in the hypogastric and the ('parasympathetic') pelvic splanchnic nerves.<sup>16,17</sup>

### The short versus long pre-ganglionic neuron argument

A commonly held concept in the classic subdivision of the autonomic outflow is the bimodal distribution of cell bodies with the sympathetic cell bodies located in ganglia close to the central nervous system, and the parasympathetic cell bodies in a distal position, within or close to the wall of target organs. This concept, however, cannot be used to subdivide the autonomic outflow, because both proximal and distal ganglia are common throughout the entire spinal outflow (Figure 5.1).

*Proximal locations*

Catecholaminergic neurons are descendants of neural crest cells.<sup>99-101</sup> Trunk neural crest cells consist of several migrating groups. The core of the developing ganglia is established by an early cohort of neural crest cells that migrates ventrally to the mesenchyme dorsolateral of the dorsal aorta.<sup>101-104</sup> Many of these proximal cell bodies subsequently nest in the sympathetic trunk. Other proximal locations, however, include the spinal nerve roots,<sup>83-98</sup> dorsal root ganglia,<sup>27,30,47-58,94</sup> and white and grey rami communicantes.<sup>84-90,94-97,105-110</sup> In the pelvic area, usually characterized as parasympathetic, these proximal locations of ganglionic cells also exist, both in sacral nerve roots<sup>83,92,98</sup> and in the proximal part of the pelvic splanchnic nerves.<sup>16,17,92,111-113</sup>

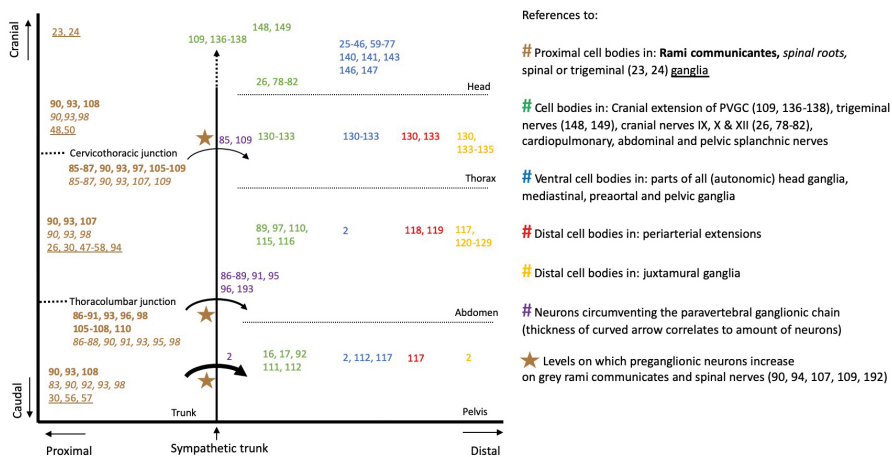


**Figure 5.1** Definitive catecholaminergic cell positions. Plotted are the references that show the position of cell bodies along the cranio-caudal (Y) and proximo-distal (X) body axes. Altogether, the data shows that both proximal and distal ganglia are common in the entire thoracolumbar and sacral autonomic outflow pathways. Other references indicate the levels at which preganglionic neurons bypass the sympathetic trunk (curved arrows), or increase on grey rami communicantes (brown stars).

*Distal locations*

Neural crest cells can run aground anywhere along their proximo-distal migration pathways. Cell bodies of trunk neural-crest cell origin exist up to the walls of the target organs, as the vascular system keeps instructing these cells to migrate.<sup>114,115</sup> In the abdomen, cell bodies are found in large amounts in all splanchnic nerves,<sup>89,97,110,116,117</sup> the preaortic ganglia,<sup>112,113</sup> all their periarterial extensions,<sup>118,119</sup> and within the walls of



organs of both the urogenital and the gastrointestinal tracts.<sup>113,120-129</sup> In the thorax, the situation is similar. Catecholaminergic cell bodies are found on the cardiopulmonary nerves,<sup>130-133</sup> in small mediastinal ganglia,<sup>130-133</sup> the ganglion cardiacum<sup>134,135</sup> and within the wall of the heart.<sup>130,133</sup> Finally, the distal position of cell bodies that are of trunk neural-crest cell origin, extends to the head. Several thousands of cell bodies exist along the intracranial course of human internal carotid arteries.<sup>109,136-138</sup>

*Within the autonomic ganglia of the head, (catecholaminergic) cell bodies are of mixed origin*

The cell bodies within the cranial autonomic ganglia develop from neural crest cells and the related Schwann-cell precursors, with the majority coming from Schwann-cell precursors.<sup>101,139,140</sup> Schwann-cell precursors associated with the oculomotor nerve,<sup>140-142</sup> chorda tympani,<sup>141,143,144</sup> greater superficial petrosal nerve and geniculate ganglion<sup>141,143,144</sup> and tympanic nerve and petrosal ganglion<sup>141,143,145</sup> populate the ciliary, submandibular, pterygopalatine and otic ganglia, respectively. Small ganglia are also present along these nerve paths.<sup>141,143,145</sup> In some species, including man, at least part of these autonomic ganglia originate directly from cranial neural-crest cells. These migrate along the ophthalmic,<sup>140,141,143,146,147</sup> maxillary,<sup>141,146</sup> and mandibular nerves,<sup>141,146</sup> and also populate the ciliary, submandibular and pterygopalatine, and otic ganglia, respectively. Similarly, these trigeminal nerve branches also harbor small ganglia that represent grounded cell bodies.<sup>148,149</sup> In addition, cells from the superior cervical ganglion were shown to populate the otic ganglion.<sup>143</sup>

The partly catecholaminergic phenotype of the autonomic ganglia of the head may arise from cranial neural-crest cells and Schwann-cell precursors, as catecholaminergic cell bodies are present in both trigeminal,<sup>23,24</sup> and petrosal<sup>25-36</sup> and geniculate ganglia, respectively. Catecholaminergic cell bodies have not yet been demonstrated in the geniculate ganglion, but we demonstrated a few in human cadavers (Figure 5.2). Of relevance, TH-positive neurons were also present in the proximal course of the greater superficial petrosal nerve. The notion that the partly catecholaminergic phenotype of the submandibular ganglion may arise from cranial neural crest cells is supported by the finding that catecholaminergic cell bodies in this ganglion are already present prior to the arrival of postganglionic neurons from the superior cervical ganglion.<sup>77</sup>

### Caveats of using the catecholaminergic phenotype

In aggregate, our inventory convincingly shows that catecholaminergic fibers and cell bodies are present in the entire tracts of peripheral nerves and ganglia throughout the

body. However, the reported prevalence of cell bodies per location varies greatly (interactive Table 2).<sup>16,18,26,29-34,36,38,40,41,43,45,50,52,53,61-66,70,71,73,79,121,123,125,150-154</sup> We hypothesize that the reasons for this variation are both biological and technical. True proportions can only be determined after histological sampling of several sections, and the fraction of catecholaminergic cells that stain is influenced by factors such as the time between death and fixation.

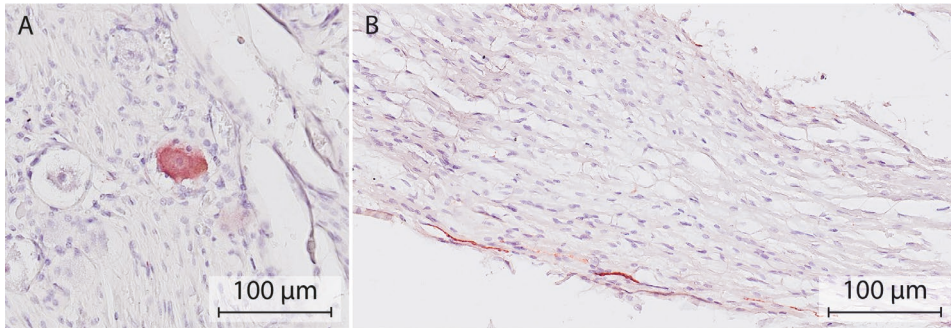


**Figure 5.2 Catecholaminergic neurons in the human geniculate ganglion and the greater superficial petrosal nerve.** Example of a TH-positive cell body (A) and nerve fiber (B) in the geniculate ganglion and proximal course of the superficial petrosal nerve, respectively. Nerve tissue was harvested from a formalin-fixed cadaver (97 years of age) of the body donation program of the Department of Anatomy and Embryology, Maastricht University. The body was preserved by intra-arterial infusion with 10 L fixative (composition (v/v): 96% ethanol (21%), glycerin (21%), 36% formaldehyde (2%), water (56%), and 2.4 g/L thymol), followed by 4 weeks of fixation in 96% ethanol (20%), 36% formaldehyde (2%) and water (78%). Antibody: ABCAM AB209487, 1:10000. Antigen retrieval TRIS-EDTA pH 9.0, 30 min. Secondary antibody GAR-bio, 1:10000. Chromogen: Vector NovaRED peroxidase substrate kit, SK-4805.

The catecholamines dopamine, noradrenaline and adrenaline are derivatives of phenylethylamine.<sup>155</sup> Tyrosine hydroxylase (TH) is the first enzyme in the biosynthetic pathway of (nor-)adrenaline. This enzyme has received the most attention in biomedical research,<sup>156</sup> and is often, incorrectly, associated with (nor-)adrenergic neurotransmission. Colocalization of TH with dopamine- $\beta$ -hydroxylase (DBH), which catalyzes the  $\beta$  hydroxylation of dopamine to noradrenaline, provides stronger evidence for such neurotransmission. DBH-positive neurons have been reported in the ciliary,<sup>60,65,66</sup> pterygopalatine,<sup>70</sup> trigeminal,<sup>24,48</sup> petrosal,<sup>48</sup> nodose<sup>46,48,154</sup> and dorsal root ganglia,<sup>48</sup> and the vestibulocochlear,<sup>157,158</sup> vagus,<sup>79,154</sup> recurrent laryngeal,<sup>80</sup> phrenic<sup>119</sup> and sciatic<sup>54,159-168</sup> nerves. Other studies measured concentrations of noradrenaline directly in the trigeminal<sup>169</sup> and nodose<sup>44</sup> ganglia, and in the facial,<sup>170</sup> vestibulocochlear,<sup>170,171</sup> vagus,<sup>169</sup> phrenic,<sup>169</sup> ilioinguinal,<sup>169</sup> genitofemoral,<sup>169</sup>

sciatic,<sup>160,166,168,172-177</sup> and fibular<sup>178</sup> nerves and spinal nerve roots.<sup>169</sup> TH-positive, but DBH-negative cell bodies have been observed in ciliary,<sup>61,63,66</sup> petrosal,<sup>30</sup> jugular,<sup>30</sup> nodose<sup>30,38</sup> and dorsal root ganglia.<sup>30,47,50</sup> Furthermore, TH-positive, but noradrenaline transporter type-1<sup>56</sup> and phenylethanolamine-N-methyl-transferase-negative cell bodies<sup>30</sup> were reported in dorsal root ganglia. Nerves in which solely TH but none of the downstream enzymes are present probably utilize dopamine as a neurotransmitter. These findings and considerations do not invalidate our model.

*Not all catecholaminergic neurons are sympathetic*

Tyrosine hydroxylase-positive staining has been observed in cell bodies that exhibit morphological features typical of primary sensory neurons in petrosal,<sup>25,33</sup> nodose<sup>25,33</sup> and dorsal root ganglia.<sup>55,56,58</sup> Some TH-positive cell bodies in the nodose ganglion are also labelled following the injection of tracer material into the nucleus of the solitary tract.<sup>38,43</sup>

*Transient catecholaminergic expression*

Within the developing ciliary and sphenopalatine ganglia, neurons are observed that express catecholamines transiently.<sup>179-181</sup> In the mouse, the nerve fibers of the vagus nerve arrive in the wall of the gastrointestinal tract only after the TH-positive neural-crest cells have settled there.<sup>182,183</sup> The TH-positive cells have largely disappeared from the vagus nerve by embryonic day 16 in the mouse, which corresponds to ~9.5 weeks of development in human embryos. Our observations suggest that a subset of these transiently TH-positive cells remain present.

*Absence of white rami communicantes at the sacral level and the 'lumbar gap'*

Another anatomical argument that is often used to define the sympathetic-parasympathetic model is the absence of white rami communicantes at the sacral level.

*The rami communicantes are part of a peripheral connection matrix*

Macroscopic studies of the distribution pattern of the rami communicantes and sympathetic trunk have shown that the rami communicantes form a true mesh, with up to 7 rami communicantes connecting the sympathetic trunk with the spinal nerves from corresponding and adjacent levels.<sup>2,93,97,184-187</sup> Interconnecting bundles of nerve fibers between the left and right sympathetic trunk are present at all levels.<sup>97</sup> In addition, the

white and grey rami communicantes can share an epineurium, and then present as a single ramus communicans.<sup>90</sup>

#### *Mixed content of white rami communicantes*

The rami communicantes are defined by their macroscopic appearance.<sup>188,189</sup> which, in turn, depends on the percentage of myelinated nerve fibers that are present. Macroscopically identifiable white rami communicantes are present between vertebral levels T1 and L2 in man. Accordingly, the absence of white rami communicantes at the sacral level has been one of the anatomical arguments to separate the sacral from the thoracolumbar autonomic outflow.<sup>1</sup> However, the nerve fibers in the rami communicantes not only represent preganglionic neurons, but also somatic neurons.<sup>86,107,190</sup> In addition, the white rami communicantes contain a great number of medium and large myelinated afferent fibers, particularly in the lower thoracic region.<sup>191</sup> The number and size of these fibers together far exceed the small (efferent) myelinated components, so that the white rami communicantes represent as much the thoracolumbar inflow as the outflow.<sup>191</sup>

#### *Mixed content of grey rami communicantes*

Myelinated pre-ganglionic neurons are also common in the grey ramus communicans.<sup>90,94,109,192</sup> At the upper and lower margins of the thoracolumbar outflow, where the white rami communicantes gradually disappear, the number of myelinated nerve fibers in the grey rami communicantes actually increases 10-fold.<sup>90,107</sup> Sporadically, sacral grey rami communicantes are so heavily myelinated, that they have been described as a 'sacral white ramus communicans'.<sup>92</sup>

#### *Preganglionic neurons can bypass the rami communicantes at the thoracolumbar outflow margins*

At the margins of the thoracolumbar outflow, a fraction of the preganglionic neurons bypass the rami communicantes and the sympathetic trunk<sup>85-89,91,95,96,109</sup> (Figure 5.3). Lumbar splanchnic nerves can arise directly from the lumbar plexus,<sup>89,193</sup> like pelvic splanchnic nerves arise from the sacral plexus. Bypassing the sympathetic trunk, therefore, is not exclusive for the sacral outflow.

#### *The lumbar gap*

The spinal preganglionic outflow levels vary between species.<sup>1,83,91,111,188,194</sup> In man, the spinal preganglionic outflow has been confined classically to the levels T1-L2 and S2-S4 based on the absence of white rami communicantes caudal to segment L2, and the

perceived discontinuity of the spinal autonomic outflow cell column. The resulting 'lumbar gap' is often quoted when describing the parallel between the parasympathetic cranial and sacral outflow. Preganglionic neurons have been described, however, at the lower lumbar level, which is within the 'lumbar gap'.<sup>94,136,192</sup> These preganglionic neurons follow, as described in the previous paragraph, the spinal nerves and grey rami communicantes.

Furthermore, from the thoracolumbar outflow margin downwards, preganglionic cell bodies increasingly nest within the ventral motor nuclei<sup>195,196</sup> (Figure 5.3). At the sacral level, the intermediolateral nucleus does not form a distinct lateral horn of gray matter,<sup>196</sup> and the ventral motor nucleus becomes highly mixed with preganglionic neurons.<sup>197</sup> Apparently, preganglionic neurons with their cell bodies in, or nearby, the ventral motor horn prefer to follow the path of the motor neurons and branch away towards their targets only distal to the position of white rami communicantes. At the sacral level, this phenomenon is structural, and the white ramus communicans disappears.

We conclude that, along the entire spinal axis, the anatomy of the autonomic outflow displays a conserved architecture, albeit that a gradient in characteristics is observed. This finding provides morphological support for the ontogenetic finding that the autonomic outflows at the thoracolumbar and sacral levels possess a highly similar molecular signature.<sup>5</sup> Surprisingly, Langley appears to have known about the limitations of the anatomical arguments supporting his model, because he was aware of the non-binary distribution of postganglionic cell bodies (see ref.<sup>111,198</sup> in interactive Table 3), the fact that the color of the rami communicantes convey no anatomical accuracy and that preganglionic fibers are present on grey rami communicantes and within the lumbar gap (see ref.<sup>192</sup> in interactive Table 3). Although Langley created a model-serving generalization, it has been hallowed by constant repetition in literature.

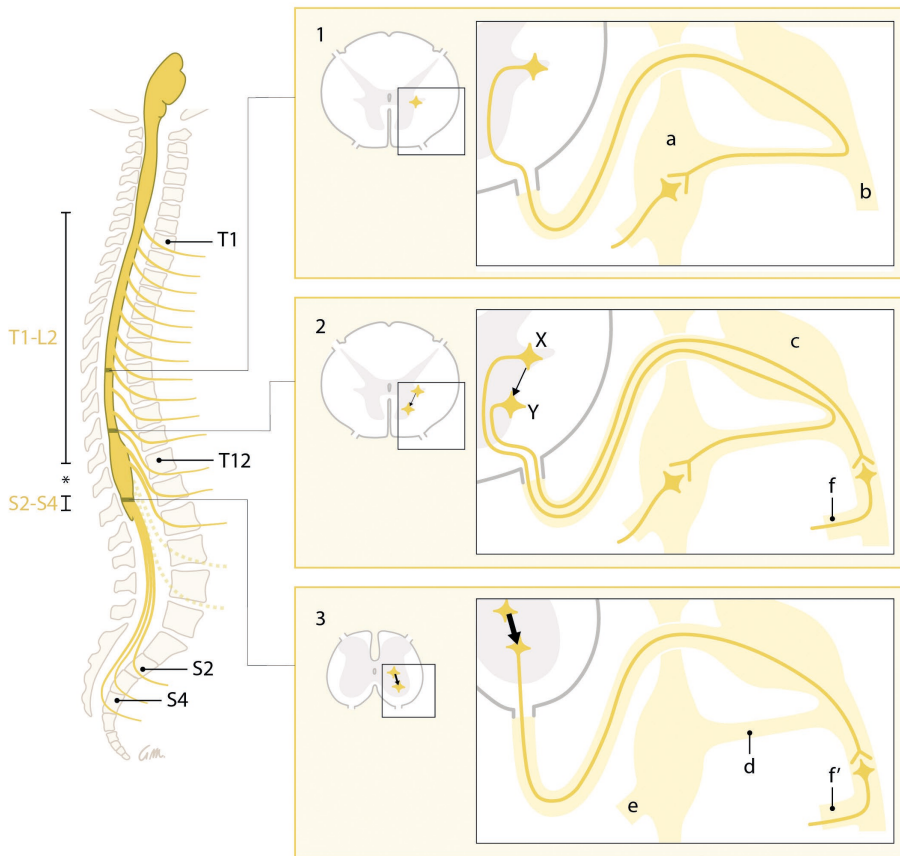


**Figure 5.3** Craniocaudal change in the position of the cell bodies and the course of the preganglionic neurons. Simplified representation. Left: Preganglionic outflow at the levels T1-L2 and S2-S4. The 'lumbar gap' is indicated by an asterisk. Dashed outflow: preganglionic neurons within the 'lumbar gap'. Right: From the lower margin of the thoracolumbar outflow downward (Panels 1-3), a gradually increasing number (represented by thickness of the arrow) of preganglionic neurons originate from cell bodies within or near the ventral motor nuclei and bypass the sympathetic trunk (Panels 2 and 3, neuron Y). Bypassing the sympathetic trunk, therefore, is not exclusive for the sacral outflow. Lumbar splanchnic nerves can arise directly from the lumbar plexus (Panel 2, f), like pelvic splanchnic nerves arise from the sacral plexus (Panel 3, f'). Panels 1 and 2, neuron X: Classic representation of a preganglionic neuron with its cell body in the intermediolateral nucleus. Labels are identical in all panels; a: sympathetic trunk ganglion, b: spinal nerve, c: spinal ganglion, d: rami communicantes, e: splanchnic nerves.

### Perspective: a peripheral connectome without dedicated nerves

Based on our findings, we propose to conceive the peripheral nervous system as a connection matrix. Different parts of this matrix embed neurons with different characteristics. Conceptually, the peripheral nerve network represents a downscaled version of the connectome in the brain.<sup>199-201</sup> The connectome-like behavior of neurons that change course from one nerve to another, is already widely accepted for preganglionic efferent neurons in the oculomotor, facial and glossopharyngeal nerves, that end up in trigeminal nerve branches.<sup>2</sup> The white and grey rami communicantes are not dedicated ‘sympathetic’ nerves, just as the vagus nerve is not exclusively ‘parasympathetic’.<sup>202,203</sup> Within the connection matrix, communications exist between the sympathetic trunk and spinal nerves, cranial nerves and ganglia. These allow neurons to switch between nerves to establish unique connections (Figure 5.4). The nerves form the scaffolding for the outgrow of neurons, resulting in the entwined anatomy of the peripheral nervous system. Examples include the reciprocal interaction between neural crest cell migration and nerve formation,<sup>182,183</sup> the Schwann-cell precursors giving rise to neurons,<sup>101,142,145</sup> and the directional guiding of the outgrowth of preganglionic neurons by epibranchial placode-derived sensory neurons.<sup>144</sup> The mesodermally derived epineurium bounds these heterogenous neurons, and makes these collections ‘nerves’. The nerves together form the connection matrix. Only by combining the results of the various research laboratories, the true architecture of the peripheral autonomic nervous system can be perceived. The upcoming task is now to fully elucidate the neuronal phenotypes and their positions in the peripheral connection matrix.

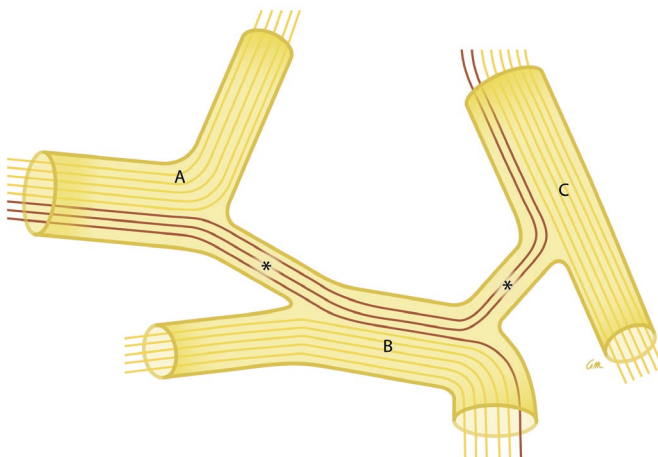


**Figure 5.4** The peripheral nervous system as a connection matrix. In this concept, neuronal function is not coupled to specific nerves. The connectome-like behavior of neurons that change course (purple) from nerve A to nerve B and C via communicating nerve branches (asterisks) is illustrated.

## Literature

1. Langley JN. The autonomic nervous system, Part I. 1921, Cambridge: W. HEFFER & SONS LTD.
2. Standing S. *Gray's Anatomy, The Anatomical Basis of Clinical Practice*. 41st Revised ed. 2016: Elsevier Health Sciences.
3. W.F., B. and B. E.L., *Medical Physiology*. 3 ed. 2016: Elsevier Health Science Division.
4. F.I.P.A.T., *Terminologia Neuroanatomica* 2017.
5. Espinosa-Medina I, et al. The sacral autonomic outflow is sympathetic. *Science*. 2016;354(6314): 893-897.
6. Janig W, et al. Renaming all spinal autonomic outflows as sympathetic is a mistake. *Auton Neurosci*. 2017;206:60-62.
7. Janig W, Neuhuber W. Reclassification of the Sacral Autonomic Outflow to Pelvic Organs as the Caudal Outpost of the Sympathetic System Is Misleading. *J Am Osteopath Assoc*. 2017;117(7):416-417.
8. Neuhuber W, McLachlan E, Janig W. The Sacral Autonomic Outflow Is Spinal, but Not "Sympathetic". *Anat Rec (Hoboken)*. 2017;300(8):1369-1370.
9. Horn JP. The sacral autonomic outflow is parasympathetic: Langley got it right. *Clin Auton Res*. 2018; 28(2):181-185.
10. Janig W, McLachlan EM, Neuhuber WL. The sacral autonomic outflow: against premature oversimplification. *Clin Auton Res*. 2018;28(1):5-6.
11. F.C.o.A.T., *Terminologia anatomica: International anatomical terminology*. 2011, Stuttgart: Thieme Publishing Group.
12. Wilson JE. Sympathetic pathways through the petrosal nerves in monkeys. *Acta Anat (Basel)*. 1985; 121(2):75-80.
13. Matthews B, Robinson PP. The course of postganglionic sympathetic fibres distributed with the facial nerve in the cat. *Brain Res*. 1986;382(1):55-60.
14. Shibamori Y, et al. The trajectory of the sympathetic nerve fibers to the rat cochlea as revealed by anterograde and retrograde WGA-HRP tracing. *Brain Res*. 1994;646(2):223-229.
15. Maklad A, Quinn T, Fritsch B. Intracranial distribution of the sympathetic system in mice: Dil tracing and immunocytochemical labeling. *Anat Rec*. 2001;263(1):99-111.
16. Takenaka A, et al. Interindividual variation in distribution of extramural ganglion cells in the male pelvis: a semi-quantitative and immunohistochemical study concerning nerve-sparing pelvic surgery. *Eur Urol*. 2005;48(1):46-52; discussion 52.
17. Imai K, et al. Human pelvic extramural ganglion cells: a semiquantitative and immunohistochemical study. *Surg Radiol Anat*. 2006;28(6):596-605.
18. Jang HS, et al. Composite nerve fibers in the hypogastric and pelvic splanchnic nerves: an immunohistochemical study using elderly cadavers. *Anat Cell Biol*. 2015;48(2):114-123.
19. Verberne ME, et al. Contribution of the cervical sympathetic ganglia to the innervation of the pharyngeal arch arteries and the heart in the chick embryo. *Anat Rec*. 1999;255(4):407-419.
20. SchrodL F, et al. Intrinsic neurons in the duck choroid are contacted by CGRP-immunoreactive nerve fibres: evidence for a local pre-central reflex arc in the eye. *Exp Eye Res*. 2001;72(2):137-146.
21. Nagatsu I, et al. Immunofluorescent and biochemical studies on tyrosine hydroxylase and dopamine-beta-hydroxylase of the bullfrog sciatic nerves. *Histochemistry*. 1979;61(2):103-109.
22. Rigon F, et al. Effects of sciatic nerve transection on ultrastructure, NADPH-diaphorase reaction and serotonin-, tyrosine hydroxylase-, c-Fos-, glucose transporter 1- and 3-like immunoreactivities in frog dorsal root ganglion. *Braz J Med Biol Res*. 2013;46(6):513-520.
23. Marfurt CF, Ellis LC., Immunohistochemical localization of tyrosine hydroxylase in corneal nerves. *J Comp Neurol*, 1993;336(4):517-531.
24. Reynolds AJ, Kaasinen SK, Hendry LA. Retrograde axonal transport of dopamine beta hydroxylase antibodies by neurons in the trigeminal ganglion. *Neurochem Res*. 2005;30(6-7):703-712.
25. Katz DM, et al. Expression of catecholaminergic characteristics by primary sensory neurons in the normal adult rat in vivo. *Proc Natl Acad Sci U S A*. 1983;80(11):3526-3530.



26. Katz DM, Black LB. Expression and regulation of catecholaminergic traits in primary sensory neurons: relationship to target innervation in vivo. *J Neurosci.* 1986;6(4):983-989.
27. Katz DM, Adler JE, Black LB. Catecholaminergic primary sensory neurons: autonomic targets and mechanisms of transmitter regulation. *Fed Proc* 1987;46(1):24-29.
28. Helke CJ, Niederer AJ. Studies on the coexistence of substance P with other putative transmitters in the nodose and petrosal ganglia. *Synapse.* 1990;5(2):144-151.
29. Katz DM, Erb MJ. Developmental regulation of tyrosine hydroxylase expression in primary sensory neurons of the rat. *Dev Biol.* 1990;137(2):233-242.
30. Kummer W, et al. Catecholamines and catecholamine-synthesizing enzymes in guinea-pig sensory ganglia. *Cell Tissue Res.* 1990;261(3):595-606.
31. Helke CJ, Rabchevsky A. Axotomy alters putative neurotransmitters in visceral sensory neurons of the nodose and petrosal ganglia. *Brain Res.* 1991;551(1-2):44-51.
32. Ichikawa H, Rabchevsky A, Helke CJ. Presence and coexistence of putative neurotransmitters in carotid sinus baro- and chemoreceptor afferent neurons. *Brain Res.* 1993;611(1):67-74.
33. Ichikawa H, Helke CJ. Parvalbumin and calbindin D-28k in vagal and glossopharyngeal sensory neurons of the rat. *Brain Res.* 1995;675(1-2):337-341.
34. Ichikawa H, Helke CJ. Coexistence of s100beta and putative transmitter agents in vagal and glossopharyngeal sensory neurons of the rat. *Brain Res.* 1998;800(2):312-318.
35. Wang ZY, et al. Expression of 5-HT3 receptors in primary sensory neurons of the petrosal ganglion of adult rats. *Auton Neurosci.* 2002;95(1-2):121-124.
36. Ichikawa H, et al. Brain-derived neurotrophic factor-immunoreactive neurons in the rat vagal and glossopharyngeal sensory ganglia; co-expression with other neurochemical substances. *Brain Res.* 2007; 1155:93-99.
37. Kawagishi K, et al. Tyrosine hydroxylase-immunoreactive fibers in the human vagus nerve. *J Clin Neurosci.* 2008;15(9):1023-1026.
38. Kummer W, et al. Tyrosine-hydroxylase-containing vagal afferent neurons in the rat nodose ganglion are independent from neuropeptide-Y-containing populations and project to esophagus and stomach. *Cell Tissue Res.* 1993;271(1):135-144.
39. Yoshida Y, et al. Ganglions and ganglionic neurons in the cat's larynx. *Acta Otolaryngol.* 1993;113(3): 415-420.
40. Zhuo H, Sinclair C, Helke CJ. Plasticity of tyrosine hydroxylase and vasoactive intestinal peptide messenger RNAs in visceral afferent neurons of the nodose ganglion upon axotomy-induced deafferentation. *Neuroscience.* 1994;63(2):617-626.
41. Zhuo H, et al. Inhibition of axoplasmic transport in the rat vagus nerve alters the numbers of neuropeptide and tyrosine hydroxylase messenger RNA-containing and immunoreactive visceral afferent neurons of the nodose ganglion. *Neuroscience.* 1995;66(1):175-187.
42. Ichikawa H, Helke CJ. Coexistence of calbindin D-28k and NADPH-diaphorase in vagal and glossopharyngeal sensory neurons of the rat. *Brain Res.* 1996;735(2):325-329.
43. Uno T, et al. Tyrosine hydroxylase-immunoreactive cells in the nodose ganglion for the canine larynx. *Neuroreport.* 1996;7(8):1373-1376.
44. Gorbunova AV. Catecholamines in rabbit nodose ganglion following exposure to an acute emotional stressor. *Stress.* 1998;2(3):231-236.
45. Sang Q, Young HM. The origin and development of the vagal and spinal innervation of the external muscle of the mouse esophagus. *Brain Res.* 1998;809(2):253-268.
46. Bookout AL, Gautron L. Characterization of a cell bridge variant connecting the nodose and superior cervical ganglia in the mouse: Prevalence, anatomical features, and practical implications. *J Comp Neurol.* 2021;529(1):111-128.
47. Price J, Mudge AW. A subpopulation of rat dorsal root ganglion neurones is catecholaminergic. *Nature.* 1983;301(5897):241-243.
48. Jonakait GM, et al. Transient expression of selected catecholaminergic traits in cranial sensory and dorsal root ganglia of the embryonic rat. *Dev Biol.* 1984;101(1):51-60.
49. Price J. An immunohistochemical and quantitative examination of dorsal root ganglion neuronal subpopulations. *J Neurosci* 1985;5(8):2051-2059.

50. Vega JA, et al. Presence of catecholamine-related enzymes in a subpopulation of primary sensory neurons in dorsal root ganglia of the rat. *Cell Mol Biol.* 1991;37(5):519-530.
51. Holmberg K, et al. Effect of peripheral nerve lesion and lumbar sympathectomy on peptide regulation in dorsal root ganglia in the NGF-overexpressing mouse. *Exp Neurol.* 2001;167(2):290-303.
52. Ichikawa H, et al. Brn-3a deficiency increases tyrosine hydroxylase-immunoreactive neurons in the dorsal root ganglion. *Brain Res.* 2005;1036(1-2):19192-5.
53. Brumovsky P, Villar MJ, Hokfelt T. Tyrosine hydroxylase is expressed in a subpopulation of small dorsal root ganglion neurons in the adult mouse. *Exp Neurol.* 2006;200(1):153-165.
54. Dina OA, et al. Neurotoxic catecholamine metabolite in nociceptors contributes to painful peripheral neuropathy. *Eur J Neurosci.* 2008;28(6):1180-1190.
55. Li L, et al. The functional organization of cutaneous low-threshold mechanosensory neurons. *Cell.* 2011;147(7):1615-1627.
56. Brumovsky PR, et al. Dorsal root ganglion neurons innervating pelvic organs in the mouse express tyrosine hydroxylase. *Neuroscience.* 2012;223:77-91.
57. McCarthy CJ, et al. Axotomy of tributaries of the pelvic and pudendal nerves induces changes in the neurochemistry of mouse dorsal root ganglion neurons and the spinal cord. *Brain Struct Funct.* 2016;221(4):1985-2004.
58. Oroszova Z, et al. The Characterization of AT1 Expression in the Dorsal Root Ganglia After Chronic Constriction Injury. *Cell Mol Neurobiol.* 2017;37(3):545-554.
59. Iacovitti L, et al. Partial expression of catecholaminergic traits in cholinergic chick ciliary ganglia: studies in vivo and in vitro. *Dev Biol.* 1985;110(2):402-412.
60. Landis SC, et al. Catecholaminergic properties of cholinergic neurons and synapses in adult rat ciliary ganglion. *J Neurosci.* 1987;7(11):3574-3587.
61. Uemura Y, et al. Tyrosine hydroxylase-like immunoreactivity and catecholamine fluorescence in ciliary ganglion neurons. *Brain Res.* 1987;416(1):200-203.
62. Tyrrell S, Siegel RE, Landis SC. Tyrosine hydroxylase and neuropeptide Y are increased in ciliary ganglia of sympathectomized rats. *Neuroscience.* 1992;47(4):985-998.
63. Kirch W, Neuhuber W, Tamm ER. Immunohistochemical localization of neuropeptides in the human ciliary ganglion. *Brain Res.* 1995;681(1-2):229-234.
64. Tan CK, Zhang YL, Wong WC. A light- and electron microscopic study of tyrosine hydroxylase-like immunoreactivity in the ciliary ganglia of monkey (*Macaca fascicularis*) and cat. *Histol Histopathol.* 1995;10(1):27-34.
65. Grimes PA, et al. Neuropeptide Y-like immunoreactivity localizes to preganglionic axon terminals in the rhesus monkey ciliary ganglion. *Invest Ophthalmol Vis Sci.* 1998;39(2):227-232.
66. Kaleczyc J, et al. Immunohistochemical characterization of neurons in the porcine ciliary ganglion. *Pol J Vet Sci.* 2005;8(1):65-72.
67. Thakker MM, et al. Human orbital sympathetic nerve pathways. *Ophthalmic Plast Reconstr Surg.* 2008;24(5):360-366.
68. Kiyokawa H, et al. Reconsideration of the autonomic cranial ganglia: an immunohistochemical study of mid-term human fetuses. *Anat Rec (Hoboken).* 2012;295(1):141-149.
69. Kuwayama Y, Emson PC, Stone RA. Pterygopalatine ganglion cells contain neuropeptide Y. *Brain Res.* 1988;446(2):219-224.
70. Simons E, Smith PG. Sensory and autonomic innervation of the rat eyelid: neuronal origins and peptide phenotypes. *J Chem Neuroanat.* 1994;7(1-2):35-47.
71. Szczurkowski A, et al. Morphology and immunohistochemical characteristics of the pterygopalatine ganglion in the chinchilla (*Chinchilla laniger*, Molina). *Pol J Vet Sci.* 2013;16(2):359-368.
72. Soinila J, et al. Met5-enkephalin-Arg6-Gly7-Leu8-immunoreactive nerve fibers in the major salivary glands of the rat: evidence for both sympathetic and parasympathetic origin. *Cell Tissue Res.* 1991;264(1):15-22.
73. Shida T, et al. Enkephalinergic sympathetic and parasympathetic innervation of the rat submandibular and sublingual glands. *Brain Res.* 1991;555(2):288-294.
74. Ng YK, Wong WC, Ling EA. A study of the structure and functions of the submandibular ganglion. *Ann Acad Med Singapore.* 1995;24(6):793-801.

75. Hosaka F, et al. Site-dependent differences in density of sympathetic nerve fibers in muscle-innervating nerves of the human head and neck. *Anat Sci Int.* 2014;89(2):101-111.
76. Yamauchi M, et al. Sympathetic and parasympathetic neurons are likely to be absent in the human vestibular and geniculate ganglia: an immunohistochemical study using elderly cadaveric specimens. *Okajimas Folia Anat Jpn.* 2016;93(1):1-4.
77. Teshima THN, Tucker AS, Lourenco SV. Dual Sympathetic Input into Developing Salivary Glands. *J Dent Res.* 2019;98(10):1122-1130.
78. Oda K, et al. A ganglion cell cluster along the glossopharyngeal nerve near the human palatine tonsil. *Acta Otolaryngol.* 2013;133(5):509-512.
79. Verlinden TJM, et al. Morphology of the human cervical vagus nerve: implications for vagus nerve stimulation treatment. *Acta Neurol Scand.* 2016;133(3):173-182.
80. Dahlqvist A, Forsgren S. Expression of catecholamine-synthesizing enzymes in paraganglionic and ganglionic cells in the laryngeal nerves of the rat. *J Neurocytol.* 1992;21(1):1-6.
81. Ibanez M, et al. Human laryngeal ganglia contain both sympathetic and parasympathetic cell types. *Clin Anat.* 2010;23(6):673-682.
82. Tubbs RS, et al. The existence of hypoglossal root ganglion cells in adult humans: potential clinical implications. *Surg Radiol Anat.* 2009;31(3):173-176.
83. Harman NB. The pelvic splanchnic nerves: an examination into their range and character. *J Anat Physiol.* 1899;33(3):386-412.
84. Marinesco G. Über die mikro-sympathischen hypospinalen Ganglien. *Neurol Zbl.* 1908. 27: p. 146-50.
85. Skoog T. Ganglia in the communicating rami of the cervical sympathetic trunk. *Lancet.* 1947;2(6474):457-460.
86. Alexander WF, et al. Sympathetic conduction pathways independent of sympathetic trunks; their surgical implications. *J Int Coll Surg.* 1949;12(2):111-119.
87. Alexander WF, et al. Sympathetic ganglion cells in ventral nerve roots. Their Relation to sympathectomy. *Science.* 1949;109(2837):484.
88. Kuntz A, Alexander WF. Surgical implications of lower thoracic and lumbar independent sympathetic pathways. *AMA Arch Surg.* 1950;61(6):1007-1018.
89. Webber RH. An analysis of the sympathetic trunk, communicating rami, sympathetic roots and visceral rami in the lumbar region in man. *Ann Surg.* 1955;141(3):398-413.
90. Hofman HH, Jacobs MW, Kuntz A. Nerve fiber components of communicating rami and sympathetic roots in man. *Anat Rec.* 1956;126(1):29-41.
91. Pick J. The identification of sympathetic segments. *Ann Surg.* 1957;145(3):355-364.
92. Kimmel DL, McCrea LE. The development of the pelvic plexuses and the distribution of the pelvic splanchnic nerves in the human embryo and fetus. *J Comp Neurol.* 1958;110(2):271-297.
93. Wreite M. The anatomy of the sympathetic trunks in man. *J Anat.* 1959;93:448-459.
94. Webber RH, et al. Myelinated nerve fibers in communicating rami attached to caudal lumbar nerves. *J Comp Neurol.* 1962;119:11-20.
95. Webber RH, Wemett A. Distribution of fibers from nerve cell bodies in ventral roots of spinal nerves. *Acta Anat.* 1966;65(4):579-583.
96. Webber RH. Accessory ganglia related to sympathetic nerves in the lumbar region. *Acta Anat.* 1967;66(1):59-66.
97. Baljet B, Boekelaar AB, Groen GJ. Retroperitoneal paraganglia and the peripheral autonomic nervous system in the human fetus. *Acta Morphol Neerl Scand.* 1985; 23(2):137-149.
98. Massrey C, et al. Ectopic sympathetic ganglia cells of the ventral root of the spinal cord: an anatomical study. *Anat Cell Biol.* 2020;53(1):15-20.
99. Jessen KR, Mirsky R. Schwann cell precursors and their development. *Glia.* 1991;4(2):185-194.
100. Serbedzija GN, McMahon AP. Analysis of neural crest cell migration in Splotch mice using a neural crest-specific LacZ reporter. *Dev Biol.* 1997;185(2):139-147.
101. Lefcort F. Development of the Autonomic Nervous System: Clinical Implications. *Semin Neurol.* 2020; 40(5):473-484.
102. Kasemeier-Kulesa JC, et al. CXCR4 controls ventral migration of sympathetic precursor cells. *J Neurosci.* 2010;30(39):13078-13088.

103. Kruepunga N, et al. Development of extrinsic innervation in the abdominal intestines of human embryos. *J Anat.* 2020; 237(4):655-671.
104. Kasemeier-Kulesa JC, Kulesa PM, Lefcort F. Imaging neural crest cell dynamics during formation of dorsal root ganglia and sympathetic ganglia. *Development.* 2005;132(2):235-245.
105. Marinesco GM. Über die mikro-sympathischen hypospinalen Ganglien. *Neurol Zbl.* 1908;27:146-150.
106. Gruss W. Über Ganglien im Ramus communicans. *Z. Anat. Entwickl. Gesch.* 1932;97:464-471.
107. Pick J, Sheehan D. Sympathetic rami in man. *J Anat.* 1946;80(Pt 1):12-20 3.
108. Wreite M. Ganglia of rami communicantes in man and mammals particularly monkey. *Acta Anat (Basel).* 1951;13(3):329-336.
109. Hoffman HH. An analysis of the sympathetic trunk and rami in the cervical and upper thoracic regions in man. *Ann Surg.* 1957;145(1):94-103.
110. Webber RH. A contribution on the sympathetic nerves in the lumbar region. *Anat Rec.* 1958;130(3): 581-604.
111. Langley JN, Andersen HK. The innervation of the pelvic and adjoining viscera. Part VII Anatomical observations. *J Physiol.* 1896;20(4-5):372-406.
112. Dail WG, Evan AP, Eason HR. The major ganglion in the pelvic plexus of the male rat: a histochemical and ultrastructural study. *Cell Tissue Res.* 1975;159(1):49-62.
113. Kuntz A, Moseley RL. An experimental analysis of the pelvic autonomic ganglia in the cat. *J Comp Neurol.* 1935;64(1):63-75.
114. Makita T, et al. Endothelins are vascular-derived axonal guidance cues for developing sympathetic neurons. *Nature.* 2008;452(7188):759-763.
115. Takahashi Y, Sipp D, Enomoto H. Tissue interactions in neural crest cell development and disease. *Science.* 2013;341(6148):860-863.
116. Kuntz A. Components of splanchnic and intermesenteric nerves. *J Comp Neurol.* 1956;105(2):251-268.
117. Kuntz A, Hoffman HH, Schaeffer EM. Fiber components of the splanchnic nerves. *Anat Rec.* 1957;128(1): 139-146.
118. Kuntz A, Jacobs MW. Components of periarterial extensions of celiac and mesenteric plexuses. *Anat Rec.* 1955;123(4):509-520.
119. Verlinden TJM, et al. The human phrenic nerve serves as a morphological conduit for autonomic nerves and innervates the caval body of the diaphragm. *Sci Rep.* 2018;8(1):11697.
120. El-Badawi A, Schenk EA. The peripheral adrenergic innervation apparatus. *Z Zellforsch.* 1968;87:218-225.
121. Morris JL, Gibbins LL. Neuronal colocalization of peptides, catecholamines, and catecholamine-synthesizing enzymes in guinea pig paracervical ganglia. *J Neurosci.* 1987;7(10):3117-3130.
122. James S, Burnstock G. Neuropeptide Y-like immunoreactivity in intramural ganglia of the newborn guinea pig urinary bladder. *Regul Pept.* 1988;23(2):237-245.
123. Houdeau E, et al. Distribution of noradrenergic neurons in the female rat pelvic plexus and involvement in the genital tract innervation. *J Auton Nerv Syst.* 1995;54(2):113-125.
124. Smet PJ, et al. Neuropeptides and neurotransmitter-synthesizing enzymes in intrinsic neurons of the human urinary bladder. *J Neurocytol.* 1996;25(2):112-124.
125. Dixon JS, Jen PY, Gosling JA. A double-label immunohistochemical study of intramural ganglia from the human male urinary bladder neck. *J Anat.* 1997;190 ( Pt 1):125-134.
126. Werkstrom V, et al. Inhibitory innervation of the guinea-pig urethra; roles of CO, NO and VIP. *J Auton Nerv Syst.* 1998;74(1):33-42.
127. Dixon JS, Jen PY, Gosling JA. Tyrosine hydroxylase and vesicular acetylcholine transporter are coexpressed in a high proportion of intramural neurons of the human neonatal and child urinary bladder. *Neurosci Lett.* 1999;277(3):157-160.
128. Muraoka K, et al. Site-dependent differences in the composite fibers of male pelvic plexus branches: an immunohistochemical analysis of donated elderly cadavers. *BMC Urol.* 2018;18(1):47.
129. Arellano J, et al. Neural interrelationships of autonomic ganglia from the pelvic region of male rats. *Auton Neurosci.* 2019;217:26-34.
130. Armour JA, Hopkins DA. Localization of sympathetic postganglionic neurons of physiologically identified cardiac nerves in the dog. *J Comp Neurol.* 1981;202(2):169-184.

131. Armour JA. Physiological studies of small mediastinal ganglia in the cardiopulmonary nerves of dogs. *Can J Physiol Pharmacol.* 1984;62(9):1244-1248.
132. Hopkins DA, Armour JA. Localization of sympathetic postganglionic and parasympathetic preganglionic neurons which innervate different regions of the dog heart. *J Comp Neurol.* 1984;229(2):186-198.
133. Janes RD, et al. Anatomy of human extrinsic cardiac nerves and ganglia. *Am J Cardiol.* 1986;57(4):299-309.
134. Hoard JL, et al. Cholinergic neurons of mouse intrinsic cardiac ganglia contain noradrenergic enzymes, norepinephrine transporters, and the neurotrophin receptors tropomyosin-related kinase A and p75. *Neuroscience.* 2008;156(1):129-142.
135. Kim JH, et al. Ganglion cardiacum or juxtaductal body of human fetuses. *Anat Cell Biol.* 2018;51(4):266-273.
136. Mitchell GAG. The cranial extremities of the sympathetic trunks. *Acta Anat.* 1953;18:195-201.
137. Kuntz, A., H.H. Hoffman, and L.M. Napolitano, Cephalic sympathetic nerves. *Arch Surg.* 1957;75:108-115.
138. Tubbs RS, et al. Does the ganglion of Ribes exist? *Folia Neuropathol.* 2006;44(3):197-201.
139. Schaper, A., The earliest differentiation in the central nervous system of vertebrates. *Science.* 1897;5(115):430-431.
140. Carpenter FW. The development of the oculomotor nerve, the ciliary ganglion and the abducent nerve in the chick. *Bull Mus Comp Zool Harvard College* 1906;48:141-228.
141. Kuntz A. The development of the sympathetic nervous system in man. *J Comp Neurol.* 1920;32(2):173-229.
142. Dyachuk V, et al. Neurodevelopment. Parasympathetic neurons originate from nerve-associated peripheral glial progenitors. *Science.* 2014;345(6192):82-87.
143. Stewart FW. The development of the cranial sympathetic ganglia in the rat. *J Comp Neurol.* 1919;31(3):163-217.
144. Coppola E, et al. Epibranchial ganglia orchestrate the development of the cranial neurogenic crest. *Proc Natl Acad Sci U S A.* 2010;107(5):2066-2071.
145. Espinosa-Medina I, et al. Neurodevelopment. Parasympathetic ganglia derive from Schwann cell precursors. *Science.* 2014;345(6192):87-90.
146. Streeter GL. *Manual of Human Embryology The development of the nervous system.* Vol. 2. 1912: Keibel and Mall.
147. Young HM, Cane KN, Anderson CR. Development of the autonomic nervous system: a comparative view. *Auton Neurosci.* 2011;165(1):10-27.
148. Andres KH, Kautzky R. Die Frühentwicklung der vegetativen Hals- und Kopfganglien des Menschen. *Z Anat Entwicklungsgesch.* 1955;119:55-84.
149. Andres KH, Kautzky R. Kleine vegetative Ganglien im Bereich der Schädelbasis des Menschen. *Deutsche Zeitschrift f. Nervenheilkunde.* 1956;174:272-282.
150. Castro J, Negrodo P, Avendano C. Fiber composition of the rat sciatic nerve and its modification during regeneration through a sieve electrode. *Brain Res.* 2008;1190:65-77.
151. Loesch A, et al. Sciatic nerve of diabetic rat treated with epoetin delta: effects on C-fibers and blood vessels including pericytes. *Angiology.* 2010;61(7):651-668.
152. Tompkins RP, et al. Arrangement of sympathetic fibers within the human common peroneal nerve: implications for microneurography. *J Appl Physiol (1985).* 2013;115(10):1553-1561.
153. Creze M, et al. Functional and structural microanatomy of the fetal sciatic nerve. *Muscle Nerve.* 2017;56(4):787-796.
154. Yang M, Zhao X, Miselis RR. The origin of catecholaminergic nerve fibers in the subdiaphragmatic vagus nerve of rat. *J Auton Nerv Syst.* 1999;76(2-3):108-117.
155. Molinoff PB, Axelrod J. Biochemistry of catecholamines. *Annu Rev Biochem.* 1971;40:465-500.
156. Daubner SC, Le T, Wang S. Tyrosine hydroxylase and regulation of dopamine synthesis. *Arch Biochem Biophys.* 2011;508(1):1-12.
157. Hozawa K, Kimura RS. Cholinergic and noradrenergic nervous systems in the cynomolgus monkey cochlea. *Acta Otolaryngol.* 1990;110(1-2):46-55.
158. Hozawa K, Takasaka T. Catecholaminergic innervation in the vestibular labyrinth and vestibular nucleus of guinea pigs. *Acta Otolaryngol Suppl.* 1993;503:111-113.

159. Dairman W, Geffen L, Marchelle M. Axoplasmic transport of aromatic L-amino acid decarboxylase (EC 4.1.1.26) and dopamine beta-hydroxylase (EC 1.14.2.1) in rat sciatic nerve. *J Neurochem.* 1973;20(6):1617-1623.
160. Keen P, McLean WH. The effect of nerve stimulation on the axonal transport of noradrenaline and dopamine-beta-hydroxylase. *Br J Pharmacol.* 1974;52(4):527-531.
161. Nagatsu I, Hartman BK, Udenfriend S. The anatomical characteristics of dopamine-beta-hydroxylase accumulation in ligated sciatic nerve. *J Histochem Cytochem.* 1974;22(11):1010-1018.
162. Reid JL, Kopin IJ. The effects of ganglionic blockade, reserpine and vinblastine on plasma catecholamines and dopamine-beta-hydroxylase in the rat. *J Pharmacol Exp Ther.* 1975;193(3):748-756.
163. Haggendal J. Axonal transport of dopamine-beta-hydroxylase to rat salivary glands: studies on enzymatic activity. *J Neural Transm.* 1980;47(3):163-174.
164. Jakobsen J, Brimijoin S. Axonal transport of enzymes and labeled proteins in experimental axonopathy induced by p-bromophenylacetylurea. *Brain Res.* 1981;229(1):103-122.
165. Evers-Von Bultzingslowen I, Haggendal J. Disappearance of noradrenaline from different parts of the rabbit external ear following superior cervical ganglionectomy. *J Neural Transm.* 1983;56(2-3):117-126.
166. Larsson PA, Goldstein M, Dahlstrom A. A new methodological approach for studying axonal transport: cytofluorometric scanning of nerves. *J Histochem Cytochem.* 1984;32(1):7-16.
167. Schmidt RE, Modert CW. Orthograde, retrograde, and turnaround axonal transport of dopamine-beta-hydroxylase: response to axonal injury. *J Neurochem.* 1984;43(3):865-870.
168. Larsson PA, et al. Reserpine-induced effects in the adrenergic neuron as studied with cytofluorimetric scanning. *Brain Res Bull.* 1986;16(1):63-74.
169. Lackovic Z, et al. Dopamine and its metabolites in human peripheral nerves: is there a widely distributed system of peripheral dopaminergic nerves? *Life Sci.* 1981;29(9):917-922.
170. Anniko M, Pequignot JM. Catecholamine content of cochlear and facial nerves. High-performance liquid chromatography analyses in normal and mutant mice. *Arch Otorhinolaryngol.* 1987;244(5):262-264.
171. Densert O. A fluorescence and electron microscopic study of the adrenergic innervation in the vestibular ganglion and sensory areas. *Acta Otolaryngol.* 1975;79(1-2):96-107.
172. Nielsen KC, Owman C, Santini M. Anastomosing adrenergic nerves from the sympathetic trunk to the vagus at the cervical level in the cat. *Brain Res.* 1969;12(1):1-9.
173. Dahlstrom A, et al. Cytofluorimetric scanning: a tool for studying axonal transport in monoaminergic neurons. *Brain Res Bull.* 1982;9(1-6):61-68.
174. Dahlqvist A, et al. Catecholamines of endoneurial laryngeal paraganglia in the rat. *Acta Physiol Scand.* 1986;127(2):257-261.
175. Dahlstrom A, et al. Immunocytochemical studies on axonal transport in adrenergic and cholinergic nerves using cytofluorimetric scanning. *Med Biol.* 1986;64(2-3):49-56.
176. Dahlstrom A, et al. The synthesis of NPY and DBH is independently regulated in adrenergic nerves after reserpine. *Neurochem Res.* 1987;12(3):221-225.
177. D'Hooge R, et al. Storage and fast transport of noradrenaline, dopamine beta-hydroxylase and neuropeptide Y in dog sciatic nerve axons. *Life Sci.* 1990;47(20):1851-1859.
178. Ben-Jonathan N, Maxson RE, Ochs S. Fast axoplasmic transport of noradrenaline and dopamine in mammalian peripheral nerve. *J Physiol.* 1978;281:315-324.
179. Leblanc GG, Landis SC. Differentiation of noradrenergic traits in the principal neurons and small intensely fluorescent cells of the parasympathetic sphenopalatine ganglion of the rat. *Dev Biol.* 1989;131(1):44-59.
180. Muller F, Rohrer H. Molecular control of ciliary neuron development: BMPs and downstream transcriptional control in the parasympathetic lineage. *Development.* 2002;129(24):5707-5717.
181. Stanzel S, et al. Distinct roles of hand2 in developing and adult autonomic neurons. *Dev Neurobiol.* 2016;76(10):1111-1124.
182. Baetge G, Gershon MD. Transient catecholaminergic (TC) cells in the vagus nerves and bowel of fetal mice: relationship to the development of enteric neurons. *Dev Biol.* 1989;132(1):189-211.
183. Young HM, et al. Expression of Ret-, p75(NTR)-, Phox2a-, Phox2b-, and tyrosine hydroxylase-immunoreactivity by undifferentiated neural crest-derived cells and different classes of enteric neurons in the embryonic mouse gut. *Dev Dyn.* 1999;216(2):137-152.

184. Kuntz A. Distribution of the sympathetic rami to the brachial plexus: Its relation to sympathectomy affecting the upper extremity. *Arch Surg.* 1927;15(6):871-877.
185. Cho HM, Lee DY, Sung SW. Anatomical variations of rami communicantes in the upper thoracic sympathetic trunk. *Eur J Cardiothorac Surg.* 2005;27(2):320-324.
186. Won HJ, et al. Topographical study of the connections of the rami communicantes from the first to the fifth thoracic sympathetic ganglia. *Clin Anat.* 2018;31(8):1151-1157.
187. Cowley R. Anatomic observations on the lumbar sympathetic nervous system. *Surgery.* 1949;25(6): 880-890.
188. Volkmann B, et al. Anatomy and physiology of the nervous system. *Brit For Med Rev.* 1844;17:379-403.
189. Snow Beck T. On the nerves of the uterus. *Philos Trans R Soc.* 1845;136:213-235.
190. Downman CBB, Hazarika NH. Somatic nerve pathways through some thoracic rami communicantes. *J Physiol.* 1962;163:340-346.
191. Sheehan DP, Pick J. The rami communicantes in the rhesus monkey. *J Anat.* 1943;77(2):125-139.
192. Langley JN. Observations on the medullated fibres of the sympathetic system and chiefly on those of the grey rami communicantes. *J Physiol.* 1896;20(1):55-76.
193. Zuckerman S. Observations on the autonomic nervous system and on vertebral and neural segmentation in Monkeys. *Trans Zool Soc Lond.* 1938;23(6):315-378.
194. Mehler WR. The anatomy and variations of the lumbosacral sympathetic trunk in the dog. *Anat Rec.* 1952;113(4):421-435.
195. Romanes GJ. The motor cell columns of the lumbo-sacral spinal cord of the cat. *J Comp Neurol.* 1951; 94(2):313-363.
196. Petras JM, Cummings JF. Autonomic neurons in the spinal cord of the rhesus monkey: A correlation of the findings of cytoarchitectonics and sympathectomy with fiber degeneration following dorsal rhizotomy. *J Comp Neurol.* 1972;146:189-218.
197. Schellino R, Boido M, Vercelli A. The Dual Nature of Onuf's Nucleus: Neuroanatomical Features and Peculiarities, in Health and Disease. *Front Neuroanat.* 2020;14:572013.
198. Langley JN. Das sympathische und verwandte nervöse Systeme der Wirbeltiere (autonomes nervöses System). *Ergebnisse der Physiologie, biologischen Chemie und experimentellen Pharmakologie.* 1903;2: 818-872.
199. Sporns O, Tononi G, Kotter R. The human connectome: A structural description of the human brain. *PLoS Comput Biol.* 2005;1(4):e42.
200. Bota M, Swanson LW. The neuron classification problem. *Brain Res Rev.* 2007;56(1):79-88.
201. Swanson LW, Bota M. Foundational model of structural connectivity in the nervous system with a schema for wiring diagrams, connectome, and basic plan architecture. *Proc Natl Acad Sci U S A.* 2010; 107(48):20610-20617.
202. Verlinden TJM, et al. Innervation of the human spleen: A complete hilum-embedding approach. *Brain Behav Immun.* 2019;77:92-100.
203. Gonzalez-Gonzalez MA, et al. Platinized graphene fiber electrodes uncover direct spleen-vagus communication. *Commun Biol.* 2021;4(1):1097.
204. Oikawa S, et al. Immunohistochemical determination of the sympathetic pathway in the orbit via the cranial nerves in humans. *J Neurosurg.* 2004;101(6):1037-1044.
205. Ruskell GL. Fibre analysis of the nerve to the inferior oblique muscle in monkeys. *J Anat* 1983;137 (Pt 3): 445-455.
206. Hosaka F, et al. Human nasociliary nerve with special reference to its unique parasympathetic cutaneous innervation. *Anat Cell Biol.* 2016;49(2):132-137.
207. Matsubayashi T, et al. Significant Differences in Sympathetic Nerve Fiber Density Among the Facial Skin Nerves: A Histologic Study Using Human Cadaveric Specimens. *Anat Rec (Hoboken).* 2016;299(8): 1054-1059.
208. Lyon DB, et al. Sympathetic nerve anatomy in the cavernous sinus and retrobulbar orbit of the cynomolgus monkey. *Ophthalmic Plast Reconstr Surg.* 1992;8(1):1-12.
209. Johnston JA, Parkinson D. Intracranial sympathetic pathways associated with the sixth cranial nerve. *J Neurosurg.* 1974;40(2):236-243.

210. Ohman-Gault L, Huang T, Krimm R. The transcription factor Phox2b distinguishes between oral and non-oral sensory neurons in the geniculate ganglion. *J Comp Neurol.* 2017;525(18):3935-3950.
211. Rusu MC, Pop F. The anatomy of the sympathetic pathway through the pterygopalatine fossa in humans. *Ann Anat.* 2010;192(1):17-22.
212. Reuss S, et al. Neurochemistry of identified motoneurons of the tensor tympani muscle in rat middle ear. *Hear Res.* 2009;248(1-2):69-79.
213. Johansson K, Arvidsson J, Thomander L. Sympathetic nerve fibers in peripheral sensory and motor nerves in the face of the rat. *J Auton Nerv Syst.* 1988;23(1):83-86.
214. Takeuchi Y, et al. Superior cervical ganglionic origin of sympathetic fibers in the facial nerve, and their preganglionic spinal inputs: a WGA-HRP study in *Macaca fuscata*. *Brain Res Bull.* 1993;32(6):661-665.
215. Fukui Y, et al. The superior cervical ganglion: origin of sympathetic fibers in the facial and hypoglossal nerves in the cat. *Brain Res Bull.* 1992;28(5):811-815.
216. Thomander L, Aldskogius H, Arvidsson J. Evidence for a sympathetic component in motor branches of the facial nerve: a horseradish peroxidase study in the cat. *Brain Res.* 1984;301(2):380-383.
217. Shimozawa A. Electron-microscopic analysis of the mouse facial nerve near the geniculate ganglion. *Acta Anat (Basel).* 1978;100(2):185-192.
218. Yau JJ, Wu JJ, Liu JC. Origins of the afferent fibers to the cat superior cervical ganglion. *Proc Natl Sci Counc Repub China B.* 1991;15(1):1-7.
219. ten Tusscher MP, et al. The allocation of nerve fibres to the anterior eye segment and peripheral ganglia of rats. II. The sympathetic innervation. *Brain Res.* 1989;494(1):105-113.
220. Yamashita H, Bagger-Sjoberg D, Sekitani T. Distribution of tyrosine hydroxylase-like immunofluorescence in guinea pig vestibular ganglia and sensory areas. *Auris Nasus Larynx.* 1992;19(2):63-68.
221. Paradiesgarten A, Spoendlin H. The unmyelinated nerve fibres of the cochlea. *Acta Otolaryngol.* 1976;82(3-4):157-164.
222. Matsumoto I, et al. DNA microarray cluster analysis reveals tissue similarity and potential neuron-specific genes expressed in cranial sensory ganglia. *J Neurosci Res.* 2003;74(6):818-828.
223. Seki A, et al. Sympathetic nerve fibers in human cervical and thoracic vagus nerves. *Heart Rhythm.* 2014;11(8):1411-1417.
224. Onkka P, et al. Sympathetic nerve fibers and ganglia in canine cervical vagus nerves: localization and quantitation. *Heart Rhythm.* 2013;10(4):585-591.
225. Satoda T, et al. The sites of origin and termination of afferent and efferent components in the lingual and pharyngeal branches of the glossopharyngeal nerve in the Japanese monkey (*Macaca fuscata*). *Neurosci Res.* 1996;24(4):385-392.
226. Nozdrachev AD, et al. Circuits and projections of cat stellate ganglion. *Arch Med Res.* 2003;34(2):106-115.
227. Forgie A, et al. In vivo survival requirement of a subset of nodose ganglion neurons for nerve growth factor. *Eur J Neurosci.* 2000;12(2):670-676.
228. Fateev MM, Nozdrachev AD. Projections of stellate ganglion sympathetic neurons in cats. *J Auton Nerv Syst.* 1995;51(2):129-134.
229. Tseng CY, et al. Ultrastructural identification of a sympathetic component in the hypoglossal nerve of hamsters using experimental degeneration and horseradish peroxidase methods. *Cells Tissues Organs.* 2005;180(2):117-125.
230. Tseng CY, et al. Evidence of neuroanatomical connection between the superior cervical ganglion and hypoglossal nerve in the hamster as revealed by tract-tracing and degeneration methods. *J Anat.* 2001;198(Pt 4):407-421.
231. Hino N, Masuko S, Katsuki T. An immunohistochemical study of sensory and autonomic innervation of the dog tongue with special reference to substance P- and calcitonin gene-related peptide-containing fibers in blood vessels and the intralingual ganglia. *Arch Histol Cytol.* 1993;56(5):505-516.
232. O'Reilly PM, FitzGerald MJ. Fibre composition of the hypoglossal nerve in the rat. *J Anat.* 1990;172:227-243.
233. Ruggiero DA, et al. Effect of cervical vagotomy on catecholaminergic neurons in the cranial division of the parasympathetic nervous system. *Brain Res.* 1993;617(1):17-27.



234. Eriksson M, et al. Distribution and origin of peptide-containing nerve fibres in the rat and human mammary gland. *Neuroscience*. 1996;70(1):227-245.
235. Ling EA, et al. Degenerative changes of neurons in the superior cervical ganglion following an injection of Ricinus communis agglutinin-60 into the vagus nerve in hamsters. *J Neurocytol*. 1990;19(1):1-9.
236. Chakravarthy Marx S, et al. Distribution of sympathetic fiber areas in the sensory nerves of forearm: an immunohistochemical study in cadavers. *Rom J Morphol Embryol*. 2011;52(2):605-611.
237. Baluk P, Gabella G. Innervation of the guinea pig trachea: a quantitative morphological study of intrinsic neurons and extrinsic nerves. *J Comp Neurol*. 1989;285(1):117-132.
238. Marx SC, et al. Microanatomical and immunohistochemical study of the human lateral antebrachial cutaneous nerve of forearm at the antecubital fossa and its clinical implications. *Clin Anat*. 2010;23(6): 693-701.
239. Marx SC, et al. Distribution of sympathetic fiber areas of radial nerve in the forearm: an immunohistochemical study in cadavers. *Surg Radiol Anat*. 2010;32(9):865-871.
240. Lucier GE, Egizii R, Dostrovsky JO. Projections of the internal branch of the superior laryngeal nerve of the cat. *Brain Res Bull*. 1986;16(5):713-721.
241. Balogh B, et al. The nerve of Henle: an anatomic and immunohistochemical study. *J Hand Surg Am*. 1999; 24(5):1103-1108.
242. Smith RV, Satchell DG. Determination of extrinsic pathways of adrenergic nerves to the guinea-pig trachealis muscle using surgical denervation and organ-bath pharmacology. *Agents Actions*. 1986;19(1-2):48-54.
243. Blessing WW, Willoughby JO, Joh TH. Evidence that catecholamine-synthesizing perikarya in rat medulla oblongata do not contribute axons to the vagus nerve. *Brain Res*. 1985;348(2):397-400.
244. Chakravarthy Marx S, et al. Microanatomical and immunohistochemical study of the human anterior branch of the medial antebrachial cutaneous nerve of forearm at the antecubital fossa and its clinical implications. *Rom J Morphol Embryol*. 2010;51(2):337-346.
245. Smith RV, Satchell DG. Extrinsic pathways of the adrenergic innervation of the guinea-pig trachealis muscle. *J Auton Nerv Syst*. 1985;14(1):61-73.
246. Hisa Y. Fluorescence histochemical studies on the noradrenergic innervation of the canine larynx. *Acta Anat (Basel)*. 1982;113(1):15-25.
247. Lundberg JM, et al. Efferent innervation of the small intestine by adrenergic neurons from the cervical sympathetic and stellate ganglia, studied by retrograde transport of peroxidase. *Acta Physiol Scand*. 1978;104(1):33-42.
248. Ungvary G, Leranath C. Termination in the stellate ganglion of axons arising from the hilar vegetative plexus of the lung. Peripheral reflex arcs. *Acta Anat (Basel)*. 1976;95(4):589-597.
249. Wang ZY, et al. Localization of zinc-enriched neurons in the mouse peripheral sympathetic system. *Brain Res*. 2002;928(1-2):165-174.
250. Li JY, et al. Proteolytic processing, axonal transport and differential distribution of chromogranins A and B, and secretogranin II (secretoneurin) in rat sciatic nerve and spinal cord. *Eur J Neurosci*. 1999;11(2): 528-544.
251. Janig W, McLachlan E. On the fate of sympathetic and sensory neurons projecting into a neuroma of the superficial peroneal nerve in the cat. *J Comp Neurol*. 1984;225(2):302-311.
252. Li JY, et al. Distribution of Rab3a in rat nervous system: comparison with other synaptic vesicle proteins and neuropeptides. *Brain Res*. 1996;706(1):103-112.
253. Li JY, Hou XE, Dahlstrom A. GAP-43 and its relation to autonomic and sensory neurons in sciatic nerve and gastrocnemius muscle in the rat. *J Auton Nerv Syst*. 1995;50(3):299-309.
254. Koistinaho J. Adrenergic nerve fibers in the human fetal sciatic nerve. *Acta Anat (Basel)*. 1991;140(4): 369-372.
255. Li JY, Jahn R, Dahlstrom A. Synaptotagmin I is present mainly in autonomic and sensory neurons of the rat peripheral nervous system. *Neuroscience*. 1994;63(3):837-850.
256. Fang F, et al. Patterns of sural nerve innervation of the sural artery with implication for reconstructive surgery. *J Surg Res*. 2017;220:261-267.
257. Nyangoh Timoh K, et al. Levator ani muscle innervation: Anatomical study in human fetus. *Neurorol Urodyn*. 2017;36(6):1464-1471.

258. Bertrand MM, et al. Anatomical basis of the coordination between smooth and striated urethral and anal sphincters: loops of regulation between inferior hypogastric plexus and pudendal nerve. *Immunohistological study with 3D reconstruction*. *Surg Radiol Anat*. 2016;38(8):963-972.
259. Studelska DR, Brimijoin S. Partial isolation of two classes of dopamine beta-hydroxylase-containing particles undergoing rapid axonal transport in rat sciatic nerve. *J Neurochem*. 1989;53(2):622-631.
260. Hinata N, et al. Histological study of the cavernous nerve mesh outside the periprostatic region: anatomical basis for erectile function after nonnerve sparing radical prostatectomy. *J Urol*. 2015;193(3):1052-9.
261. Hieda K, et al. Nerves in the intersphincteric space of the human anal canal with special reference to their continuation to the enteric nerve plexus of the rectum. *Clin Anat*. 2013;26(7):843-854.
262. Alsaid B, et al. Autonomic-somatic communications in the human pelvis: computer-assisted anatomic dissection in male and female fetuses. *J Anat*. 2011;219(5):565-573.
263. Alsaid B, et al. Coexistence of adrenergic and cholinergic nerves in the inferior hypogastric plexus: anatomical and immunohistochemical study with 3D reconstruction in human male fetus. *J Anat*. 2009;214(5):645-654.
264. Roppolo JR, Nadelhaft I, de Groat WC. The organization of pudendal motoneurons and primary afferent projections in the spinal cord of the rhesus monkey revealed by horseradish peroxidase. *J Comp Neurol*. 1985;234(4):475-488.
265. Moszkowicz D, et al. Neural supply to the clitoris: immunohistochemical study with three-dimensional reconstruction of cavernous nerve, spongiosus nerve, and dorsal clitoris nerve in human fetus. *J Sex Med*. 2011;8(4):1112-1122.
266. Colombel M, et al. Caverno-pudendal nervous communicating branches in the penile hilum. *Surg Radiol Anat*. 1999;21(4):273-276.
267. Hinata N, et al. Topohistology of sympathetic and parasympathetic nerve fibers in branches of the pelvic plexus: an immunohistochemical study using donated elderly cadavers. *Anat Cell Biol*. 2014;47(1):55-65.
268. Hinata N, et al. Nerves and fasciae in and around the paracolpium or paravaginal tissue: an immunohistochemical study using elderly donated cadavers. *Anat Cell Biol*. 2014;47(1):44-54.
269. Deng YS, Zhong JH, Zhou XF. BDNF is involved in sympathetic sprouting in the dorsal root ganglia following peripheral nerve injury in rats. *Neurotox Res*. 2000;1(4):311-322.
270. Jones MG, Munson JB, Thompson SW. A role for nerve growth factor in sympathetic sprouting in rat dorsal root ganglia. *Pain*. 1999;79(1):21-29.
271. Thoenen H, Mueller RA, Axelrod J. Phase difference in the induction of tyrosine hydroxylase in cell body and nerve terminals of sympathetic neurones. *Proc Natl Acad Sci U S A*. 1970;65(1):58-62.
272. Ma W, Bisby MA. Partial sciatic nerve transection induced tyrosine hydroxidase immunoreactive axon sprouting around both injured and spared dorsal root ganglion neurons which project to the gracile nucleus in middle-aged rats. *Neurosci Lett*. 1999;275(2):117-120.
273. Shinder V, et al. Structural basis of sympathetic-sensory coupling in rat and human dorsal root ganglia following peripheral nerve injury. *J Neurocytol*. 1999;28(9):743-761.
274. Morellini N, et al. Expression of the noradrenaline transporter in the peripheral nervous system. *J Chem Neuroanat*. 2019;104:101742.
275. Thompson SW, Majithia AA. Leukemia inhibitory factor induces sympathetic sprouting in intact dorsal root ganglia in the adult rat in vivo. *J Physiol*. 1998;506 ( Pt 3):809-816.
276. Karlsson M, Hildebrand C. Invasion of the rat ventral root L5 by putative sympathetic C-fibers after neonatal sciatic nerve crush. *Brain Res*. 1994;667(1):39-46.



# Chapter 6

Impact



## Impact

Progress in science is dependent on (interdisciplinary) collaboration. Appropriate collaboration is dependent on language. The anatomical nomenclature is one of the fundamental languages of neuroscience important for (interdisciplinary) communication. The unambiguous description of thousands of structures is made possible with an extensive number of highly specialized terms that are used to the exclusion of any other. In this thesis we conclude that neurons, nerves and ganglia are best labelled according to topography.

### Implications from this thesis for peripheral nerve stimulation treatments

A common form of generalization is the classification of nerves and ganglia based on their dominant feature alone. The vagus nerve for example has become known as a parasympathetic nerve, and the phrenic nerve as a somatic nerve (Chapters 2,3).

Direct implications from such classifications can be observed in “peripheral nerve stimulation treatments”. This therapy involves delivering electrical impulses to specific nerves. The treatment involves surgery in which a small generator is usually implanted under the patients’ skin. Lead wires from the generator are tunneled up to the area of interest where the electrode is then wrapped around the entire nerve.

Well known examples are vagus and phrenic nerve stimulation treatments. Because of the classification of nerves on their dominant physiologic characteristic, phrenic nerve stimulation is mainly known for pacing the diaphragm (Chapter 2). Vagus nerve stimulation has, as such, become known for increasing ‘parasympathetic tone’ (Chapter 3). Other events that appear on vagus nerve stimulation, such as voice alteration and hoarseness, cough and dysphagia are called adverse effects, but are common and can be ascribed to other properties of the vagus nerve.

In this thesis, we studied the morphological composition of both vagus and phrenic nerves at the typical levels of nerve stimulation therapies. We demonstrated that both nerves also contain catecholaminergic fibers. We described the distribution of myelinated and non-myelinated nerve fibers within the left and right or along the proximo-distal course of these nerves. Such information is important for nerve stimulation, because myelinated nerve fibers have a much lower amplitude-duration threshold than non-myelinated fibers. Typical stimulation protocols for nerve stimulation can vary up to a hundred-fold in intensity, 5-fold in duration and 2-fold in frequency. If

applied for central sleep apnea, we suggest that the stimulation should target the myelinated fibers and should, therefore, be accomplished with the lowest possible amplitude-duration thresholds that result in the intended rhythmic activation of the diaphragm. This is necessary to prevent any undesired stimulation of the nonmyelinated catecholaminergic fibers that we demonstrated within the phrenic nerve (Chapter 2). Stimulation of these fibers may further increase the chronic upregulation of sympathetic activity that is already present in patients with central sleep apnea and is associated with increased mortality these patients. Furthermore, we demonstrated that the right cervical vagus nerve contains significantly more catecholaminergic fibers than the left (Chapter 3).

### Providing morphological support for novel molecular findings

The universally accepted model of the sympathetic and parasympathetic efferent limbs of the autonomic nervous system was formulated at the turn of the 19<sup>th</sup> to the 20<sup>th</sup> century. The tenability of this classic model, however, is challenged by progressive insights from novel molecular techniques (Chapter 5). Collectively, these studies however, struggle in refuting the longstanding anatomical arguments that are used for the classic subdivision of the spinal autonomic outflow in sympathetic (thoracolumbar) and sacral (parasympathetic) divisions. The proposed paradigm shift to classify the sacral autonomic outflow as sympathetic, met as such, considerable resistance in the field.

In this thesis, we assembled all available data on the peripheral distribution of catecholaminergic neurons, and used the outcome to re-evaluate the anatomical arguments on which the sympathetic-parasympathetic model is based (Chapter 5). We conclude that the anatomy of the autonomic outflow actually displays a conserved architecture along the entire spinal axis. The perceived differences in the anatomy of the thoracolumbar and sacral outflow are the result of a gradient of anatomical characteristics that progressively change from the thoracic level towards those that are typical for the sacral autonomic outflow. This finding provides the morphological support that, up until now, was lacking for the novel molecular finding that the autonomic outflows at the thoracolumbar and sacral levels possess a highly similar molecular signature. Aiding to appropriate interdisciplinary communication, we also show in this thesis (Chapter 5) that it is better to label preganglionic neurons according to topography (i.e. spinal vs. cranial), since the term sympathetic has become polysemous over time (Chapter 1).

## Samenvatting





## Samenvatting

Het perifere zenuwstelsel bestaat onder andere uit neuronen (zenuwcellen). Elk neuron is opgebouwd uit een cellichaam met daarin de celkern, en uitlopers (axonen en dendrieten) waarover de elektrische impuls wordt doorgeleid. Dikwijls maakt de elektrische impuls neurotransmitters vrij aan het einde van de cel. Er bestaan verschillende typen neuronen en neurotransmitters afhankelijk van de richting van geleiding en het beoogde effect op de doelcel. Neuronen verzamelen zich tot zenuwen zodat elektrische impulsen door het hele lichaam verspreid kunnen worden. Een gangbare opvatting is dat neuronen gewijd zijn aan specifieke zenuwen, waardoor zenuwen zelf ook fysiologisch geïnclassificeerd worden.

**Hoofdstuk 1** geeft achtergrondinformatie over deze classificaties. Binnen het zenuwstelsel wordt een viscerale component onderscheiden dat het autonome zenuwstelsel wordt genoemd. Het bestaat uit neuronen die zich zowel in het centrale als in het perifere deel van het zenuwstelsel bevinden. Deze viscerale efferente trajecten worden gekenmerkt door een opeenvolging van ten minste twee neuronen tussen het centrale zenuwstelsel en de doelstructuur. Deze worden respectievelijk preganglionaire en postganglionaire neuronen genoemd. Het is gebruikelijk om paren van pre- en postganglionaire neuronen samen als sympathisch of parasympathisch te bestempelen. Zenuwen en ganglia zelf worden ook wel geïnclassificeerd als sympathisch of parasympathisch. De paravertebrale ganglia en witte en grijze rami communicantes staan bekend als sympathische structuren, terwijl de autonome ganglia van het hoofd en pelvische splanchnische zenuwen typische parasympathische structuren zouden zijn.

**Hoofdstuk 2** is het eerste hoofdstuk dat laat zien dat neuronen niet altijd gewijd zijn aan specifieke zenuwen. We laten zien dat catecholaminerge (sympathische) neuronen ook aanwezig zijn op de 'somatische' nervus phrenicus. De gehele nervi phrenici van 35 menselijke stoffelijke overschotten werden morfometrisch en immunohistochemisch geanalyseerd. Verder werd de rechter abdominale tak van de nervus phrenicus serieel doorgesneden en gereconstrueerd. De nervus phrenicus bevat  $3 \pm 2$  zenuwbundels in de nek die samensmelten tot een enkele zenuwbundel in de thorax en weer splitsen in  $3 \pm 3$  zenuwbundels boven het diafragma. Alle onderzochte zenuwen bevatten catecholaminerge (sympathische) neuronen. Deze zijn homogeen verdeeld of aanwezig als afzonderlijke gebieden binnen een zenuwbundel of als afzonderlijke bundels. Verder observeerden we dat de phrenicoabdominale tak van de rechter nervus phrenicus eigenlijk een tak is van de plexus coeliacus. Deze wordt daarom beter de "phrenische tak van de plexus coeliacus" genoemd.

Tenslotte vonden we in deze studie dat de wand van de vena cava inferior in het diafragma longitudinale strengen van myocardium bevat en atriale natriuretische peptide-positieve paraganglia ("cavale lichamen") die worden geïnnerveerd door de rechter nervus phrenicus.

In **hoofdstuk 3** demonstreren we catecholaminerge (sympathische) neuronen op de nervus vagus. We bestudeerden 11 cervicale paren van de menselijke nervus vagus op het niveau waar de electrode wordt geïmplantéerd bij nervus vagus stimulatie. Daarbij werden nog 4 extra intracraniale paren geanalyseerd. Er werd vastgesteld dat de rechter cervicale nervus vagus een gemiddeld 1,5 maal groter effectief oppervlak heeft dan de linker zenuw (respectievelijk  $1.089.492 \pm 98.337 \mu\text{m}^2$  vs.  $753.915 \pm 102.490 \mu\text{m}^2$  ( $P < 0,05$ )) en dat er een brede spreiding is binnen de individuele zenuwen. Aan de rechterzijde is de gemiddelde effectieve oppervlakte op cervicaal niveau ( $1.089.492 \pm 98.337 \mu\text{m}^2$ ) groter dan op het niveau binnen de schedelbasis ( $630.921 \pm 105.422$ ) ( $P < 0,05$ ). Dit zou kunnen betekenen dat de nervus vagus anastomoserende en "meeliftende" takken ontvangt uit andere gebieden dan de hersenstam. Bovendien konden overvloedig tyrosine hydroxylase (TH) en dopamine  $\beta$  hydroxylase (DBH) positief gekleurde zenuwvezels worden geïdentificeerd, wat wijst op de catecholaminerge neurotransmissie. In 2 van de 22 cervicale zenuwen werden ganglioncellen gevonden die ook positief kleurden voor TH en DBH. Stimulatie van de nervus vagus kan dus het vrijkomen van dopamine en noradrenaline induceren. Een sympatische activatie zou daarom deel kunnen uitmaken van het werkingsmechanisme van VNS. Bovendien werd aangetoond dat de rechter cervicale nervus vagus gemiddeld 2 maal meer TH positieve zenuwvezels bevat dan de linker zenuw ( $P < 0,05$ ), een feit dat van belang zou kunnen zijn bij de keuze van de stimulatie zijde. We suggereren ook dat de hoeveelheid epineuraal weefsel een belangrijke variabele zou kunnen zijn voor het bepalen van de individuele effectiviteit van VNS, omdat de absolute hoeveelheid epineuraal weefsel sterk verdeeld is tussen de individuele zenuwen (variërend van  $2.090.000 \mu\text{m}^2$  tot  $11.683.000 \mu\text{m}^2$ ). We besluiten dit hoofdstuk met te stellen dat men de nervus vagus, net als de nervus phrenicus, moet zien als een morfologische entiteit van het perifere zenuwstelsel, een composiet van verschillende vezels en (communicerende en liftende) takken van verschillende oorsprong met verschillende neurotransmitters. Elektrisch stimuleren van de nervus vagus is dus niet hetzelfde als het verhogen van de "fysiologische parasympatische tonus", maar kan dus ook catecholaminerge (sympatische) effecten teweegbrengen.

**Hoofdstuk 4** borduurt voort op het principe van zenuwstimulatie. Er wordt verondersteld dat de milt een rol speelt in de neuraal gemedieerde controle van de

gastheer verdediging. Het neuro-anatomisch bewijs voor deze veronderstelling berust echter op een schaars aantal studies, die het onderling oneens zijn over het bestaan van cholinerge of vagale innervatie van de milt. Wij voerden een immuno- en enzym-histochemische studie uit, naar de innervatie van de menselijke milt, gebruik makend van een benadering waarbij het volledige hilum van 46 stoffelijke overschotten werd ingebed. Dit om er zeker van te zijn dat alleen zenuwen die de milt binnenkwamen of verlieten werden bestudeerd, en dat alle zenuwen van de milt werden opgenomen in het bemonsterde gebied. Additioneel werd 1 compleet ingebedde milt serieel doorsneden zodat een 3D-reconstructie van de hilaire zenuwplexus kon worden gemaakt. Onze resultaten waren als volgt: Alle zenuwen van de milt komen voort uit de zenuw plexus die takken van de arteria splenica omringt en zijn catecholaminerg. Binnen de milt gaan deze zenuwen verder in de adventitia van de centrale arteriën van de witte, en de arteriolen van de rode pulpa. Kleuring voor choline acetyltransferase of acetylcholinesterase leverde geen aanwijzingen op voor cholinerge innervatie van de menselijke milt, ongeacht het type fixatie (standaard gefixeerd, vers-ingevroren post gefixeerd of vers-ingevroren cryo coupes). Bovendien werd geen positieve VIP-kleuring waargenomen (VIP wordt vaak mede aangetroffen in postganglionaire parasympatische zenuwen). We concluderen in dit hoofdstuk dat onze uitgebreide benadering geen bewijs kon leveren voor een directe cholinerge (of VIP-erge) innervatie van de milt. Deze bevinding sluit niet uit dat er een (indirecte) vagale innervatie via niet-cholinerge vezels bestaat, zoals we die in hoofdstuk 3 aantoonde.

Naar aanleiding van onze eigen onderzoeken besloten we een systematische review te doen naar de perifere distributie van catecholaminerge neuronen (**hoofdstuk 5**). We gebruikten het resultaat om de anatomische argumenten waarop het huidige binaire sympatische-parasympatische model gebaseerd is, opnieuw te evalueren. Pubmed werd doorzocht op originele studies bij zoogdieren die de aanwezigheid van catecholaminerge neuronen immunohistochemisch aantoonde of de communicatie tussen zenuwen en sympatische structuren bevestigde met gevalideerde technieken. 144 Zoekopdrachten identificeerden 1.239 studies die informatie gaven over 389 anatomische structuren. 168 Studies voldeden aan alle inclusiecriteria. We vonden dat catecholaminerge zenuwvezels aanwezig zijn in vele spinale en alle craniale zenuwen en ganglia, inclusief zenuwen en ganglia die bekend staan om hun parasympatische functie.

Langs de gehele spinale autonome weg komen zowel proximale als distale catecholaminerge cellichamen voor. Zowel in het hoofd, de borstkas en het abdominale en bekken gebied, hetgeen het argument van "korte versus lange pre-ganglionaire neuronen" ontkracht. Deze bevindingen tonen opnieuw aan dat neuronen niet gewijd

zijn aan specifieke zenuwen, en toont aan dat het concept van het connectoom in de hersenen ook van toepassing is op het perifere zenuwstelsel.

In tegenstelling tot de klassiek begrensde uittrede niveau's T1-L2 en S2-S4, zijn preganglionaire neuronen ook gevonden op het lagere lumbale niveau. Preganglionaire cellen die zich bevinden in de intermediolaterale zone van het thoracolumbale ruggenmerg, nestelen zich geleidelijk aan meer ventraal in de ventrale motorkernen op lumbaal en sacraal niveau, en hun vezels omzeilen de witte ramus communicans en de sympathische grensstreng, om rechtstreeks uit de spinale zenuwen uit te treden. Het omzeilen van de sympathische grensstreng is dus niet exclusief voor sacrale neuronen. Wij concluderen dat de anatomie van het autonoom zenuwstelsel een geconserveerde architectuur vertoont langs de gehele spinale as.

Tenslotte wordt in **hoofdstuk 6** de potentiële impact van dit proefschrift en het daarin beschreven onderzoek besproken. Stimulatie van catecholaminerge vezels binnen de nervus phrenicus kunnen de chronische verhoging van sympathische activiteit, die reeds aanwezig is bij patiënten met centrale slaapapneu en geassocieerd is met een verhoogde mortaliteit bij deze patiënten, mogelijk extra verhogen. Bovendien toonden we aan dat de rechter cervicale nervus vagus significant meer catecholaminerge vezels bevat dan de linker.

Onze bevinding dat de anatomie van het autonoom zenuwstelsel een geconserveerde architectuur vertoont langs de gehele spinale as, biedt de morfologische ondersteuning die tot nu toe ontbrak voor de nieuwe moleculaire bevinding dat de autonome uitlopers op thoracolumbaal en sacraal niveau een sterk gelijke moleculaire signatuur bezitten.

Dankwoord



## Dankwoord

Nieuwe inzichten komen tot stand door samenwerking. Tussen groepen en doorheen generaties. Ik wil iedereen van onze vakgroep Anatomie & Embryologie dan ook bedanken.

Extra dank gaat uit naar Paul van Dijk, Els Terwindt en Marjolein Verhesen-Herfs voor hun enorme aandeel in het laboratorium, inclusief de inspanningen die reeds zijn gedaan aan de voortgekomen vraagstukken.

Dank aan Jill Hikspoors en Greet Mommen voor hun expertise in histologische 3D-reconstructies en het maken van de prachtige illustraties.

In het bijzonder bedank ik Andreas Herrler, Wouter Lamers en Leo Köhler. Leo ben ik enorm dankbaar voor de manier waarop zij ons leidt. Het is zeer speciaal dat ik in deze tijd mijn eigen onderzoek, van A tot Z, uiteen heb mogen zetten. Daarvoor ook heel veel dank aan Wout en Andreas. Door hen lukte het om te denken buiten het veronderstelde. De constante vragen van Wout stimuleerden mij om door te blijven zoeken. Dat is de kern van leren. 'Question everything...'

Breder gezien heb ik natuurlijk zo veel te danken aan mijn ouders, voor alles wat ik zomaar meekreeg. Ik voel mij een zondagskind.

Tenslotte ook zo veel dank aan mijn vrouw, Nicole. Wij vormen een droomteam, dat nog eens werd uitgebreid met onze prachtige jongens, Floris en Lucas. Samen kunnen wij elke catecholamine aan!





## Curriculum vitae



## Curriculum vitae

Thomas Verlinden werd geboren op 17 mei 1985 te Roermond. Hij groeide op in Maasbracht en rondde in 2002 zijn middelbare school in Echt af. Na het afronden van verschillende studies, waaronder initieel fysiotherapie, behaalde hij in 2010 (cum laude) zijn masterdiploma aan de Universiteit van Maastricht in de richting Metabolism and Nutrition. Sindsdien is hij zelf werkzaam aldaar als docent en onderzoeker binnen de vakgroep Anatomie & Embryologie. Daarnaast houdt Thomas nog een praktijk waarin hij een vorm van manuele therapie beoefend. Zijn behandelingen zijn veelal gericht op het verbeteren van de functie van de gewrichten van de wervelkolom die tekenen van artrose vertonen.

